DU 2354
EDSF 748

PCCF T 1302

UNIVERSITÉ BLAISE PASCAL DE CLERMONT-FERRAND
U.F.R Sciences et Technologies

ÉCOLE DOCTORALE DES SCIENCES FONDAMENTALES

THÈSE

présentée pour obtenir le grade de

Docteur d'Université
Spécialité: PHYSIQUE DES PARTICULES

par:

Siavash NESHATPOUR

Recent B-decay implications beyond the Standard Model

Thèse soutenue publiquement le 23 mai 2013, devant la commission d'examen:

Mme. Marie-Hélène SCHUNE	*Président*
M. Damir BĚCIREVIĆ	*Rapporteur*
Mme. Gudrun HILLER	*Rapporteur*
M. Gilbert MOULTAKA	*Examinateur*
M. Jean ORLOFF	*Directeur de thèse*
Mme. Nazila MAHMOUDI	*Codirecteur de thèse*

Abstract

There are fast progresses in the experimental study of rare decays of mesons containing a b-quark, and involving a pair of leptons and an s-quark. The present work measures the indirect implications of these progresses on the supersymmetric extensions of the Standard Model. Even within constrained models, the indirect limits obtained in this way can in some cases be stronger than those coming from direct searches of supersymmetric particles. The accuracy gained by the form factors and higher order corrections newly implemented in the public code "SuperIso" are then fully relevant.

Résumé

Des progrès expérimentaux importants sont en cours dans l'étude des désintégrations rares de mésons contenant un quark beau et impliquant un quark étrange et une paire de leptons. Le travail présent mesure la portée indirecte de ces progrés sur des extensions supersymétriques du modèle standard. Même dans des modèles contraints, les limites indirectes ainsi obtenues peuvent dans certains cas être plus fortes que celles provenant de la recherche directe de particules supersymétriques. La précision gagnée par les facteurs de forme et les corrections d'ordre supérieur nouvellement implémentés dans le programme public "SuperIso" montrent alors leur importance.

Acknowledgements

I would like to thank the Laboratoire de Physique Corpusculaire de Clermont-Ferrand for hosting me during my PhD studies; I am indebted to the LPC, and in particular to Alain Falvard and Jean Orloff, for the additional grant on the final stages of my PhD. I would like to acknowledge the French Ministère de l'Enseignement Supérieur et de la Recherche for the financial support during the PhD thesis.

The Theory Group at the LPC offered a very warm and welcoming environment, and I am particularly thankful to Jean-François Mathiot, Jean Orloff, Vincent Morénas, Nazila Mahmoudi, and Ana Teixeira for the stimulating atmosphere, constant help in physics and computer crises. I am also thankful for the many moments we shared during these past years and for introducing me to the wibbly-wobbly nature of time.

I would like to thank my supervisor Jean Orloff and my co-supervisor Nazila Mahmoudi for motivating me to study B-physics, and for their extensive advice, guidance and availability during my PhD thesis. I am also grateful for having been given the possibility to participate in international Schools and scientific meetings.

I am particularly indebted to Jean Orloff for the endless hours we spent discussing and exchanging about numerous topics, physics related and otherwise! I have enormous gratitude for your patience and understanding, and for your constant support throughout the thesis. I cannot thank you enough for all I have learnt from you, for your interest and concern, and your continuous availability. It is an honour to have been your student!

My deep gratitude to Jean Orloff, Nazila Mahmoudi and Alexandre Arbey for their generous help and assistance upon my arrival at Clermont.

I am also indebted to Jean Orloff, Nazila Mahmoudi and Ana Teixeira for the many remarks and valuable suggestions regarding the preparation of this thesis, as well as for a careful and critical reading of the manuscript.

I want to express my enormous gratitude to Ana Teixeira, a person without whom this thesis would not have been completed. An enlightening, friendly, patient and helpful researcher, who shares her experience generously. I have utterly enjoyed and learned a lot from the many discussions we have had on various (physics and non-physics) topics. Thank you very much Ana, for being always ready to help and for your concern, scientifically and otherwise! Your encouraging words during difficult times have been instrumental to my PhD studies.

Many thanks to Stephane Monteil, an illuminating and open researcher with whom I had my first French physics education, and many nice discussions.

My gratitude goes to my office mates and fellow graduate students, for their friendship and for creating a great working environment - Bruno, Mariam, Mustafa and Natalia. Many thanks to all the new friends I met in Clermont, Cécile, Chantelle, Elena, Krzysztof, Lukasz, Ola, Samantha and Teresa, who introduced me to Berthom's Kriek.
Albeit not physically present, a special thank you to my friends back from Iran: Ali Chenani, Ali Nejat, Azadeh, Behrang, Ehsan, Farzaneh, Hamzeh, Mehdi, Mohammad, Mohsen, Negar, Roham, Saman, Samaneh and Shahab, with whom I spent hours and hours and of laughing, discussing, arguing and having fun. Many of you literally went to great lengths to be physically present.
My special gratitude to my family, my Mom and Dad and to my Sisters, Ani and Kati, for their unconditional love and support. Kati, for all the talks which were always uplifting and joyful, and Ani and Amir for their care and kindness. My heart goes to my nephew Danny, and my little niece, Rose with whom our "chats" were always the highlight of the day. I am enormously grateful and indebted to my parents for the education they offered me and for having always supported and encouraged me to pursue my goals.
Last but not least, a heartfelt thank goes out to Golnoosh for all her love, support and patience when I was only thinking about strange formulas. Golnoosh, thank you for your invaluable support in so many moments, for listening to me and offering your advice whenever I needed. Your support, encouragement, quiet patience and unwavering love were undeniably the bedrock upon which the past years of my life have been built. Thank you with all my heart!

To my Parents.

Contents

List of Figures

List of Tables

CHAPTER 1

Introduction

The Standard Model (SM) is an elaborate theoretical construction that has met remarkable empirical success. However, the SM has shortcomings. Some are observational deficiencies, such as the inability to account for neutrino masses and mixings, and to provide an explanation for the baryon asymmetry of the universe, or a viable dark matter candidate. Moreover, the SM has theoretical caveats (of a more conceptual and/or aesthetic nature). Among the latter are the incomplete unification of gauge symmetries, the hierarchy problem, the flavour problem, etc.

In the SM there are 19 arbitrary parameters, many of which are related to flavour dynamics. In particular, in the quark sector the difficulty of explaining why there are so many different types of fermions and why their weak interactions behave in the peculiar way observed, is referred to as the flavour problem. Specifically, it is important to understand whether the Cabibbo-Kobayashi-Maskawa matrix fully describes the flavour dynamics in the quark sector. In the past years, substantial theoretical and experimental progress has been achieved in flavour physics. These progresses, in addition to testing the SM description, also provide a powerful tool to indirectly probe possible underlying New Physics (NP) effects.

The SM has two features that are crucial to its successful description of the (so far) observed mixing pattern in the quark sector. The first is the unitarity of the CKM matrix and its small mixing angles. The second is the suppression of flavour changing neutral current (FCNC) processes due to the Glashow-Iliopoulos-Maiani (GIM) mechanism. Since within the Standard Model, FCNC processes vanish at tree level, NP effects can be comparable with the SM loop level contributions. Hence, these processes offer sensitive probes of extensions of the Standard Model. In particular rare B decays with quark level transition $b \to s$ can provide strong constraints on many new physics models.

Since there are several energy scales involved in the weak decay of mesons, there are subtleties in studying FCNC processes. The energy scales pertinent to B decays are: the

QCD scale ($\Lambda_{\rm QCD}$), the mass of the b quark, m_b, the electroweak scale which is of the order of the masses of the W and Z bosons and the top quark, and higher scales of possible new physics. An important theoretical tool which allows for the description of separate scales as well as the convenient inclusion of NP effects, is operator product expansion (OPE). Within the OPE framework, the weak (and higher) scales are separated, leading to an effective weak Hamiltonian. This Hamiltonian is described in terms of effective operators and their associated effective couplings, referred to as Wilson coefficients. While all the short distance effects are contained in the Wilson coefficients, there are long distance contributions from the hadronic matrix elements of the effective operators. The long distance effects usually include non-perturbative QCD effects which are the major source of theoretical uncertainties.
In B decays, since $m_b \gg \Lambda_{\rm QCD}$, the otherwise troublesome long distance strong interaction effects are generally less important than for the lighter mesons and further simplifications are possible. Hence $b \to s$ and $b \to d$ quark level transitions are of great interest. However, the amplitude for $b \to d$ transitions are suppressed by a factor of $|V_{td}/V_{ts}|$ compared to $b \to s$ transition amplitudes, and current experimental results for $b \to d$ transitions are not yet at the level of precision to constrain NP effects. On the other hand, for $b \to s$ transitions, there are many results already available from past B-physics experiments such as CLEO, BaBar and Belle, as well as CDF and D0. The experimental results for exclusive B decays have recently made significant progress with the LHCb collaboration, thanks to the massive b-quark production at the LHC.

In particular, the LHCb has provided remarkable experimental results for two rare $b \to s$ transitions: the leptonic and semileptonic decays, $B_s \to \mu^+\mu^-$ and $B \to K^*\mu^+\mu^-$, respectively. The leptonic decay is free of hadronic final states, and hence theoretically cleaner. However, the only observable it provides is a branching ratio (BR). On the other hand, the semileptonic decay is theoretically more challenging as it has a hadron in its final state and requires information on $B \to K$ form factors. Nonetheless, with large enough statistics, this decay offers a variety of angular observables, in addition to the branching ratio. The angular observables can be designed to minimise the hadronic dependence. Moreover, they have different dependences on different Wilson coefficients, and can provide information on some of the Wilson coefficients which are otherwise not accessible from the branching ratio of the leptonic decay. All this renders the study of the semileptonic decay specially interesting.

In this thesis, we discuss the theoretical description of the $B_s \to \ell^+\ell^-$ and $B \to K^*\ell^+\ell^-$ decays. We present the Standard Model predictions and carefully estimate the theoretical errors. To demonstrate the NP effects in these decays, we consider one specific extension of the SM: supersymmetric models. In minimal supersymmetric standard model (MSSM), new particles such as charged Higgs, charginos and squarks can modify the predicted values of flavour changing observables. In particular we consider constrained MSSM (CMSSM) and study the implications of the recent measurements of $B \to K^*\mu^+\mu^-$ observables and update the constraints from BR($B_s \to \mu^+\mu^-$).

This thesis is organised as follows: in Chapter 2, we give a brief description of the Standard Model and address the topic of flavour changing neutral currents. Chapter 3 contains an overview of the minimal supersymmetric standard model (MSSM) , with possible FCNC contributions within the MSSM. In Chapter 4, we introduce the effective Hamiltonian within the operator product expansion framework. In Chapter 5, the generic effective Hamiltonian for $b \to s$ transitions is introduced. We later discuss the theoretical description of the $B \to K^* \ell^+ \ell^-$ decay, and present the associated observables along with the SM predictions, concentrating mostly on the large recoil region. We continue with the description of the $B_s \to \ell^+ \ell^-$ decay, and discuss the SM value for its branching ratio. In Chapter 6, we present recent LHCb results and discuss the effect of supersymmetric particles (within CMSSM) on the different Wilson coefficients. We later discuss the constraining power of BR($B_s \to \mu^+ \mu^-$) and $B \to K^* \mu^+ \mu^-$ observables on the parameters of the CMSSM and a less constrained model (NUHM). Finally in the last Chapter, we outline the most relevant aspects discussed in this thesis.

CHAPTER 2

Standard Model

In this chapter we give a brief description of the Standard Model (SM), focusing on the charged and neutral currents, as well as flavour changing neutral currents (FCNC) in the quark sector.

2.1 Standard Model with unbroken symmetry

The Standard Model [1] is a gauge theory invariant under the local symmetry group $SU(3)_c \times SU(2)_L \times U(1)_Y$, where $SU(3)$ describes the symmetries of the strong interactions, and $SU(2) \times U(1)$ the electroweak sector in the massless limit. The charges associated with $SU(2)$ and $U(1)$ are weak isospin (T) and hypercharge (Y), respectively. The hypercharge is defined by requiring the particles to have the correct charge according to the quasi-Gell-Man-Nishijima relation

$$Q = T_3 + \frac{Y}{2}, \tag{2.1}$$

where T_3 is the third component of the weak isospin. The L in $SU(2)_L$ corresponds to the fact that for fermions, only left-handed states transform nontrivially under weak isospin. Here, left- and right-handed, refers to the decomposition of Dirac four component spinors via the chirality projectors P_L and P_R

$$\psi_R = P_R\psi \equiv \frac{1+\gamma_5}{2}\psi, \qquad \psi_L = P_L\psi \equiv \frac{1-\gamma_5}{2}\psi. \tag{2.2}$$

The different behaviour of left- and right-handed particles under $SU(2)_L$ transformations is addressed by writing the left-handed particles as doublets (Q, L), and the right-handed ones as singlets (D, U, E), as given in Table 2.1.
The free field Lagrangian, constructed only with the fermion fields, does not preserve local gauge invariance, due to the appearance of derivative terms of the type $(\partial_\mu\psi)$.

Fields	$SU(3)_c \times SU(2)_L \times U(1)_Y$	Q	T_3
Fermion lepton fields			
$L \equiv \begin{pmatrix} \nu'_L \\ \ell'_L \end{pmatrix}$	$(1, 2, -1)$	$\begin{pmatrix} 0 \\ -1 \end{pmatrix}$	$\begin{pmatrix} 1/2 \\ -1/2 \end{pmatrix}$
$E \equiv \ell'_R$	$(1, 1, -2)$	-1	0
Fermion quark fields			
$Q \equiv \begin{pmatrix} u'_L \\ d'_L \end{pmatrix}$	$(3, 2, 1/3)$	$\begin{pmatrix} 2/3 \\ -1/3 \end{pmatrix}$	$\begin{pmatrix} 1/2 \\ -1/2 \end{pmatrix}$
$U \equiv u'_R$	$(3, 1, 4/3)$	$2/3$	0
$D \equiv d'_R$	$(3, 1, -2/3)$	$-1/3$	0
Gauge fields			
B_μ	$(1, 1, 0)$		
$W^a_\mu, (a = 1, 2, 3)$	$(1, 3, 0)$		
$G^a_\mu, (a = 1, \ldots, 8)$	$(8, 1, 0)$		
Scalar field			
$\Phi \equiv \begin{pmatrix} \phi^+ \\ \phi^0 \end{pmatrix}$	$(1, 2, 1)$	$\begin{pmatrix} 1 \\ 0 \end{pmatrix}$	$\begin{pmatrix} 1/2 \\ -1/2 \end{pmatrix}$

Table 2.1.: Gauge, fermion and scalar fields of the SM. The fermion fields each appear in three generations: (e, μ, τ) for the charged lepton fields (and corresponding ν_e, ν_μ, ν_τ), and (u, c, t) and (d, s, b) for the up- and down-type quarks, respectively.

The Lagrangian can be made locally gauge invariant by introducing spin 1 gauge fields, coupling minimally to the fermion fields by the replacement of ∂_μ with

$$D_\mu = \partial_\mu + ig_1 B_\mu \frac{Y}{2} + ig_2 W_\mu^a \tau^a + ig_s G_\mu^a T^a. \tag{2.3}$$

Here, g_1, g_2 and g_s are the coupling constants associated with $U(1)_Y, SU(2)_L$ and $SU(3)_c$, respectively, indicating the strength with which the gauge fields couple to the fermion fields. The gauge fields B_μ, $W_\mu^a (a = 1, 2, 3)$ and $G_\mu^a (a = 1, \cdots, 8)$ are respectively associated with the symmetries $U(1)_Y, SU(2)_L$ and $SU(3)_c$, while τ^a and T^b are the generators of the latter. For these generators we use

$$\tau^a = \frac{\sigma^a}{2}, \qquad\qquad T^a = \frac{\lambda^a}{2}, \tag{2.4}$$

where σ^a and λ^a are the Pauli and Gell-Mann matrices, respectively. The Lagrangian, including fermion and gauge fields then becomes

$$\mathcal{L}_{\text{Fermion-Gauge}} = \bar{Q} i\gamma^\mu D_\mu Q + \bar{U} i\gamma^\mu D_\mu U + \bar{D} i\gamma^\mu D_\mu D + \bar{L} i\gamma^\mu D_\mu L + \bar{E} i\gamma^\mu D_\mu E, \tag{2.5}$$

where summation over the three generations for both lepton and quarks is implied.

In order for the gauge fields to become dynamical, the locally gauge invariant kinetic terms must be added

$$\mathcal{L}_{\text{Kinetic Gauge}} = -\frac{1}{4} B_{\mu\nu} B^{\mu\nu} - \frac{1}{4} W_{\mu\nu}^a W^{a,\mu\nu} - \frac{1}{4} G_{\mu\nu}^a G^{a,\mu\nu}. \tag{2.6}$$

Here $B_{\mu\nu}, W_{\mu\nu}^a$ and $G_{\mu\nu}^a$ are the field strength tensors

$$B_{\mu\nu} = \partial_\mu B_\nu - \partial_\nu B_\mu, \tag{2.7}$$
$$W_{\mu\nu}^a = \partial_\mu W_\nu^a - \partial_\nu W_\mu^a - g_2 \epsilon^{abc} W_\mu^b W_\nu^c, \tag{2.8}$$
$$G_{\mu\nu}^a = \partial_\mu G_\nu^a - \partial_\nu G_\mu^a - g_s f^{abc} G_\mu^b G_\nu^c, \tag{2.9}$$

where ϵ^{abc} and f^{abc} are the structure constants of $SU(2)_L$ and $SU(3)_c$, respectively.

Dirac mass terms for the fermions ($m\bar{\psi}\psi = m\bar{\psi}_L\psi_R + m\bar{\psi}_R\psi_L$) are not allowed in the SM Lagrangian since left- and right-handed fermions transform differently under $SU(2)_L$. Moreover, local gauge invariance requires all the gauge bosons to be massless. This is obviously at odds with observation and can be successfully addressed via spontaneous breaking of the $SU(2)_L \times U(1)_Y$ symmetry.

2.2 Mass terms of the SM Lagrangian

Spontaneous symmetry breaking

Mass terms can be included into the Lagrangian through the Englert-Brout-Higgs mechanism [2] by introducing a scalar $SU(2)_L$ doublet

$$\Phi = \begin{pmatrix} \phi^+ \\ \phi^0 \end{pmatrix} = \begin{pmatrix} \frac{1}{\sqrt{2}}(\phi^3 + i\phi^4) \\ \frac{1}{\sqrt{2}}(\phi^1 + i\phi^2) \end{pmatrix}. \tag{2.10}$$

In the above, ϕ^+ and ϕ^0 are both complex fields and the superscripts denote their electric charges; alternatively they can be written in terms of four real scalar fields $\phi^{1...4}$. Considering that the scalar potential has a renormalisable (Mexican hat) form

$$V(\Phi) = -\mu^2 \Phi\Phi^\dagger + \lambda(\Phi\Phi^\dagger)^2, \tag{2.11}$$

and provided that $\lambda, \mu^2 > 0$, the lowest energy classical solution for the scalar field (Φ_0) becomes nonzero. For the vacuum expectation value (VEV) of the scalar field we then have

$$\langle \Phi_0^\dagger \Phi_0 \rangle = \frac{\mu^2}{2\lambda} \equiv \frac{v^2}{2}. \tag{2.12}$$

This is known as spontaneous symmetry breaking (SSB), where the Lagrangian is invariant under the gauge transformations, but the vacuum state is not. A particular gauge can be chosen in such a way that three of the four real degrees of freedom of the scalar doublet vanish ($\phi^2 = \phi^3 = \phi^4 = 0$), hence for the ground state we find

$$\langle \Phi_0 \rangle = \begin{pmatrix} 0 \\ \frac{v}{\sqrt{2}} \end{pmatrix}. \tag{2.13}$$

For excitations above the vacuum, the scalar field can be written as

$$\Phi = \begin{pmatrix} \phi^+ \\ \frac{v+h+i\phi^2}{\sqrt{2}} \end{pmatrix}, \tag{2.14}$$

where $h(x) = \phi^1(x) - v$. Using the local symmetry, different $SU(2)_L$ transformations may be performed at each point in space so that Φ gets reduced to[1]

$$\Phi = \begin{pmatrix} 0 \\ \frac{v+h(x)}{\sqrt{2}} \end{pmatrix}. \tag{2.15}$$

The scalar field coupling to the fermion and gauge fields further gives rise to mass terms.

[1] The unphysical scalars, $\phi_{2,3,4}$ are the would-be Goldstone bosons, absorbed as the longitudinal degrees of freedom of the weak bosons.

Gauge fields mass terms

The scalar field couples the the gauge fields in a gauge invariant way as follows

$$\mathcal{L}_{\text{Scalar-Gauge}} = (D_\mu\Phi)^\dagger(D^\mu\Phi) - V(\Phi) = (D_\mu\Phi)^\dagger(D^\mu\Phi) + \mu^2\Phi\Phi^\dagger - \lambda(\Phi\Phi^\dagger)^2, \tag{2.16}$$

with D_μ given in (2.3). Considering Φ as mentioned in (2.15), from the above Lagrangian one can obtain the mass terms for the weak gauge bosons

$$(D_\mu\Phi)^\dagger(D_\mu\Phi) = \frac{1}{2}(\partial_\mu h)^2 + \frac{g_2^2v^2}{8}\left[(W_\mu^1)^2 + (W_\mu^2)^2\right] + \frac{v^2}{8}\left[g_2W_\mu^3 - g_1B_\mu\right]^2 + \cdots . \tag{2.17}$$

The gauge fields mass eigenstates are related to the interaction ones as

$$W_\mu^\pm = \frac{1}{\sqrt{2}}(W_\mu^1 \mp iW_\mu^2), \qquad \begin{pmatrix} A_\mu \\ Z_\mu \end{pmatrix} = \begin{pmatrix} \cos\theta_W & \sin\theta_W \\ -\sin\theta_W & \cos\theta_W \end{pmatrix}\begin{pmatrix} B_\mu \\ W_\mu^3 \end{pmatrix}, \tag{2.18}$$

where $W^\pm$ and Z_μ are the charged and neutral fields associated with the weak bosons and θ_W is the Weinberg angle defined via

$$\cos\theta_W = \frac{g_2}{(g_1^2+g_2^2)^{1/2}}, \qquad \sin\theta_W = \frac{g_1}{(g_1^2+g_2^2)^{1/2}}. \tag{2.19}$$

A_μ corresponds to photon with the electromagnetic coupling constant

$$e = g_1\cos\theta_W = g_2\sin\theta_W. \tag{2.20}$$

Finally, the masses of $W_\mu^\pm$ and Z_μ can be written as

$$M_{W^\pm} = \frac{g_2v}{2}, \qquad M_Z = \frac{(g_1^2+g_2^2)^{1/2}v}{2}, \tag{2.21}$$

while the gauge field of the photon remains massless ($M_A = 0$).
The mentioned process is known as electroweak symmetry breaking (EWSB) and can be expressed as $SU(2)_L \times U(1)_Y \to U(1)_{EM}$, since the $U(1)$ to which the photon corresponds remains unbroken.

Fermion fields mass terms

Moreover, fermion fields couple to the scalar field and obtain mass terms

$$\mathcal{L}_{\text{Scalar-Fermion}} = -\sum_{i,j}\left(\bar{Q}_i(Y^u)_{ij}U_j\Phi^c + \bar{Q}_i(Y^d)_{ij}D_j\Phi + \bar{L}_i(Y^e)_{ij}E_j\Phi\right) + h.c., \tag{2.22}$$

with,

$$\Phi^c = i\sigma^2\Phi^*, \tag{2.23}$$

and i, j denote the three generations of fermions. The couplings of the scalar field to the fermion fields are referred to as Yukawa couplings (Y^u, Y^d, Y^e) which are 3×3 complex matrices.[2]

Upon EWSB, the scalar VEV (v) produces quadratic mass terms in $\mathcal{L}_{\text{SF}}$ (2.22), which in the gauge basis (primed) can be expressed as

$$\mathcal{L}_{\text{Scalar-Fermion}} \to \mathcal{L}_{\text{mass}} = -\bar{u}'_{R_i} M^{U\prime}_{ij} u'_{L_j} - \bar{d}'_{R_i} M^{D\prime}_{ij} d'_{L_j} - \bar{e}'_{R_i} M^{E\prime}_{ij} e'_{L_j} + h.c., \tag{2.24}$$

with

$$M'_U = \frac{v^2}{\sqrt{2}}(Y^u)^T, \qquad M'_D = \frac{v^2}{\sqrt{2}}(Y^d)^T, \qquad M'_E = \frac{v^2}{\sqrt{2}}(Y^e)^T. \tag{2.25}$$

In general the Yukawa couplings, and hence the mass matrices, are not diagonal. The mass matrices can be diagonalised via unitary field transformations that relate the interaction (primed) and physical mass basis (unprimed) as follows

$$\begin{aligned} &u_L = V^u_L u'_L, \qquad u_R = V^u_R u'_R, \qquad d_L = V^d_L d'_L, \qquad d_R = V^d_R d'_R, \\ &e_L = V^e_L e'_L, \qquad e_R = V^e_R e'_R. \end{aligned} \tag{2.26}$$

The mass matrices then become diagonal

$$\begin{aligned} &M_U = V^u_R M'_U V^{u\dagger}_L = \text{diag}(m_u, m_c, m_t), \quad M_D = V^d_R M'_D V^{d\dagger}_L = \text{diag}(m_d, m_s, m_b), \\ &M_E = V^e_R M'_E V^{e\dagger}_L = \text{diag}(m_e, m_\mu, m_\tau). \end{aligned} \tag{2.27}$$

In summary, the Standard Model Lagrangian can be written as

$$\mathcal{L} = \mathcal{L}_{\text{FG}} + \mathcal{L}_{\text{KG}} + \mathcal{L}_{\text{SG}} + \mathcal{L}_{\text{SF}}, \tag{2.28}$$

where $\mathcal{L}_{\text{FG}}, \mathcal{L}_{\text{KG}}, \mathcal{L}_{\text{SG}}$ and $\mathcal{L}_{\text{SF}}$ are given in (2.5),(2.6),(2.16) and (2.22) respectively.

2.3 Quark interactions

In this work we are mostly interested in flavour changing neutral current (FCNC) processes in the quark sector; the rest of this Chapter will thus be focused on flavour violating interactions and processes in the quark sector.

[2] In the SM, as originally proposed, no ν_R is present, and neutrinos remain massless.

Charged current interactions

Using the $SU(2)_L \times U(1)_Y$ formulation introduced above, the charged part of the interaction Lagrangian for the quark sector in $\mathcal{L}_{\rm FG}$ can be written as

$$\mathcal{L}_{\text{Charged Current}} = -\frac{g_2}{\sqrt{2}} J^{+\mu} W_\mu^+ + h.c., \tag{2.29}$$

with the charged current given by

$$\begin{aligned} J^{+\mu} &= \sum_i \bar{u}'_{L_i} \gamma^\mu d'_{L_i}, = \begin{pmatrix} \bar{u}'_L & \bar{c}'_L & \bar{t}'_L \end{pmatrix} \gamma^\mu \begin{pmatrix} d'_L \\ s'_L \\ b'_L \end{pmatrix} W_\mu^+ \\ &= -\frac{g_2}{\sqrt{2}} \begin{pmatrix} \bar{u}_L & \bar{c}_L & \bar{t}_L \end{pmatrix} \gamma^\mu \left(V_L^u V_L^{d\dagger} \right) \begin{pmatrix} d_L \\ s_L \\ b_L \end{pmatrix} W_\mu^+ , \end{aligned} \tag{2.30}$$

where the first line corresponds to the interaction basis while and the second line is cast in the mass basis; moreover, $J^{-\mu} = (J^{+\mu})^\dagger$. The matrix $(V_L^u V_L^{d\dagger})$ is the so called Cabibbo-Kobayashi-Maskawa (CKM) matrix [3, 4]. In general, both the up- and down-type gauge eigenstates are different from the mass eigenstates. However, either the up- or down-type quarks can be chosen in such a way that they are the same in both mass and gauge basis. Usually it is the up-type quarks that are considered to be the same ($V_L^u \equiv \mathbb{1}$), in this case the down-type gauge eigenstates (d', s', b') are related to the mass eigenstates (d, s, b) via the CKM matrix ($V_L^d \equiv V_{\rm CKM}$)

$$\begin{pmatrix} d'_L \\ s'_L \\ b'_L \end{pmatrix} = V_{\rm CKM} \begin{pmatrix} d_L \\ s_L \\ b_L \end{pmatrix} = \begin{pmatrix} V_{ud} & V_{us} & V_{ub} \\ V_{cd} & V_{cs} & V_{cb} \\ V_{td} & V_{ts} & V_{tb} \end{pmatrix} \begin{pmatrix} d_L \\ s_L \\ b_L \end{pmatrix}. \tag{2.31}$$

The CKM matrix is a unitary 3×3 matrix, as it is the product of two unitary matrices. It can be parametrised by three mixing angles and one complex phase which means it can be viewed as an Eulerian construction of three rotation matrices and a phase matrix. The standardised parametrisation of the Particle Data Group (GDP) is of this sort. There are other parametrisations of $V_{\rm CKM}$; an approximate form of $V_{\rm CKM}$ due to Wolfenstein [5]

$$V_{\rm CKM} = \begin{pmatrix} 1 - \frac{1}{2}\lambda^2 & \lambda & A\lambda^3(\rho - i\eta) \\ -\lambda & 1 - \frac{1}{2}\lambda^2 & A\lambda^2 \\ A\lambda^3(1 - \rho - i\eta) & -A\lambda^2 & 1 \end{pmatrix} + \mathcal{O}(\lambda^4), \tag{2.32}$$

separates a Cabibbo suppression parameter $\lambda \sim 0.22$, from $\mathcal{O}(1)$ parameters (A, ρ) and a phase (η). Within this approximate representation, the unitarity of $V_{\rm CKM}$ only holds up to corrections of $\mathcal{O}(\lambda^4)$. Nonetheless, in the SM the unitarity of $V_{\rm CKM}$ is exact. The

unitarity relations for the CKM matrix can be written as

$$\sum_{k=u,c,t} V_{ki}^* V_{kj} = \delta_{ij}, \qquad i,j = d,s,b. \tag{2.33}$$

The fact that the CKM matrix is not diagonal results in tree level flavour changing charged current (FCCC) processes.

Neutral current interactions

While the misalignment between interaction and mass eigenstates results in FCCC processes, neutral currents do not give rise to flavour changing processes. In the interaction basis, considering (2.5), neutral current interactions among quarks are given by terms $\propto g_1 \bar{q}'_{L(R)} \gamma^\mu q'_{L(R)} B_\mu$ and $g_2 \bar{q}'_L \gamma^\mu q'_L W^3_\mu$ with $q = u, d$. However, expressed in the quark mass basis, the primes can simply be removed since the rotation matrices are unitary ($V^q_{L(R)} V^{q\dagger}_{L(R)} = \mathbb{1}$). For completeness, the neutral part of interactions among quarks in the mass basis are given below

$$\mathcal{L}_{\text{Neutral Current}} = -e J^\mu_{\text{em}} A_\mu - \frac{e}{\sin\theta_W \cos\theta_W} \left(J^\mu_3 - \sin^2\theta_W J^\mu_{\text{em}} \right) Z_\mu, \tag{2.34}$$

where the neutral currents are

$$J^\mu_{\text{em}} = \sum_i Q^a \left(\bar{u}_{L_i} \gamma^\mu u_{L_i} + \bar{u}_{R_i} \gamma^\mu u_{R_i} \right) + Q^d \left(\bar{d}_{L_i} \gamma^\mu d_{L_i} + \bar{d}_{R_i} \gamma^\mu d_{R_i} \right), \tag{2.35}$$

$$J^\mu_3 = \sum i T^u_3 \bar{u}_{L_i} \gamma^\mu u_{L_i} + T^d_3 \bar{d}_{L_i} \gamma^\mu d_{L_i}. \tag{2.36}$$

Here Q^q and T^q_3 denote the charge and third component of the isospin of the quarks, respectively. The relevant charges for the fields can be found in Table 2.1.

2.4 FCNCs in the Standard Model

As mentioned, tree level FCNCs are not allowed in the SM, nonetheless, at the loop level they can appear through the so called penguin[3] and box diagrams[4] as shown in Figure 2.1. However, these processes are very rare in the SM due to GIM and CKM suppressions. It is possible to have FCNCs both for external up-type quark transitions (e.g. $b \to s$) and down-type ones (e.g. $c \to u$).

[3] The etymology of this diagram is described in [6].

[4] Notice these are 4-point functions; loop corrections to 2-point function FCNCs between on-shell quarks are reabsorbed by renormalising the quark fields and mass terms.

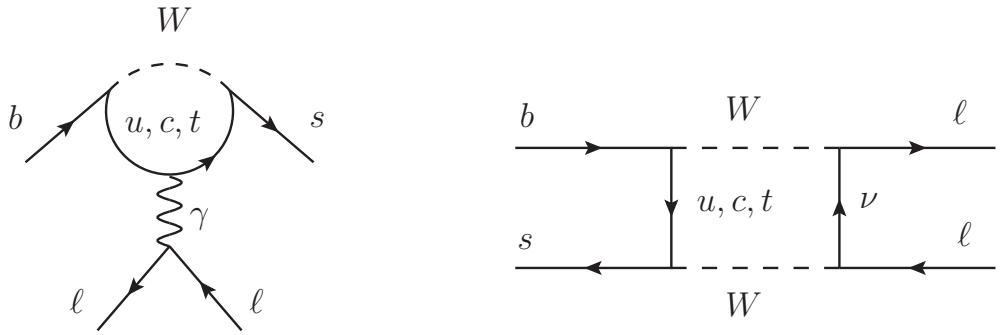

Figure 2.1.: Typical FCNC penguin and box diagrams for $b \to s\ell\ell$ transitions.

Down-type FCNCs

For instance, in the case of $b \to s$ transitions, the relevant one-loop amplitude can schematically be expressed as

$$\mathcal{M} = V_{ub}V_{us}^* \ F(m_u^2/M_W^2) + V_{cb}V_{cs}^* \ F(m_c^2/M_W^2) + V_{tb}V_{ts}^* \ F(m_t^2/M_W^2), \tag{2.37}$$

where $F(m_i^2/M_W^2)$ are Inami-Lim loop functions [7]. If all the up-type quark masses were degenerate, these functions could be factored out, and from the unitarity relation (2.33)

$$V_{ub}V_{us}^* + V_{cb}V_{cs}^* + V_{tb}V_{ts}^* = 0, \tag{2.38}$$

the amplitude would vanish. This is known as "GIM cancellation", named after Glashow, Iliopoulos and Maiani [8]. However, due the large mass difference between the top quark and the charm and up quarks, $b \to s$ transitions are not highly GIM suppressed.

Up-type FCNCs

By the same argument, the GIM suppression is very efficient for the the up-type FCNCs, since the down-type quarks appearing in the loops are much more degenerate in mass, than the up-type quarks. Hence FCNCs are more "visible" i.e. likely to be experimentally observed in the down sector.

Overall, both the GIM and CKM suppressions, embedded in the structure of the SM, play an important part in limiting the size of FCNC processes. On the other hand, new physics, present at some high energy scale Λ, can introduce additional sources of FCNCs. In our work we consider supersymmetry as the new physics model. A brief description of the minimal supersymmetric standard model and possible new sources of FCNCs are given in the next chapter.

CHAPTER 3

Minimal Supersymmetric Standard Model

In recent years many experiments have tested the Standard Model (SM) of electroweak and strong interactions to unprecedented accuracy. So far, the SM has provided a remarkably successful description of the observed particles and their interactions. Nevertheless, the SM is not the ultimate theory of fundamental particles and their interactions. To understand why this is so, let us first point out that although being able to interpret and account for the experimental data, the SM does not explain fundamental issues, like the particle quantum numbers, such as electric charge, weak isospin, hypercharge and colour, and contains 19 arbitrary parameters. The latter include three gauge couplings, one CP violating strong interaction parameter, six quark and three charged lepton masses, three weak mixing angles, one CP violating phase, and two independent masses for a weak boson and a scalar.
Moreover, we are yet to understand the reasons behind the choice of the $SU(3)_c \times SU(2)_L \times U(1)_Y$ gauge group, the existence of three chiral families, and the mixings of the different quark flavours under weak interactions. The SM also offers little insight into the true nature of electroweak symmetry breaking processes, and the generation of mass – the Brout-Englert-Higgs mechanism [2].
At energies above the Planck scale, quantum gravitational effects become significant, and the SM must necessarily be replaced by a more fundamental theory that incorporates gravity. It is also conceivable that the SM breaks down at an intermediate scale, so that the SM degrees of freedom are no longer appropriate to describe physics above that scale and new physics (NP) must enter. Note that these scales are separated by several orders of magnitude, in particular 17 orders of magnitude spread between the weak and the Planck scales. This introduces another fundamental issue: the understanding of the gap between the two major energy scales of the four fundamental interactions. This is usually referred to as the hierarchy problem: why the weak scale is so small when compared to the Planck scale, $M_P \simeq 10^{19}$GeV, or equivalently why the Newton constant is so much smaller than the Fermi constant $G_N \ll G_F$. Since in the SM there is no mechanism to protect the mass of a scalar boson (chiral and gauge symmetries protect fermion and gauge boson masses), radiative corrections to the Higgs mass can be arbitrarily large, since

$\delta m_H^2 = \mathcal{O}(\alpha/\pi)\,\Lambda^2$, where Λ is an ultraviolet cut-off scale that reflects the appearance of new physics beyond the SM. By adjusting the Lagrangian counterterm so to cancel this large quantum correction, one can bring down the renormalised Higgs mass to the electroweak scale. Note that this cancellation must be done order-by-order, and amounts to a fine-tuning of one part in 10^{32}. Such an unnatural cancellation is in the very heart of the hierarchy problem and it poses a serious problem to any theory which aims at naturalness as a guiding principle.
In summary, the standard model of electroweak interactions is not a fundamental theory. At best it is an effective field theory, that provides an extremely good description of all observable low energy phenomena. One of the most acclaimed candidates for a theory that naturally includes the SM and establishes a bridge to gravity is supersymmetry or "SUSY" for short.

3.1 Supersymmetry

The basic idea of supersymmetry is the existence of transformations that convert a bosonic state into a fermionic state and vice-versa. These transformations are generated by an operator Q, that relates bosons and fermions,

$$Q\,|\text{Boson}\rangle = |\text{Fermion}\rangle\,, \qquad Q\,|\text{Fermion}\rangle = |\text{Boson}\rangle\,. \tag{3.1}$$

The Hermitian conjugate of Q, $Q^\dagger$, can be shown to be a distinct symmetry generator. Note that Q and $Q^\dagger$ are fermionic operators, which means that they carry spin angular momentum 1/2, so it is clear that in addition to being an internal symmetry, SUSY must be a spacetime symmetry. In this case the Poincaré group of spacetime transformations is extended to Q and $Q^\dagger$.
As first noticed by Wess and Zumino [9], SUSY evades the Coleman-Mandula no-go theorem [10], which states that one cannot mix internal and spacetime symmetries, if the spin of the new symmetry generators are integer. The Haag-Lopuzanski-Sohnius extension of the theorem [11] shows that the no-go condition can be evaded with half-integer spins, provided the generators Q and $Q^\dagger$ satisfy an algebra of commutation relations that has the schematic form:

$$\{Q, Q^\dagger\} = P^\mu\,, \quad \{Q, Q\} = \{Q^\dagger, Q^\dagger\} = 0\,, \qquad [P^\mu, Q] = [P^\mu, Q^\dagger] = 0\,. \tag{3.2}$$

The appearance of the momentum generator of spacetime translations, P^μ, on the right hand side of the first equation is not surprising, since it transforms under Lorentz boosts and rotations as a spin-1 object, while Q and $Q^\dagger$ are spin-1/2 objects. Introducing the Weyl two-component spin notation (see for example [12]), let us summarise explicitly the algebra of the SUSY generators:

$$\begin{aligned} &\{Q_\alpha, Q_\beta\} = \{\bar{Q}_{\dot\alpha}, \bar{Q}_{\dot\beta}\} = 0\,, \qquad \{Q_\alpha, \bar{Q}_{\dot\beta}\} = 2\,(\sigma^\mu)_{\alpha\dot\beta}\,P_\mu\,, \\ &[P^\mu, Q_\alpha] = 0\,, \qquad [M^{\mu\nu}, Q_\alpha] = -i\,(\sigma^{\mu\nu})_\alpha{}^\beta\,Q_\beta\,, \end{aligned} \tag{3.3}$$

where $M^{\mu\nu}$ is the 4-angular momentum tensor and $\overset{(.)}{\alpha}$ and $\overset{(.)}{\beta}$ are Weyl spinor indices running from 1 to 2.

In order to reconcile Special Relativity and Quantum Mechanics, Dirac postulated a doubling of states, by introducing an antiparticle for each particle. The generators Q have a similar effect, causing a further splitting into particle and superparticle (or "sparticle"). Due to the spinorial nature of Q, the superpartners differ the SM partners in spin, by an amount of 1/2. Each fermion and sfermion (a scalar), as well as each gauge boson and gaugino (a fermion) are joined together to form irreducible representations of the algebra, called supermultiplets. Each supermultiplet contains both fermion and boson states, which can be related one to the other by means of some combination of the generators, up to a spacetime translation or rotation.

Since the squared-mass operator P^2 commutes with Q and $Q^\dagger$, as well as with all spacetime and translation operators, it follows that the members of a supermultiplet must have the same eigenvalue of P^2, that is, the same mass.

The anticommutation of Q and $Q^\dagger$ with the operator $(-1)^{2s}$ where s is the spin angular momentum, results in the number of bosonic degrees of freedom (n_B) to be equal to the number of fermionic degree of freedom (n_F), for a supermultiplet. Depending on the number of distinct copies of supersymmetry generators Q and $Q^\dagger$, supermultiplets can be written as various combinations of particle with spins that satisfy $n_F = n_B$. If the interactions are to be renormalisable and there is only one supersymmetry generator ($N = 1$ supersymmetry), the supermultiplets can be written as chiral and gauge supermultiplets. The chiral (matter) supermultiplet consists of a two-component Weyl fermion and a complex scalar field called the sfermion. The vector (gauge) supermultiplet consists of a massless spin-1 gauge boson and a massless spin-1/2 Weyl fermion called the gaugino. For both of these multiplets $n_F = n_B = 2$. The superpartners within a supermultiplet differ in spin by 1/2 unit.

In the first page of this Chapter, we have mentioned a number of unsettling issues of the SM. Although SUSY does not offer an answer to all of them, supersymmetric extensions of the SM do manage to provide a viable and elegant solution to many of those issues. Let us discuss a few examples:

Hierarchy problem

The hierarchy problem [13, 14] is related to the large radiative corrections to the Higgs boson mass. To overcome the associated fine-tuning problem, one requires a mechanism that acts in the same fashion as gauge and chiral symmetries in protecting the gauge boson and fermion masses. In particular, quantum corrections to fermion masses are only logarithmically sensitive to the cut-off scale Λ. If SUSY was an exact symmetry, then both elements of a chiral multiplet would have the same mass (radiative effects included). Since the Higgs boson would be associated with a higgsino (fermion), it would display an analogous logarithmic sensitivity to Λ. In particular, since the couplings and the masses of the particles entering the radiative corrections are the same, but fermion and scalar loops contribute with opposite sign, the corrections would vanish. Given that no sparticle has yet been observed, we have good reasons to believe that SUSY is in

fact broken. In this case, we have non-vanishing, yet mild corrections to the Higgs mass ($\delta m_H^2 = \mathcal{O}(\alpha/\pi)\ \delta m^2$, where δm^2 would be the mass splitting between partners and spartners). In particular, if the masses of the superpartners are in the TeV range, a Higgs mass around the electroweak breaking scale can be naturally obtained, without any miraculous cancellations.

It is worth mentioning that even though SUSY was not originally developed having in view a solution to the hierarchy problem, the fact that SUSY eliminates many divergences in certain quantum field theories became one of its most attractive and motivating aspects: it is only one of the many theoretical virtues of building maximal extensions of the Poincaré algebra.

Unification of gauge couplings

Although perhaps accidental, this feature has often been identified as the only quantitative prediction (or even as the only s-experimental hint) of supersymmetry, and is related to the strengths of the different interactions. In Grand Unified theories (GUT), the energy-scale evolution of the three gauge couplings is such that they should meet in one common point at some large energy. In a theory of particle physics, the behaviour of a parameter as a function of the energy scale is given by the renormalisation group equations (RGE), and these depend on the specific model being considered. If we take the SM RGEs, the requirement of unification at some high energy scale would translate into a low-energy measurement of the Weinberg weak mixing angle, $\sin^2\theta_W = 0.214 \pm 0.004$, that would not be compatible with the current experimental value, $\sin^2\theta_W = 0.23116 \pm 0.00012$ [15]. Including SUSY in the RGEs, the couplings unify at a scale around 2×10^{16} GeV [16] safe from the experimental lower limit on the lifetime of the proton, and the low-energy value of $\sin^2\theta_W$ predicted by minimal SUSY GUTs is $\sin^2\theta_W \sim 0.232$, in fair agreement with the experiment. Note that the SUSY prediction depends on the value of the sparticle masses, that were here estimated to be in the $0.1 \to 10$ TeV range.

Spontaneous electroweak symmetry breaking

As we will discuss at a later stage, in minimal SUSY models we have necessarily at least two Higgs doublets. In the presence of a heavy top quark, radiative corrections to the mass of the Higgs associated with the up-quark sector induce its running from a positive value at the ultraviolet scale, down to negative values in the infrared, thus triggering electroweak symmetry breaking (see, for example [17]). Unlike in the SM, where the negative value of the squared scalar mass is put by hand, in SUSY we have a natural framework for the radiative breaking of $SU(2)_L \times U(1)_Y$. From a wider perspective, SUSY also provides a symmetry argument for the necessary existence of fundamental scalar doublets, whose existence is now established.

3.2 MSSM

3.2.1 Particle content

The minimal supersymmetric extension of the standard model (MSSM) [17–19] consists of taking the SM particles, and adding the corresponding SUSY partners, so that a gauge or matter supermultiplet is formed. In Table 3.1, we summarise the MSSM superfield content, splitting the multiplets, which are denoted by a hat superscript, into their fermionic and bosonic components, and presenting their common gauge quantum numbers.

Superfields	Boson Fields	Fermionic Partners	$SU(3)_c \times SU(2)_L \times U(1)_Y$
Gauge Multiplets			
$\hat{B}$	B	$\tilde{B}$	$(1,1,0)$
$\hat{V}$	W	$\tilde{W}$	$(1,3,0)$
$\hat{G}$	g	$\tilde{g}$	$(8,1,0)$
Matter Multiplets			
$\hat{L}$	$\tilde{L} \equiv \begin{pmatrix} \tilde{\nu}_L \\ \tilde{\ell}_L \end{pmatrix}$	$L \equiv \begin{pmatrix} \nu_L \\ \ell_L \end{pmatrix}$	$(1,2,-1)$
$\hat{E}$	$\tilde{E} \equiv \tilde{\ell}_R^*$	$E \equiv (\ell_R)^c$	$(1,1,+2)$
$\hat{Q}$	$\tilde{Q} \equiv \begin{pmatrix} \tilde{u}_L \\ \tilde{d}_L \end{pmatrix}$	$Q \equiv \begin{pmatrix} u_L \\ d_L \end{pmatrix}$	$(3,2,1/3)$
$\hat{U}$	$\tilde{U} \equiv \tilde{u}_R^*$	$U \equiv (u_R)^c$	$(3^*,1,-4/3)$
$\hat{D}$	$\tilde{D} \equiv \tilde{d}_R^*$	$D \equiv (d_R)^c$	$(3^*,1,2/3)$
$\hat{H}_1$	$H_1 \equiv \begin{pmatrix} H_1^0 \\ H_1^- \end{pmatrix}$	$\tilde{H}_1 \equiv \begin{pmatrix} \tilde{H}_1^0 \\ \tilde{H}_1^- \end{pmatrix}$	$(1,2,-1)$
$\hat{H}_2$	$H_2 \equiv \begin{pmatrix} H_2^+ \\ H_2^0 \end{pmatrix}$	$\tilde{H}_2 \equiv \begin{pmatrix} \tilde{H}_2^+ \\ \tilde{H}_2^0 \end{pmatrix}$	$(1,2,+1)$

Table 3.1.: Gauge and matter supermultiplets of the MSSM.

Note that in Table 3.1 we listed the interaction eigenstates, and not the physical particles, and we did not consider flavour or colour dependence. Two Higgs supermultiplets were introduced in the superfield content. This is done to ensure the cancellation of the anomalies induced by chiral fermion partners, and to give mass to both up and down quarks, without violating the analytical properties of the superpotential. It should be stressed that all the SM fermions are chiral, which means that the left parts of the fields interact differently from the right parts. Hence they can only be members of the chiral supermultiplet.

It is also worth emphasising that all supersymmetric partners are indeed new particles, and cannot be identified with any of the original SM bosons or fermions. Originally, and

from the comparison of the quantum numbers, it was attempted to assign the sneutrino and one of the Higgs scalars as members of the same supermultiplet [20]. Although an appealing attempt, it was soon realised that it would not work; even ignoring the problem of anomaly cancellation, phenomenological inconsistencies were present, like sizable lepton number violation, and a large mass for one of the neutrinos.

Regarding the labeling of these new particles, we have a spin-1/2 gluino $\tilde{g}$ as the spartner of the $SU(3)_c$ gluon. In association with the electroweak gauge symmetry spin-1 bosons, we have the spin-1/2 superpartners $\tilde{W}^0$, $\tilde{W}^{\pm}$ and $\tilde{B}^0$, called Winos and Bino, respectively. After electroweak symmetry breaking the mixtures of $\tilde{W}^0$ and $\tilde{B}^0$ give mass eigenstates zino $\tilde{Z}^0$ and photino $\tilde{\gamma}$. The Higgs spartners are labeled higgsinos, and symbolically denoted $\tilde{H}_i^{0,\pm}$, or $\tilde{h}_i^{0,\pm}$. Depending on the SUSY breaking Lagrangian (discussed later in the text) the neutral components mix with the neutral Bino and Wino, and give rise to the physical neutralinos $\tilde{\chi}^0$, while the admixture of the charged components with the charged winos forms the physical charginos $\tilde{\chi}^{\pm}$. The fermionic and leptonic matter content finds its superpartners in the squarks, sleptons and sneutrinos.

In general, supersymmetric extensions of the SM can have gauge invariant interactions that violate baryon and lepton numbers. This leads to some disturbing results such as unacceptably fast proton decay. To avoid these types of phenomenological results, the MSSM is postulated to preserve a new symmetry called R-parity. The R-parity is a multiplicative quantum number

$$P_R = (-1)^{3(B-L)+2s}, \tag{3.4}$$

where s refers to the spin and B and L are the baryon and lepton number, respectively. All the SM particles and the Higgs bosons have even R-parity ($P_R = +1$), while their supersymmetric partners have odd R-parity ($P_R = -1$). The fact that the MSSM is R-parity conserving leads to useful phenomenological results. All supersymmetric particles are produced in pairs and the lightest supersymmetric particle (LSP) is automatically stable. The existence of such a stable LSP is well motivated by the need for non-baryonic dark matter [21]. Another welcome result of R-parity conservation is the elimination of tree level flavour changing neutral currents.

3.2.2 Supersymmetric Lagrangian

Chiral Lagrangian

The Lagrangian of the chiral supermultiplet can be obtained from a superpotential that is assumed to preserve R-parity

$$W = W_{\text{Yukawa}} + W_{\text{Higgs}}, \tag{3.5}$$

with

$$W_{\text{Yukawa}} = \epsilon_{\alpha\beta}\left(\hat{Q}_i^\alpha Y_{ij}^u \hat{U}_j \hat{H}_2^\beta - \hat{Q}_i^\alpha Y_{ij}^d \hat{D}_j \hat{H}_1^\beta - \hat{L}_i^\alpha Y_{ij}^e \hat{E}_j \hat{H}_1^\beta\right), \tag{3.6}$$

$$W_{\text{Higgs}} = -\mu\epsilon_{\alpha\beta}\hat{H}_1^\alpha \hat{H}_2^\beta, \tag{3.7}$$

where $i, j = 1, 2, 3$ denote generation indices, $\alpha, \beta = 1, 2$ are SU(2) indices, and ϵ is a completely antisymmetric 2×2 matrix with $\epsilon_{12} = 1$. The matrices Y^u, Y^d, and Y^e give rise to the usual Yukawa interactions, which generate the masses of quarks and leptons. Including the fermion fields of the chiral supermultiplet, the Lagrangian can be expressed as[1]

$$\mathcal{L}_{\text{chiral}} = \partial_\mu \phi_i^\dagger \partial^\dagger \phi_i + i\bar{\psi}_i \bar{\sigma}^\mu \partial_\mu \psi_i - \frac{1}{2}\left(\frac{\partial^2 W}{\partial\phi_i \partial\phi_j}\psi_i\psi_j + h.c.\right) - \left(\frac{\partial W}{\partial\phi_i}\right)^* \left(\frac{\partial W}{\partial\phi_i}\right). \tag{3.8}$$

Here ϕ refers to a massless complex spin-0 field and ψ corresponds to a massless left-handed Weyl spinor. In the above equation i and j stand for different superfields of the chiral supermultiplet (e.g. $\hat{L}, \hat{E}, \hat{Q}, ...$) of the chiral supermultiplet.

Gauge Lagrangian

The gauge Lagrangian can be expressed in terms of the massless gauge boson fields (A_μ^a) and of the Weyl fermion gaugino fields (λ^a), which form the gauge supermultiplets

$$\mathcal{L}_{\text{gauge}} = -\frac{1}{4}F_{\mu\nu}^a F^{\mu\nu\ a} + i\lambda^{\dagger a}\bar{\sigma}^\mu D_\mu \lambda^a + \frac{1}{2}D^a D^a. \tag{3.9}$$

Here D^a is the nonpropagating auxiliary field of the gauge supermultiplet and D_μ is the covariant derivative

$$D_\mu \lambda^a = \partial_\mu \lambda^a + g f^{abc}\lambda^c, \tag{3.10}$$

with f^{abc} the totally antisymmetric structure constant that defines the gauge group ($[T^a,\ T^b] = if^{abc}T^c$), and T_G^a the generators of the gauge group. For the Yang-Mills field strength tensor we have

$$F_{\mu\nu}^a = \partial_\mu A_\nu^a - \partial_\nu A_\mu^a + g f^{abc} A_\mu^b A_\nu^c. \tag{3.11}$$

SUSY Lagrangian

While the gauge Lagrangian is both SUSY and gauge invariant, the chiral Lagrangian is only SUSY invariant. For $\mathcal{L}_{\text{chiral}}$ to respect gauge invariance, and similar to what occurs

[1] The superfields of the superpotential can alternatively be considered as their corresponding scalar fields [17].

in the SM, the partial derivative can be replaced with the covariant derivative

$$\partial_\mu \phi_i \longrightarrow D_\mu \phi_i = \partial_\mu \phi_i - igA^a_\mu (T^a \phi)_i, \tag{3.12}$$
$$\partial_\mu \psi_i \longrightarrow D_\mu \psi_i = \partial_\mu \psi_i - igA^a_\mu (T^a \phi)_i. \tag{3.13}$$

The covariant derivative restores gauge invariance but it introduces new interaction terms that break the SUSY invariance (the second terms in the above equations). To restore SUSY invariance new interaction terms have to be included. Considering renormalisability and gauge invariance, there are three possible terms that can be added

$$(\phi_i^* T^a \psi_i)\lambda^a, \qquad \lambda^{\dagger a}(\psi_i^\dagger T^a \phi_i), \qquad (\phi_i^* T^a \phi_i) D^a. \tag{3.14}$$

Combining the chiral and gauge Lagrangians, and adding the above gauge-restoring terms with the appropriate numerical factors, the supersymmetric Lagrangian can be schematically expressed as

$$\begin{aligned} \mathcal{L}_{\text{SUSY}} = & -\frac{1}{4} F^a_{\mu\nu} F^{\mu\nu\, a} + i\lambda^{\dagger a} \bar{\sigma}^\mu D_\mu \lambda^a + D_\mu \phi_i^\dagger D^\dagger \phi_i + i\bar{\psi}_i \bar{\sigma}^\mu D_\mu \psi_i \\ & - \frac{1}{2}\left(\frac{\partial^2 W}{\partial \phi_i \partial \phi_j} \psi_i \psi_j + h.c. \right) - \left(\frac{\partial W}{\partial \phi_i} \right)^* \left(\frac{\partial W}{\partial \phi_i} \right) \\ & - \sqrt{2} g \left[(\phi_i^* T^a \psi_i)\, \lambda^a + h.c. \right] - \frac{1}{2} g^2 \left(\phi_i^* T^a \phi_i \right)^2, \end{aligned} \tag{3.15}$$

where the auxiliary field (D^a) has been eliminated using the equation of motion. As aforementioned, in an unbroken SUSY theory, both members of a multiplet are degenerate in mass.

3.2.3 Soft breaking Lagrangian

Since we have not observed any sparticles with the same mass as their SM partners, for instance a scalar with the same quantum numbers of the electron and couplings, we have to admit that the mass of the selectron has to be high enough for it to have so far escaped detection. Therefore SUSY must be broken. To ensure that the supersymmetric Lagrangian remains free of quadratic divergences - an original motivation of supersymmetry, only a small set of terms are allowed to be present in the so called "soft SUSY breaking" Lagrangian. For detailed analyses, we refer the reader to [12, 17, 19, 22–24].

As a consequence, in addition to the superpotential given by (3.5), we have to specify the SUSY soft-breaking terms. These are given by

$$
\begin{aligned}
\mathcal{L}_{\rm SB} = & \frac{1}{2}\left(M_1\tilde{B}\tilde{B} + M_2\tilde{W}\tilde{W} + M_3\tilde{g}\tilde{g} + h.c.\right) \\
& - \tilde{Q}_i^{\alpha *}\left(M^2_{\tilde{Q}}\right)_{ij}\tilde{Q}_j^{\alpha} - \tilde{U}_i\left(M^2_{\tilde{U}}\right)_{ij}\tilde{U}_j^{*} - \tilde{D}_i\left(M^2_{\tilde{D}}\right)_{ij}\tilde{D}_j^{*} - \tilde{L}_i^{\alpha *}\left(M^2_{\tilde{L}}\right)_{ij}\tilde{L}_j^{\alpha} - \tilde{E}_i\left(M^2_{\tilde{E}}\right)_{ij}\tilde{E}_j^{*} \\
& - \epsilon_{\alpha\beta}\left[\tilde{Q}_i^{\alpha}(A^u_{ij}Y^u_{ij})\tilde{U}_j H_2^{\beta} - \tilde{Q}_i^{\alpha}(A^d_{ij}Y^d_{ij})\tilde{D}_j H_1^{\beta} - \tilde{L}_i^{\alpha}(A^u_{ij}Y^e_{ij})\tilde{E}_j H_1^{\beta}\right] \\
& - m^2_{H_1}H_1^{*\alpha}H_1^{\alpha} - m^2_{H_2}H_2^{*\alpha}H_2^{\alpha} + B\mu\,\epsilon_{\alpha\beta}\,H_1^{\alpha}\,H_2^{\beta},
\end{aligned}
\tag{3.16}
$$

where the first line contains the gaugino mass terms and the second line the soft squared masses for the squarks and sleptons. The third line contains the trilinear soft breaking terms (also referred to as A terms).

The origin of SUSY breaking is still unknown. Constructing models that break supersymmetry in an acceptable way is highly non-trivial mostly because the breaking cannot be brought by one of the MSSM supermultiplets, and must thus occur in a "hidden" sector and later communicate to the MSSM (see, for instance [25] for an overview). Many mechanisms have been presented since the 1980's. To account for the set of terms appearing in the soft breaking Lagrangian, there are several proposals for the mediation of SUSY breaking. Let us just cite supergravity [26, 27], gauge mediation [28] and anomaly mediation [29] models.

The soft breaking Lagrangian has several new parameters compared to the SM. Overall, the MSSM Lagrangian introduces 62 real parameters and 43 CP-violating phases in addition to the SM parameters which brings the total number of physical degree of freedom to:

$$
\text{Unconstrained MSSM:} \quad 79\ \text{real} \quad + \quad 45\ \text{imaginary} \quad = \quad 124\ \text{d.o.f.}\ . \tag{3.17}
$$

However, the MSSM is not phenomenologically viable in a large region of its parameter space: unless we impose some conditions on the parameters, we encounter some fine-tuning problems, as the μ problem, naturalness paradigms like the electric dipole moment problems, unsuppressed contributions to flavour changing neutral currents - the SUSY flavour problem, just to cite a few issues.

To reduce the MSSM parameter freedom, one can either assume some simplification criteria at high or low energies. Let us just mention that at low energies we can impose some alignment between quark Yukawa terms and squark soft masses, or assume universality of the soft breaking terms in the flavour space, for example. At high energies, one treats the MSSM parameters as running parameters, and imposes some structure for the soft breaking terms at some common scale (GUT, or even M_P). The initial conditions depend on the mechanism for SUSY breaking one is considering. For example, in minimal supergravity scenarios (mSUGRA), relations of universality among the soft breaking parameters, and the use of the above referred symmetries, allow us to parameterise the high energy model by means of five independent parameters: the common soft scalar mass at the GUT scale (m_0), the unified gaugino mass ($m_{1/2}$), the universal trilinear coupling (A_0), the ratio of the Higgs vacuum expectation values ($\tan\beta$) and finally the sign of the bilinear Higgs

term in the superpotential ($\operatorname{sgn}\mu$). By running the RGEs one can then derive the low energy MSSM parameters. The running of the MSSM parameters can generate a vacuum instability where the Higgs mass runs from a positive value at the GUT scale to a negative one at the electroweak scale, thus triggering spontaneous electroweak symmetry breaking, induced by SUSY breaking.

3.2.4 Low energy spectrum

Depending on the high-energy model we are assuming, different predictions for the low energy scenario will emerge. Overlooking the fact that each high scale model will establish specific patterns between the low energy parameters, the phenomenology of the MSSM can be described by enumerating the properties of the physical states, that is, their interactions and their masses.
The essential tool to obtain the high-low energy relations is the (RGE) [30] adapted for the MSSM.
The Feynman rules, particle interaction, and mass matrices of the MSSM have been extensively listed in the literature, for example in Refs. [17, 22, 23, 31–33]. Here, we shall pay special attention to the definition of the mass matrices, and hence to the relations between the interaction and the physical states, which play an essential role in flavour physics.
We will give a brief description of the mass matrices of the matter sector, that is, fermions and sfermions, as well as the mixtures of the gauge boson partners and Higgs fermions, when discussing the charginos and the neutralinos. However, before advancing, we will consider the implications of finding stable minima for the scalar potential, and present the MSSM spectrum of scalar Higgs particles.

Minimisation of the potential
As stated before, SUSY requires the presence of - two complex doublets, rather than the single one present in the SM. The classical standard potential for the Higgs scalar fields in the MSSM is given by

$$\begin{aligned} V_{scalar} &= (\mu^2 + m_{H_1}^2)\,(|H_1^0|^2 + |H_1^-|^2) + (\mu^2 + m_{H_2}^2)\,(|H_2^0|^2 + |H_2^+|^2) \\ &\quad + \left[B\,\mu\,(H_1^-\,H_2^+ - H_1^0\,H_2^0) + \text{c.c.}\right] \\ &\quad + \frac{1}{8}\,(g_1^2 + g_2^2)\,\left(|H_2^0|^2 + |H_2^+|^2 - |H_1^0|^2 - |H_1^-|^2\right)^2 \\ &\quad + \frac{1}{2}\,g_2^2\,|H_1^{0*}\,H_2^+ + H_1^{-*}\,H_2^0|^2\,, \end{aligned} \tag{3.18}$$

where some terms arise from soft SUSY breaking and others are F- (those proportional to μ) and D-terms (the ones associated with the weak gauge couplings).
As mentioned before, having a negative value for one of the soft Higgs masses ($m_{H_1}^2 < 0$) is not only natural, but in fact essential for the spontaneous breaking of electroweak symmetry (SSB).
Using $SU(2)_L$ gauge transformations, and requiring that the potential has a minimum

with respect to the four Higgs components, lead us to setting $\langle H_1^- \rangle = \langle H_2^+ \rangle = 0$, where $\langle \phi \rangle$ denotes the vacuum expectation value of the field ϕ. This has the appealing feature of preserving electromagnetism, and forcing the product $\langle H_1^0 \rangle \langle H_2^0 \rangle$ to be real and positive at the minimum of the potential.

The minimisation of the tree level potential after electroweak symmetry breaking leads to a pair of equations, which can be rewritten as

$$\begin{aligned} |\mu|^2 + m_{H_1}^2 &= B\ \mu\ \tan\beta - (M_Z^2/2)\ \cos(2\beta)\ , \\ |\mu|^2 + m_{H_2}^2 &= B\ \mu\ \cot\beta + (M_Z^2/2)\ \cos(2\beta)\ , \end{aligned} \tag{3.19}$$

where we are already introducing the physical Z boson mass, $M_Z^2 = (v^2)\ (g_1^2 + {g_2}^2)/4$ with the numerical value $v = \sqrt{v_1^2 + v_2^2} \simeq 246$ GeV and $\tan\beta = v_2/v_1$ is the ratio of the Higgs VEVs

$$\langle H^1 \rangle = \begin{pmatrix} \frac{v_1}{\sqrt{2}} \\ 0 \end{pmatrix} \equiv \begin{pmatrix} \frac{v\cos\beta}{\sqrt{2}} \\ 0 \end{pmatrix}, \qquad \langle H^2 \rangle = \begin{pmatrix} 0 \\ \frac{v_2}{\sqrt{2}} \end{pmatrix} \equiv \begin{pmatrix} 0 \\ \frac{v\sin\beta}{\sqrt{2}} \end{pmatrix}. \tag{3.20}$$

.

Requiring the minimum to be stable, and that it corresponds to an electroweak symmetry breaking minimum (that is, $v_{1,2} \neq 0$), impose 2 additional conditions,

$$\begin{aligned} (B\ \mu)^2 &> (\mu^2 + m_{H_1}^2)\ (\mu^2 + m_{H_2}^2)\ , \\ m_{H_1}^2 + m_{H_2}^2 + 2\ \mu^2 &> |B\ \mu|\ . \end{aligned} \tag{3.21}$$

Equations (3.19) allow us to eliminate two of the Lagrangian parameters, namely μ and B, just with the requirement of SSB. The disadvantage this introduces is the so-called "μ-problem" of supersymmetry. In other words, if μ is a superpotential parameter, defined at some very high-scale, *e.g.* the GUT scale, why should its value be close to that of the soft masses appearing in the SUSY breaking Lagrangian, which are not related to the superpotential? This is one of SUSY's naturalness problems. The above statement becomes mathematically clear if we take $|\mu|^2$, B and $m_{H_i}^2$ as input parameters and M_Z and $\tan\beta$ as output parameters, and rewrite (3.19) to obtain

$$|\mu|^2 = -\frac{1}{2}\ M_Z^2 + \frac{m_{H_2}^2\ \sin^2\beta - m_{H_1}^2\ \cos^2\beta}{\cos(2\ \beta)}\ . \tag{3.22}$$

If we dismiss the possibility of cancellations between the parameters on the right hand side, we should expect that all parameters present in the equation should be roughly within one or two orders of magnitude of M_Z^2. Therefore, we are led to believe that there must exist some mechanism at very high energies that somehow relates the value of μ with the soft supersymmetry breaking mechanism [34].

Scalar Higgs spectrum

Although we will skip the presentation of the Higgs mixing matrices here (see, for instance Refs. [35, 36]), we shall discuss the physical Higgs scalar eigenstates of this two-Higgs doublet model. We originally have 4 complex (or 8 real) degrees of freedom associated with the 2 doublets. Three of them are "eaten up" by the SM gauge bosons, $W^\pm$ and Z^0, and the remaining five are associated to 5 physical Higgs bosons: two charged scalars ($H^\pm$) and three neutral states. Of the latter, one is a CP-odd state, the pseudoscalar A, and the other two are CP even (H^0 and h^0), where the upper (lower) case refers to the heaviest (lightest) state. Their tree level masses are given by

$$\begin{aligned} m_A^2 &= m_{H_1}^2 + m_{H_2}^2 + 2\,\mu^2 \,, \\ m_{H^\pm}^2 &= m_A^2 + M_W^2 \,, \\ m_{H^0,h^0}^2 &= \frac{1}{2}\left[m_A^2 + M_Z^2 \pm \sqrt{(m_A^2 + M_Z^2)^2 - 4\, m_A^2\, M_Z^2\, \cos^2 2\,\beta} \right] . \end{aligned} \tag{3.23}$$

Notice that at tree level we have $m_{H^\pm} \geq M_W$, $m_{H^0} \geq M_Z$ and $m_{h^0} \leq M_Z$, which means that in these conditions we have a light Higgs boson. This is a consequence of having the Higgs quartic coupling defined by the gauge couplings in the supersymmetric framework. Observe however that radiative corrections play a very important role in the MSSM: regarding the light Higgs mass, m_h, the leading radiative corrections arise from the top-stop loops, and grow as the fourth power of the top mass,

$$m_h^2 \to m_h^2 + \delta m_h^2 \,, \qquad \text{with} \qquad \delta m_h^2 \sim \mathcal{O}(\alpha)\, \frac{m_t^4}{M_W^2}\, \ln\left(\frac{m_{\tilde{t}}^2}{m_t^2}\right) , \tag{3.24}$$

so that the upper limit can be pushed up to around 150 GeV. The upper limit depends on various parameters such as $\tan\beta$ and the supersymmetry breaking scale [37]. A detailed summary of radiative corrections to m_{h^0} can be found in [38].

Quark and lepton mass matrices

In the weak interaction basis, the quark mass Lagrangian is given by

$$\mathcal{L} \;=\; \bar{d}'_R\, M'_D\, d'_L + \bar{u}'_R\, M'_U\, u'_L + \bar{e}'_R\, M'_E\, e'_L + h.c. \,, \tag{3.25}$$

with the mass matrices written in terms of the Higgs VEV's and the Yukawa couplings,

$$M'_D = \frac{v_1}{\sqrt{2}}\,(Y^d)^T \,, \qquad M'_U = \frac{v_2}{\sqrt{2}}\,(Y^u)^T \,. \qquad M'_E \;=\; \frac{v_1}{\sqrt{2}}\,(Y^e)^T \,. \tag{3.26}$$

The physical and weak (primed) eigenstates are related according to (2.26), and the diagonalised mass matrices are given in (2.27). The Cabibbo-Kobayashi-Maskawa matrix, that parameterises the flavour mixing in charged weak interactions is defined as $V_{\rm CKM} = V_L^u\, V_L^{d\dagger}$ (see Section 2.2).

Squark mass matrices

A convenient basis when addressing problems of CP violation, or flavour physics, is the so called "super-CKM" (SCKM) basis [39], where left and right handed squarks are rotated parallel to the left and right handed quarks. In this basis, the 6×6 mass matrices of the up-squark $(\tilde{u}_L, \tilde{c}_L, \tilde{t}_L, \tilde{u}_R, \tilde{c}_R, \tilde{t}_R)$ and down-squarks $(\tilde{d}_L, \tilde{s}_L, \tilde{b}_L, \tilde{d}_R, \tilde{s}_R, \tilde{b}_R)$, can each be expressed as

$$M^2_{\tilde{u}} = \begin{pmatrix} M^2_{U_{LL}} & M^2_{U_{LR}} \\ M^{2\dagger}_{U_{LR}} & M^2_{U_{RR}} \end{pmatrix}, \qquad M^2_{\tilde{d}} = \begin{pmatrix} M^2_{D_{LL}} & M^2_{D_{LR}} \\ M^{2\dagger}_{D_{LR}} & M^2_{D_{RR}} \end{pmatrix} \tag{3.27}$$

The 3×3 submatrices are given by

$$M^2_{U_{LL}} = M^2_{\tilde{U}_L} + M^2_U + \frac{1}{6} M^2_Z \cos 2\beta (3 - 4s^2_W) \mathbb{1}, \tag{3.28}$$

$$M^2_{U_{LR}} = M_U (A^{u*} - \mu \cot \beta \mathbb{1}), \tag{3.29}$$

$$M^2_{U_{RR}} = M^2_{\tilde{U}_R} + M^2_U + \frac{2}{3} M^2_Z \cos 2\beta s^2_W \mathbb{1}, \tag{3.30}$$

$$M^2_{D_{LL}} = M^2_{\tilde{D}_L} + M^2_D - \frac{1}{6} M^2_Z \cos 2\beta (3 - 2s^2_W) \mathbb{1}, \tag{3.31}$$

$$M^2_{D_{LR}} = M_D (A^{d*} - \mu \tan \beta \mathbb{1}), \tag{3.32}$$

$$M^2_{D_{RR}} = M^2_{\tilde{D}_R} + M^2_D - \frac{1}{3} M^2_Z \cos 2\beta s^2_W \mathbb{1}. \tag{3.33}$$

where $s^2_W \equiv \sin^2 \theta_W$. In the above relations, $M_{\tilde{X}_{L,R}} (X = U, D)$ are the soft breaking mass-squared matrices in the SCKM basis which are related to the interaction basis via

$$M^2_{\tilde{U}_L} = V^u_L M^2_{\tilde{Q}} V^{u\dagger}_L , \qquad M^2_{\tilde{U}_R} = V^u_R M^{2T}_{\tilde{U}} V^{u\dagger}_R , \tag{3.34}$$

$$M^2_{\tilde{D}_L} = V^d_L M^2_{\tilde{Q}} V^{d\dagger}_L , \qquad M^2_{\tilde{D}_R} = V^d_R M^{2T}_{\tilde{D}} V^{d\dagger}_R . \tag{3.35}$$

Due to $SU(2)$ gauge symmetry, $M^2_{\tilde{D}_L}$ and $M^2_{\tilde{U}_L}$ are connected through the CKM matrix, this can readily be seen by considering the above relations

$$M^2_{\tilde{D}_L} = V^\dagger_{\rm CKM} M^2_{\tilde{U}_L} V_{\rm CKM}. \tag{3.36}$$

While the mass matrices (M_U, M_D) are diagonal in the SCKM basis, the squark mass-squared matrices are not. The matrices $M^2_{\tilde{u}}$ and $M^2_{\tilde{d}}$ can be diagonalised by unitary field rotations to obtain the mass eigenstates of the squarks

$$\Gamma^U M^2_{\tilde{u}} \Gamma^{U\dagger} = \mathrm{diag}(m^2_{\tilde{u}_1}, \cdots, m^2_{\tilde{u}_6}), \tag{3.37}$$

$$\Gamma^D M^2_{\tilde{d}} \Gamma^{D\dagger} = \mathrm{diag}(m^2_{\tilde{d}_1}, \cdots, m^2_{\tilde{d}_6}). \tag{3.38}$$

Finally it proves useful to define the 6×6 mixing matrices Γ^U and Γ^D in terms of their

6×3 block components,

$$\Gamma^U_{6\times 6} = \begin{pmatrix} \Gamma^{U_L}_{6\times 3} & \Gamma^{U_R}_{6\times 3} \end{pmatrix}, \tag{3.39}$$

$$\Gamma^D_{6\times 6} = \begin{pmatrix} \Gamma^{D_L}_{6\times 3} & \Gamma^{D_R}_{6\times 3} \end{pmatrix}. \tag{3.40}$$

Slepton mass matrices

Similar to the squark case, the slepton mass matrices can also be built from four, 3×3 submatrices,

$$M^2_{\tilde{\ell}} = \begin{pmatrix} M^2_{E_{LL}} & M^2_{E_{LR}} \\ M^{2\dagger}_{E_{LR}} & M^2_{E_{RR}} \end{pmatrix}, \tag{3.41}$$

where the 3×3 submatrices are

$$M^2_{E_{LL}} = M^2_{\tilde{L}_L} + M^2_E - \frac{1}{2} M^2_Z \cos 2\beta (1 - 2s^2_W) \mathbb{1}, \tag{3.42}$$

$$M^2_{E_{LR}} = M_E (A^{e*} - \mu \tan\beta \mathbb{1}), \tag{3.43}$$

$$M^2_{E_{RR}} = M^2_{\tilde{L}_R} + M^2_E - M^2_Z \cos 2\beta s^2_W \mathbb{1}. \tag{3.44}$$

$M_{\tilde{L}_L}$ and $M_{\tilde{L}_R}$ are the soft breaking mass matrices in the basis where the charged leptons are diagonal, they are related to the interaction basis through

$$M^2_{\tilde{L}_L} = V^e_L M^2_{\tilde{L}} V^{e\dagger}_L , \qquad M^2_{\tilde{L}_R} = V^e_R M^{2T}_{\tilde{E}} V^{e\dagger}_R . \tag{3.45}$$

For the sneutrinos we have

$$M^2_{\tilde{\nu}} = M^2_{\tilde{L}_L} + \frac{1}{2} M^2_Z \cos 2\beta \mathbb{1}. \tag{3.46}$$

In this basis, the matrices $M^2_{\tilde{\ell}}$ and $M^2_{\tilde{\nu}}$ are not diagonal. Similar to the squark mass matrices, the mass eigenstates of the sleptons and sneutrinos can be obtained by the mixing matrices $(\Gamma^E)_{6\times 6}$ and $(\Gamma^N)_{3\times 3}$

$$\Gamma^E M^2_{\tilde{\ell}} \Gamma^{E\dagger} = \mathrm{diag}(m^2_{\tilde{\ell}_1}, \cdots, m^2_{\tilde{\ell}_6}), \tag{3.47}$$

$$\Gamma^N M^2_{\tilde{\nu}} \Gamma^{N\dagger} = \mathrm{diag}(m^2_{\tilde{\nu}_1}, \cdots, m^2_{\tilde{\nu}_3}). \tag{3.48}$$

As before, the 6×6 mixing matrix Γ^E can be defined in terms of 6×3 submatrices

$$\Gamma^E_{6\times 6} = \begin{pmatrix} \Gamma^{E_L}_{6\times 3} & \Gamma^{E_R}_{6\times 3} \end{pmatrix}. \tag{3.49}$$

Chargino mass matrices

We now turn our attention to the four-component Dirac fermions, $\tilde{\chi}^\pm_{1,2}$, which arise from the mixing of the W-gauginos and the charged higgsinos. Within the MSSM, the chargino

mass terms in the Lagrangian are

$$\mathcal{L} \;=\; -\frac{1}{2}(\psi^{\pm})^T \begin{pmatrix} 0 & M_{\chi^{\pm}}^T \\ M_{\chi^{\pm}} & 0 \end{pmatrix} \psi^{\pm} + h.c., \tag{3.50}$$

where $\psi^{\pm} = (\tilde{W}^+, \tilde{H}_2^+, \tilde{W}^-, \tilde{H}_1^-)$. In a general SUSY model, the chargino mass matrix is given by

$$M_{\chi^{\pm}} \;=\; \begin{pmatrix} M2 & \sqrt{2}\, M_W\, \sin\beta \\ \sqrt{2}\, M_W\, \cos\beta & \mu \end{pmatrix}, \tag{3.51}$$

where M_2 is the soft $SU(2)$ gaugino mass. This mass matrix can be diagonalised by means of a biunitary transformation,

$$U^*\, M_{\chi^{\pm}}\, V^{\dagger} \;=\; M_{\chi^{\pm}}^{\mathrm{diag}}\,. \tag{3.52}$$

The positive and negative eigenstates are then defined as

$$\left(\tilde{\chi}_1^+, \tilde{\chi}_2^+\right)^T \;=\; V\,(\tilde{W}^+, \tilde{H}_2^+)^T\,, \qquad \left(\tilde{\chi}_2^-, \tilde{\chi}_2^-\right)^T \;=\; U\,(\tilde{W}^-, \tilde{H}_1^-)^T\,, \tag{3.53}$$

and we emphasise that positively and negatively charged states mix in a different fashion.

Neutralino mass matrices

The mixture of the four Majorana spinors (photino, zino and neutral higgsinos) is parametrised by the mass term in the Lagrangian

$$\mathcal{L} \;=\; -\frac{1}{2}\,(\psi^0)^T\, M_{\chi^0}\, \psi^0 + h.c., \tag{3.54}$$

where $(\psi^0)^T = (\tilde{B}, \tilde{W}^0, \tilde{H}_1^0, \tilde{H}_1^0)^T$, and the neutralino mass matrix can be written in terms of the physical masses as

$$M_{\tilde{\chi}^0} \;=\; \begin{pmatrix} M_1 & 0 & -M_Z\, s_W\, c_\beta & M_Z\, s_W\, s_\beta \\ 0 & M_2 & M_Z\, c_W\, c_\beta & -M_Z\, c_W\, s_\beta \\ -M_Z\, s_W\, c_\beta & M_Z\, c_W\, c_\beta & 0 & -\mu \\ M_Z\, s_W\, s_\beta & -M_Z\, c_W\, s_\beta & -\mu & 0 \end{pmatrix}, \tag{3.55}$$

where $s_W \equiv \sin\theta_W$, $c_W \equiv \cos\theta_W$, $s_\beta \equiv \sin\beta$, $c_\beta \equiv \sin\beta$, and $M_{1,2}$ are the soft gaugino masses. This matrix can be diagonalised by an orthogonal matrix

$$N^*\, M_{\tilde{\chi}^0}\, N^{\dagger} \;= \mathrm{diag}(M_{\tilde{\chi}_1^0}, M_{\tilde{\chi}_2^0}, M_{\tilde{\chi}_3^0}, M_{\tilde{\chi}_4^0}), \tag{3.56}$$

with $(M_{\tilde{\chi}_1^0} < M_{\tilde{\chi}_2^0} < M_{\tilde{\chi}_3^0} < M_{\tilde{\chi}_4^0})$.

Physical particles in the MSSM

The additional physical particles to the SM which were discussed in this section are listed in Table 3.2.

Mass eigenstates	Composed of
CP-even neutral Higgs h^0 and H^0	Re(H_1^0) and Re(H_2^0)
CP-odd neutral Higgs A^0 (and $Z^0_{\text{long.}}$)	Im(H_1^0) and Im(H_2^0)
charged Higgs $H^\pm$ (and $W^\pm_{\text{long.}}$)	$H_1^\pm$ and $H_2^\pm$
charged sleptons $\tilde{\ell}_{i=,\cdots,6}$	LH and RH charged sleptons ($\tilde{\ell}_{i=e,\mu,\tau;L,R}$)
sneutrinos $\tilde{\nu}_{i=1,2,3}$	LH sneutrinos ($\tilde{\nu}_{i=e,\mu,\tau;L}$)
up-squarks $\tilde{u}_{i=1,\cdots,6}$	LH and RH up-squarks ($\tilde{u}_{i=u,c,t;L,R}$)
down-squarks $\tilde{d}_{i=1,\cdots,6}$	LH and RH down-squarks ($\tilde{d}_{i=d,s,b;L,R}$)
neutralino $\tilde{\chi}_{i=1,2,3,4}$	neutral Higgsinos (H_1^0, H_2^0), Wino ($\tilde{W}^3$) and Bino ($\tilde{B}$)
charginos $\tilde{\chi}^\pm_{i=1,2}$	charged Higgsinos ($\tilde{H}_1^\pm$ and $\tilde{H}_2^\pm$) and charged Winos ($\tilde{W}^\pm$)

Table 3.2.: Physical particles in the MSSM.

MSSM interactions contributing to down type FCNC

As mentioned in Chapter 2, in the SM tree-level flavour changing interactions can only take place via the exchange of a charged W between up- and down-quarks (u-d-$W^\pm$). In the MSSM there are additional interactions that result in change of flavour. In terms of the mass eigenstates, the most relevant vertices leading to $d_i \to d_j$ transitions are

- down-quark - up-quark - charged Higgs (d-u-$H^\pm$)
- down-quark - up-squark - chargino (d-$\tilde{u}$-$\chi^\pm$)
- down-quark - down-squark - neutralino (d-$\tilde{d}$-χ^0)
- down-quark - down-squark - gluino(d-$\tilde{d}$-g)

In the SCKM basis, the Lagrangian for the above interactions can be expressed as [40, 41]

$$\mathcal{L}_{duH^\pm} = \frac{g_2}{\sqrt{2}M_W}\Big[\bar{u}(\cot\beta\ M_U V_{\rm CKM} P_L\ +\ \tan\beta\ V_{\rm CKM} M_D P_R)d\Big]H^+ + h.c., \tag{3.57}$$

$$\mathcal{L}_{d\tilde{u}\tilde{\chi}^\pm} = \sum_{i=1}^{2}\Big\{\overline{\tilde{\chi}_i^-}\ \big[\tilde{u}^\dagger(X_i^{U_L}P_L + X_i^{U_R}P_R)d\big]\Big\} + h.c., \tag{3.58}$$

$$\mathcal{L}_{d\tilde{d}\tilde{\chi}^0} = \sum_{i=1}^{4}\Big\{\overline{\tilde{\chi}_i^0}\ \Big[\tilde{d}^\dagger(Z_i^{D_L}P_L + Z_i^{D_R}P_R)d\Big]\Big\} + h.c., \tag{3.59}$$

$$\mathcal{L}_{d\tilde{d}\tilde{g}} = -\sqrt{2}g_3\sum_{a=1}^{8}\Big\{\overline{\tilde{g}_a}\ \Big[\tilde{d}^\dagger(\Gamma^{D_L}P_L - \Gamma^{D_R}P_R)T^a d\Big]\Big\} + h.c., \tag{3.60}$$

where

$$X_i^{U_L} = -g_2\left[V_{i1}^*\Gamma^{U_L} - V_{i2}^*\Gamma^{U_R}\frac{M_U}{\sqrt{2}M_W\sin\beta}\right]V_{\rm CKM}, \tag{3.61}$$

$$X_i^{U_R} = g_2 U_{i2}\Gamma^{U_L}V_{\rm CKM}\frac{M_D}{\sqrt{2}M_W\cos\beta}, \tag{3.62}$$

$$Z_i^{D_L} = -\frac{g_2}{\sqrt{2}}\Big[(-N_{i2}^* + \frac{1}{3}\tan\theta_W N_{i1}^*)\Gamma^{D_L} + N_{i3}^*\Gamma^{D_R}\frac{M_D}{M_W\cos\beta}\Big], \tag{3.63}$$

$$Z_i^{D_R} = -\frac{g_2}{\sqrt{2}}\Big[\frac{2}{3}\tan\theta_W N_{i1}\Gamma^{D_R} + N_{i3}\Gamma^{D_L}\frac{M_D}{M_W\cos\beta}\Big]. \tag{3.64}$$

The flavour changing nature of these interactions is due to the CKM matrix ($V_{\rm CKM}$) and/or the squark-mixing matrices (Γ^U, Γ^D). The flavour mixing effect of Γ^U and Γ^D can be understood by noting that for instance in the SCKM basis the squark mass-squared matrices ($M_{\tilde{u}}^2$) and ($M_{\tilde{d}}^2$) are in general not flavour diagonal which results in Γ^U and Γ^D to have flavour off-diagonal entries. All terms proportional to $M_{U,D}$ come from higgsino interactions; the others from Winos.

At one-loop level, charged Higgs contributions to down-type FCNC processes are only due to the CKM matrix. On the other hand, gluino and neutralino contributions emerge only from flavour mixing among the down squarks. However, charginos contribute to down-type FCNC processes due to both the CKM matrix and flavour mixing among the up squarks.

Depending on the structure of $M_{\tilde{u}}^2$ and $M_{\tilde{d}}^2$ there can be different contributions from d-$\tilde{u}$-$\tilde{\chi}^\pm$ and d-$\tilde{d}$-$(\tilde{\chi}^0, \tilde{g})$ interactions at one-loop level. Consider the following illustrative limits:

- $M_{\tilde{d}}^2$ block-diagonal: while left- and right-handed mixing in the same flavour is allowed, no flavour mixing takes place among the down-squarks. Hence there will be no FCNC contributions from gluinos and neutralinos since the only source of flavour violation from $\tilde{\chi}^0$ and $\tilde{g}$ is due to flavour off-diagonal entries in Γ^D (which in this limit is diagonal in flavour space).

- $M^2_{\tilde{u}}$ block-diagonal: left- and right-handed mixing among up-squarks is present. However, even if flavour mixing does not occur and Γ^U will be flavour diagonal there are still chargino contributions to FCNC processes at one-loop level from the CKM matrix.

3.3 MFV

Although illustrative, the simple limiting cases discussed in the previous section are not realistic: the many new degrees of freedom introduced by the (in general) complex and non-diagonal soft breaking terms give rise to abundant sources of flavour and CP-violation The appearance of various degrees of freedom in the MSSM results in new sources of FCNCs as well as CP violation. These flavour- and CP-violating interactions lead to phenomenologically unacceptable results (see for example [42] and references therein). Hence any realistic low energy manifestation of the MSSM requires flavour- and CP-violating parameters to be small. However, according to the naturalness principle as formulated by 't Hooft [43]: small numbers are natural only if the symmetry of the theory increases in the limit where they vanish. Equivalently, these terms should be protected by a symmetry, and generated only through a breaking of that symmetry. One of the main challenges in supersymmetry is to understand the smallness of flavour- and CP-violating effects from a theoretical viewpoint. The difficulty of explaining the smallness of these parameters is referred to as the "flavour problem" and "CP problem" [44], as an extension of the "strong CP problem" of the SUSY models.
There are various methods to guarantee the smallness of flavour and CP-violation. For instance, one way to suppress large FCNCs is to have squarks with the same electric charge to be highly degenerate [45]. This is automatically implemented in the low energy limit of spontaneously broken supergravity theories [46], or minimal supergravity inspired models, as is the case of the constrained MSSM (CMSSM). Models of new physics (supersymmetric or not), where no sources of flavour violation - other than the CKM - are present, are known a Minimal Flavour Violating (MFV) scenarios. There are various formal definitions of MFV [47, 48]; from a phenomenological point of view, a common feature of these realisations is that FCNC processes are, to a very good approximation, governed by the CKM matrix.
In MFV SUSY scenarios, and in order to avoid large FNCNs, it can be assumed that $A^u, A^d, M^2_{\tilde{U}_R}$ and $M^2_{\tilde{D}_R}$ are to a good approximation, diagonal in flavour space

$$A^u \approx \mathrm{diag}(A_u, A_c, A_t), \qquad A^d \approx \mathrm{diag}(A_d, A_s, A_b), \tag{3.65}$$

$$M^2_{\tilde{U}_R} \approx \mathrm{diag}(m_{\tilde{u}_R}, m_{\tilde{c}_R}, m_{\tilde{t}_R}), \qquad M^2_{\tilde{D}_R} \approx \mathrm{diag}(m_{\tilde{d}_R}, m_{\tilde{s}_R}, m_{\tilde{b}_R}). \tag{3.66}$$

Moreover, to avoid CP-violating phases besides the CKM, the matrices A^u, A^d as well as μ are considered to be real. Within the latter conditions, $M^2_{\tilde{u}}$ and $M^2_{\tilde{d}}$ are not necessarily flavour diagonal and can still induce flavour violation due to the off-diagonal terms in $M^2_{\tilde{U}_L}$ and $M^2_{\tilde{D}_L}$. As already mentioned in (3.36), due to $SU(2)$ gauge invariance, $M^2_{\tilde{U}_L}$ and $M^2_{\tilde{D}_L}$ are intimately connected.

CHAPTER 4

Effective field theory

At any energy scale there can be various physical effects from known and unknown particles. If we needed the *full theory* that describes the physics of these particles at any given scale, we would not be able to do much. Fortunately this is not the case, effective theories are one way of getting around complicated computations or more importantly unknown underlying physics from heavy particles. Effective theories are used all the time in physics. For example Hooke's law is an effective theory, used to describe the behavior of a spring and while it would be possible to derive it by considering the particle structure, it would not be very convenient to do so for most applications.
The main idea in effective theories is to divide the parameter space into different regions to achieve a more convenient effective description of the region of interest. In particle physics the only relevant parameter in the relativistic and quantum limit is the distance scale, or alternatively the energy scale. In effective field theory (EFT) the parameters that are either very large or very small compared to the regime of interest, are respectively put to infinity and zero, in a first approximation. Setting these parameters to their true values have small effects which can be treated as perturbations. In the case of effective quantum field theory (EQFT), all the short distance effects due to the heavier particles, that cannot be produced at the energy under consideration, are integrated out and the result is a framework that is considerably simpler than the full quantum field theory. In the full theory, the effect of these heavy particles can be integrated out, resulting in nonlocal interactions, while in the effective theory these interactions will be described by local interactions in such a way as to match the full theory at low energies. The resulting effective theory's validity is bounded from above in energy by the masses of the heavy particles that have been integrated out. The reason this can be done is due to the decoupling theorem of Appelquist and Carazzone [49] which states that for a renormalisable theory with different mass scales, the heavy fields can be effectively decoupled and the low-momentum behavior of the theory can be described by the light particles only. Part of the effects of the heavy fields can be absorbed into finite renormalisation of the fields and of the free parameters (e.g. coupling constant) of the underlying theory. An unavoidable consequence of this procedure is a nonrenormalisable

theory [50]. But from an EFT point of view that is only a problem if we want the effective theory to be also capable of describing the physics of energies higher than the heavy particles.
One of the processes for which the decoupling theorem is useful is the weak decay of a meson where the relevant energy of the process is of the order of the decaying hadron mass, while the weak interactions involve scales of the order of the weak boson mass, M_W. To study these processes where two disparate energy scales appear, based on the decoupling theorem it is possible to construct an effective field theory where the explicit dynamical degrees of freedom due to the W and Z bosons and the top quark and any other heavier particle existing beyond the Standard Model, can be integrated out.
Furthermore, while weak interactions are responsible for the hadrons' decay, it is the strong force that binds quarks into hadrons. The theory describing the strong interactions among quarks is a non-Abelian gauge theory (quantum chromodynamics, QCD), where the gauge group is an $SU(3)_c$ that acts on the colour degree of freedom. However, the observed processes involve hadrons, thus presenting some theoretical subtleties since the latter do not possess the same degrees of freedom as the SM Lagrangian for quarks. The phenomenon that quarks cannot be observed individually and only appear as hadronic volumes of quarks and gluons, is addressed by colour confinement which postulates that the appearance of isolated colour charged particles are not allowed. One of the characteristics of QCD is the negative value of the β-function, which causes an increase in the coupling constant at large distances, and so the quarks and gluons can not be separated enough to form individual quarks which leads to confinement.[1]
The coupling constant at small energies ($\Lambda_{QCD} \approx 300$MeV) can become so large that perturbation theory is no longer applicable. However, at higher energies the constituents of hadrons behave almost as free particles and their effective interactions are relatively weak. The fact that the coupling constant progressively decreases at short distances is a proven property of non-Abelian gauge theories, known as asymptotic freedom. Asymptotic freedom then allows for perturbative calculations. The running of the coupling constant is essential to asymptotic freedom: the fact that the value of the coupling constant depends on the energy at which the process is taking place involves concepts such as renormalisation scale and renormalisation group which will be needed for the discussion of the effective theory.
There are two approaches to effective theories. One is the "bottom up" application of effective theory where the full underlying theory is not known, an example of this is the historical development of the description of weak interactions. Another approach is the "top down" application used when the fundamental theory is known and using the EFT can be helpful in making the calculations simpler or just possible, as in the case of QCD (where separation of the perturbative calculable contributions from the more delicate non-perturbative ones is needed). By exploring approximate symmetries which would be hidden in the fundamental theory, EFTs can offer stronger predictive power.Another reason for using EFT is that a common feature when dealing with disparate energy scales is the appearance of large logs ($\ln \frac{M_{\text{Heavy}}}{M_{\text{Light}}}$) which need resummation in order to keep the

[1] This has not yet been proved at the level of mathematical rigor. It is known as the Yang Mills problem and remains as one of the unsolved problems of the Clay Institute Millennium Prize [51].

perturbation theory under control; this is easier to perform in EFT.

4.1 "Bottom up" approach to weak interactions

The Fermi interaction is a perfect example of the "bottom up" approach in EFT. In 1933, Fermi made the first attempt to construct a weak interaction to explain the β-decay [52]. Fermi considered a 4-point interaction (Figure 4.1), and in accordance with

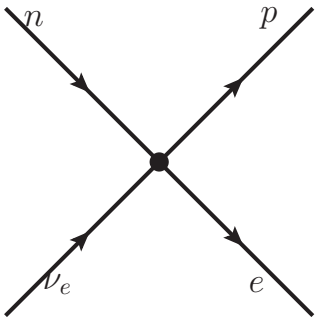

Figure 4.1.: 4-point interaction

the electromagnetic interaction he introduced the following current-current interaction

$$\mathcal{L}_{\beta-decay} = G_F j_\mu^{n\to p} j_{e\to\nu}^\mu = G_F(\bar{p}\gamma_\mu n)(\bar{e}\gamma^\mu \nu). \tag{4.1}$$

This interaction was successful in also describing some other weak processes such as pion and muon decay. All these processes showed nearly the same strength in weak interactions which suggested a universality of weak interactions. However, some unexplainable behaviour was observed in other weak processes, such as the theta-tau puzzle (θ and τ which had the same mass and lifetime would decay into final states with different parities). This peculiarity was resolved in 1956 by the bold assumption of Lee and Yang, who considered the weak interactions to be parity violating [53] and that θ and τ are in fact the same particle (now known as K^+). In 1957-1958, Marshak and Sudarshan [54] and Feynman and Gell-Mann [55] incorporated parity violation into the Lagrangian by modifying it to a V-A (Vector-Axial vector) theory. At that time, experiments suggested that there was a suppression of strangeness-changing processes compared to the strangeness-conserving ones in weak decays and the universality of weak interactions was again questioned. To keep the universality of weak interactions, in 1963 Cabibbo used current algebra to show that the V-A current should have unit length [3]. In the quark language (which would be later developed), the Hamiltonian that Cabibbo proposed is

$$H = \bar{u}\gamma_\mu(1-\gamma_5)[d\cos\theta + s\sin\theta], \tag{4.2}$$

where θ is the Cabibbo angle. Cabibbo's hypothesis further implied that flavour-changing neutral current (FCNC) processes should be of the same order as those mediated by flavour-changing charged currents, and this was in contradiction with observation. To solve this problem, in 1970 Glashow, Iliopoulos and Maiani suggested a mechanism (the GIM mechanism) which required a fourth quark (the charm quark), and which would lead to a cancellation of FCNC processes [8]. Still there remained some theoretical problems with the now modified Fermi interaction: when parity violation was observed, it was assumed that charge conjugation accompanied with parity would be conserved (CP-conservation). However, in 1964, CP violation was observed in the decay of some neutral Kaons [56] while there was no theoretical explanation to justify it. To explain and accommodate CP violation observed in experiments, Kobayashi and Maskawa postulated in 1974 the existence of a third family of quarks, and replaced the orthogonal Cabibbo rotation of down quarks with a unitary rotation (the CKM matrix) which allows for CP violation. Another lingering problem was the nonrenormalisability of Fermi's interaction, since until the late 1960s, weak interactions were described by a set of nonrenormalisable dimension 6 four-fermion operators. The nonrenormalisability of the Fermi interaction would work as one of the strongest incentives for the construction of the SU(2)×U(1) gauge structure which is now incorporated into the Standard Model.
An effective description which began as a way to explain β-decays proved to be crucial in the development of the Standard Model. Even in modern particle physics, where the full theory that describes weak interactions is well known, it is still convenient to use an effective electroweak theory to describe the low energy behavior of weak interactions. Not only does it simplify some calculations, but it also allows for higher order calculations by resummation of large logarithms. Moreover, new physics effects is conveniently implemented in the effective framework.

4.2 Effective field theory for quark weak interactions

In this section we will present the EFT for weak transitions of quarks using the top down approach. To demonstrate how this is done, it is interesting to derive Fermi's interaction from the full electroweak theory. One of the fundamental tools in deriving an effective theory is operator product expansion (OPE), introduced by Kenneth Wilson [57, 58]; in this framework if two operators $A(x_1)$ and $B(x_2)$ are separated by a small distance ($(x_1 - x_2) \approx 0$), then the product of operators can be replaced with a linear combination of local operators

$$A(x_1)B(x_2) \underset{(x_1-x_2)_\mu \to 0}{\approx} \sum_i C_i(x_1 - x_2) O_i \left(\frac{x_1 + x_2}{2} \right), \tag{4.3}$$

where the $C_i(x_1 - x_2)$ are c-number functions – Wilson coefficients –, and O_i are local operators that have the same quantum numbers as AB. The Wilson coefficients $C_i(x)$ are singular at $x \to 0$ and dimensional analysis shows the dimension of $C_i(x)$ to be $d_{C_i} = d_A + d_B - d_{O_i}$, where d_A, d_B and d_{O_i} are the dimensions of the operators A, B

and O_i, respectively. The higher the dimension of the corresponding operator O_i, the less singular will the coefficients $C_i(x)$ be; this makes the operators with the smallest dimension the most relevant, and usually a small number of operators is sufficient in the expansion. For renormalisable theories, the expansion is valid to any finite order of perturbation provided $(x_1 - x_2)$ is sufficiently small. The Wilson coefficients contain the short distance physics contribution and are process independent, which makes them relevant for different decays.

As an example of the top down approach, we use the electroweak theory to write the amplitude of the quark transition $c \to su\bar{d}$ at tree level (Figure 4.2);

$$\mathcal{M}_{full} = (i)\frac{ig_2}{2\sqrt{2}}V_{cs}^{*}\,\bar{s}\gamma^{\mu}(1-\gamma^5)c\left(\frac{-ig_{\mu\nu}}{q^2 - M_W^2}\right)\frac{ig_2}{2\sqrt{2}}V_{ud}\,\bar{u}\gamma^{\nu}(1-\gamma^5)d, \tag{4.4}$$

where q is the four momentum of the W boson. The amplitude contains the product of two dimension 3 operators, $(\bar{s}P_Lc)$ and $(\bar{u}P_Ld)$, at two different points, with P_L defined in (2.2). We would like to replace the product of the operators with a linear combination of local operators; an effective Hamiltonian containing local operators can be written as

$$\mathcal{H}_{eff} = \frac{4G_F}{\sqrt{2}}V_{cs}^{*}V_{ud}\Big\{C \times [(\bar{s}P_Lc)(\bar{u}P_Ld)] + \dots\Big\}, \tag{4.5}$$

where C is the Wilson coefficient and $O = [(\bar{s}P_Lc)(\bar{u}P_Ld)]$ the local dimension six operator, the ellipsis denotes higher dimension operators which usually involve derivative terms and G_F is the Fermi constant

$$\frac{G_F}{\sqrt{2}} = \frac{g_2^2}{8M_W^2}. \tag{4.6}$$

The operator O can be considered as an effective vertex and the Wilson coefficient C the corresponding coupling. The value of the Wilson coefficient can be obtained by equating the full and effective amplitudes since the amplitudes should be the same in both "theories". This procedure is called *matching*, and is the first step in constructing the effective theory.

In the full theory, if we consider that the momentum of the W propagator is much smaller than the W boson mass ($q^2 \ll M_W^2$), the propagator can be expanded in powers of the small ratio (q^2/M_W^2), so that in this limit the amplitude in (4.4) becomes

$$\mathcal{M}_{full} = \frac{4G_F}{\sqrt{2}}V_{cs}^{*}V_{ud}(\bar{s}\gamma^{\mu}P_Lc)(\bar{u}\gamma_{\mu}P_Ld) \times \left(1 + \frac{q^2}{M_W^2} + \dots\right). \tag{4.7}$$

On the other hand, for the amplitude of the effective theory we find

$$\mathcal{M}_{eff} = \langle\mathcal{H}_{eff}\rangle = \frac{4G_F}{\sqrt{2}}V_{cs}^{*}V_{ud}\Big\{C \times \langle O\rangle + \dots\Big\}. \tag{4.8}$$

Figure 4.2.: The $c \to su\bar{d}$ transition in the full theory on left and in the effective theory on right.

Matching the first terms in (4.7) and (4.8), the Wilson coefficient is obtained

$$C = 1. \tag{4.9}$$

However, this value for the Wilson coefficient is only valid at tree-level and gets modified at loop-level. In terms of Feynman diagrams, the effective operators are obtained by contracting the lines corresponding to heavy particles to a point. In Figure 4.2, the tree level W-exchange diagram corresponding to the full theory is shown on the left while the diagram corresponding to the first term in the effective Hamiltonian is depicted on the right.

To better see how OPE is crucial in obtaining the effective theory, the W propagator can alternatively be expanded in position space

$$\begin{aligned} \langle 0|\mathbf{T}\{W_\mu(x_1)W_\nu(x_2)\}|0\rangle &= \int \frac{d^4q}{(2\pi)^4} e^{-iq(x_1-x_2)} \frac{-ig_{\mu\nu}}{M_W^2 - q^2} \\ &= \frac{-ig_{\mu\nu}}{M_W^2}\left(1 - \frac{\partial^2}{M_W^2} + \dots\right)\delta^4(x_1 - x_2), \end{aligned} \tag{4.10}$$

where $\mathbf{T}$ is the time ordering operator. The nonlocality of the product of the charged currents in the full theory is determined by the Compton wavelength, $1/M_W$. Since for small momenta of the W, the distance between the currents is close to zero, it is appropriate to use OPE. From (4.10), it is clear that if higher dimension operators in (4.5) were to be considered, they would correspond to the derivative terms.

Considering the underlying quark process involved in the β-decay (Figure 4.3), Fermi's interaction can now be obtained from the effective theory. Replacing the charm-strange-W vertex in (4.5) with an electron-antineutrino-W vertex we get

$$\mathcal{H}_{d\to u\, e\, \bar{\nu}} = \frac{G_F}{\sqrt{2}} V_{ud}[(\bar{e}\nu)_{V-A}\,(\bar{u}d)_{V-A}] + \cdots . \tag{4.11}$$

Noting that $V_{ud} \approx 1$, Fermi's interaction is recovered with the neutron and proton replaced

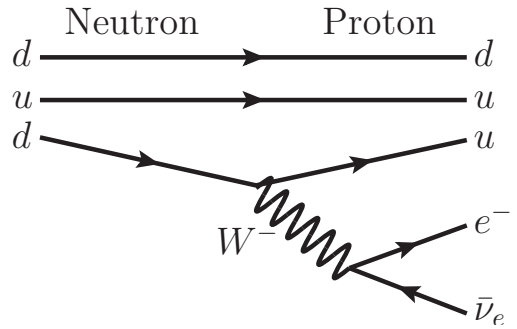

Figure 4.3.: The tree level quark process of the β-decay where a d-quark decays to a u-quark, with the emission of an electron-antineutrino pair.

with a d- and u-quark, respectively. The other two quarks are spectators and do not play a role in the decay.
So far QCD effects were neglected in obtaining the effective Hamiltonian in (4.5). The inclusion of QCD effects will result in the appearance of new operators, as well as in modifications in Wilson coefficients. To include the QCD corrections, further integrations over virtual momenta has to be done, resulting in infinite terms which require renormalisation. We proceed to address these issues in the following section.

4.3 Renormalisation procedure

The QCD Lagrangian is [59]:

$$\begin{aligned}\mathcal{L}_{QCD} = &-\frac{1}{4}(\partial_\mu A^a_\nu - \partial_\nu A^a_\mu)(\partial^\mu A^{a\nu} - \partial^\nu A^{a\mu}) - \frac{1}{2\xi}(\partial^\mu A^a_\mu)^2 \\ &+ \bar{q}_\alpha(i\ \partial\!\!\!/ - m_q)\delta_{\alpha\beta}q_\beta + \chi^{a*}\partial^\mu\partial_\mu\chi^a \\ &- \frac{g_s}{2}f^{abc}(\partial_\mu A^a_\nu - \partial_\nu A^a_\mu)A^{b\mu}A^{c\nu} - \frac{g_s^2}{4}f^{abe}f^{cde}A^a_\mu A^b_\nu A^{c\mu}A^{d\nu} \\ &+ g_s\bar{q}_\alpha T^a_{\alpha\beta}\gamma^\mu q_\beta A^a_\mu + g_s f^{abc}(\partial^\mu\chi^{a*})\chi^b A^c_\mu. \end{aligned} \tag{4.12}$$

Here A^a_μ and χ^a are the gluon and ghost fields, respectively, and ξ is the gauge parameter. For q_α, $\alpha(=1,2,3)$ indicates the colour of the quark flavour q ($q = u, d, c, s, t, b$) and g_s is the QCD coupling. T^a, f^{abc} (a, b, $c = 1,\ldots,8$) are the generators and structure constants of $SU(3)$, respectively.
Using the Feynman rules derived from $\mathcal{L}_{QCD}$, the amplitude of any process can be calculated at any order in perturbation theory. However, going beyond tree level calculations necessarily includes contributions of divergent loop integrals, but these divergences can be isolated by regularisation, where the divergent integral is written as the limit of a convergent integral. These mathematically manageable integrals can then be taken care

of by renormalisation. There are several techniques of regularisation such as dimensional regularisation [60], the cut-off method [61] and Pauli-Villars regulator method [62]. Depending on the method of regularisation, some of the underlying physical requirements such as Lorentz invariance, unitarity and gauge invariance might be violated. Unlike the cut-off method, dimensional regularisation preserves the gauge invariance of the regularised theory. It further preserves Lorentz invariance and unitarity, and is hence suitable for gauge theories.

4.3.1 Dimensional regularisation

The basic idea of dimensional regularisation is rendering a divergent integral into a convergent one, by reducing the number of multiple integrals. For example, while $\int d^4k/k^3$ is divergent in 4-dimensional spacetime, it is convergent in 2-dimensions. By reducing the $D = 4$ spacetime to $D = 4-2\epsilon$, the D-dimensional integral $\int d^Dk$ becomes convergent and can be expressed in terms of an analytical function of D. The original divergence can be recovered in the limit $D \to 4$. Since the action $S = \int d^Dx\mathcal{L}$, has to be dimensionless, the Lagrangian should have dimension D. As a result, the different parameters of the QCD Lagrangian will have modified dimensions. In D-dimensions, the strong coupling constant g_s acquires mass dimension $(4 - D)/2$. To keep the coupling constant dimensionless, as it was in $D = 4$, one uses the following replacement

$$g_s \to g_s\mu^{(4-D)/2}, \tag{4.13}$$

where μ is an arbitrary mass scale, called the renormalisation scale. With the replacement in relation (4.13), we now have a dimensionless coupling constant on the right hand side. The divergences will then manifest themselves as $1/\epsilon$ poles.
Dimensional regularisation preserves all of the physical requirements (e.g. gauge invariance, unitarity), but there is no mathematically consistent generalisation of γ^5, in D dimension. However, various computational rules are available, where an operational definition of γ^5 is used. Among the different schemes available are, Naive Dimensional Regularisation (NDR) [63–65], and the 't Hooft-Veltman (HV) scheme [66–68].

4.3.2 Renormalisation

In the renormalised theory, the divergences emerging from loop integrals can be removed by adjusting the parameters and fields in the Lagrangian. The unrenormalised, so-called *bare* quantities, can be written as products of suitable multiplicative factors and renormalised quantities

$$\begin{aligned} m^B &= Z_m m, & g_s^B &= Z_g g_s \mu^\epsilon, & \xi^B &= Z_3 \xi, \\ A_\mu^{a,B} &= Z_3^{1/2} A_\mu^a, & q^B &= Z_q^{1/2} q, & \chi^{B,a} &= \tilde{Z}_3^{1/2} \chi^a, \end{aligned} \tag{4.14}$$

where the superscript B stands for bare. On the right hand side of the above equations, the quantities without superscript are the renormalised parameters. The multiplicative

factors $Z_i (i = m, g, 3 \text{ and } q)$ are called renormalisation constants, and are chosen such that they compensate the divergences. The unrenormalised truncated connected Green function $\tilde{G}^{tc}(p; g_s^B, m^B)$, with n_F quark and n_G gluon external legs, is thus related to the renormalised Green function by

$$\tilde{G}^{tc}(p; g_s^B, m^B) = Z_3^{-n_G/2} Z_q^{-n_F/2} \tilde{G}_R^{tc}(p; g_s, m, \mu). \tag{4.15}$$

However, there is an ambiguity in defining the divergent piece within the Green function. This leads to further ambiguities in the values of the renormalisation constants. The prescription to choose the renormalisation constants is called the renormalisation scheme, and the most common one for QCD calculations is the modified minimal subtraction ($\overline{MS}$) scheme [69]. In this scheme, the $1/\epsilon$ poles, and the accompanying $(-\gamma_E + \ln 4\pi)$ term, which is peculiar to dimensional regularisation are removed from the unrenormalised theory.
Regardless of the choice of scheme, any two renormalisation schemes are connected by a finite renormalisation. Even though calculations depend on the chosen scheme, the physical predictions should not: this statement leads to the Renormalisation Group Equations (RGE).

4.3.3 Renormalisation Group Equation

Let us consider two different renormalisation procedures, R and R', since both are derived from the same bare Lagrangian we must have

$$\mathcal{L}^R(R\text{-quantities}) = \mathcal{L}^{R'}(R'\text{-quantities}). \tag{4.16}$$

In terms of these two schemes, for the quark fields we can write

$$q^B = Z_q^{1/2}(R) q^R = Z_q^{1/2}(R') q^{R'}, \tag{4.17}$$

and therefore

$$q^{R'} = Z_q^{-1/2}(R, R') q^R, \tag{4.18}$$

where

$$Z_q(R', R) = \frac{Z_q(R')}{Z_q(R)}. \tag{4.19}$$

The quark field renormalisation constants in different schemes are related by a multiplicative factor which is finite [70]. Similar equations can be written for other fields and parameters as well as for the Green function. The operators that relate one scheme to another can be viewed as transformations between different schemes. Nonetheless, the physics of the theory should be invariant under these transformations. The set of all these transformations form the renormalisation group, and the differential equations which encode the effect of change in renormalisation scale μ, on the Green functions and on the

different parameters are renormalisation group equations.
Using (4.14) and noting that the bare coupling constant and mass are independent of μ, we find

$$\frac{dg^B}{d\mu} = \frac{dZ_g}{d\mu} g_s \mu^\epsilon + \frac{dg_s}{d\mu} Z_g \mu^\epsilon + \epsilon \mu^{\epsilon-1} Z_g g_s = 0, \tag{4.20}$$

$$\frac{dm^B}{d\mu} = \frac{dZ_m}{d\mu} m + \frac{dm}{d\mu} Z_m = 0. \tag{4.21}$$

Defining the β-function and γ_m through

$$\beta \equiv \frac{dg(\mu)}{d\ln\mu}, \tag{4.22}$$

$$-m\gamma_m \equiv \frac{dm}{d\ln\mu}, \tag{4.23}$$

we can obtain the RGEs for the coupling constant and mass:

$$\beta = -\epsilon g_s - g_s \mu \frac{1}{Z_g}\frac{dZ_g}{d\mu}, \tag{4.24}$$

$$\gamma_m = \frac{1}{Z_m}\frac{dZ_m}{d\ln\mu}, \tag{4.25}$$

where γ_m is called the anomalous mass dimension[2].
Although in general Z_g and Z_m are functions of μ, g_s, m and ξ, in the MS ($\overline{MS}$) scheme, they are only explicitly dependent on g_s, making this scheme of particular interest in QCD. The fact that in the MS ($\overline{MS}$) scheme, β and γ_m become independent of m is why the MS scheme is referred to as the mass-independent renormalisation scheme.
The RGEs are crucial for deriving the properties of QCD. The β-function encodes the dependence of the coupling constant on the scale μ and the energy-dependence of the coupling constant manifests in its designation: effective or running coupling constant $g_s(\mu)$. The β-function has the perturbative expansion

$$\beta(g) = -\frac{g_s^3}{16\pi^2}\beta_0 - \frac{g_s^5}{(16\pi^2)^2}\beta_1 - \frac{g_s^7}{(16\pi^2)^4}\beta_2 + \cdots . \tag{4.26}$$

The calculation of the leading term in β-function (β_0), requires the renormalisation constant Z_g up to one loop. Considering the loop correction to the gluon-quark-quark vertex, we have

$$Z_g = 1 - \frac{g_s^2}{16\pi^2}\frac{1}{2}\left(\frac{11N_c - 2N_f}{3}\right) + \mathcal{O}(g_s^4), \tag{4.27}$$

where N_C is the number of colours and N_f is the number of active quark flavours. Hence

[2]It is called the anomalous dimension since it indicates the deviation of the canonical dimension from the scale dimension [71].

using (4.24), we get

$$\beta_0 = \frac{11N_c - 2N_f}{3}. \tag{4.28}$$

The lowest order solution to the coupling constant RGE, in terms of $\alpha_s = g_s^2/4\pi$, gives us the relation between the coupling constant at two different scales, μ and μ_0

$$\alpha_s(\mu) = \frac{\alpha_s(\mu_0)}{1 - \frac{\alpha_s(\mu_0)}{4\pi}\beta_0 \ln\frac{\mu_0^2}{\mu^2}}. \tag{4.29}$$

The sign of β_0 is crucial in describing the behavior of the coupling constant: since for QCD $N_c = 3$, if the number of flavours is less than $33/2$, β_0 has a positive sign: and this means that by increasing the energy scale, the QCD coupling constant decreases, resulting in the theory being asymptotically free [72,73]. Conversely, for quantum electrodynamics, the sign of β_0 is negative and hence QED is not an asymptotically free theory. On the other hand, decreasing the energy scale implies that the QCD coupling constant becomes stronger, up to the point where perturbation theory is no longer suitable. The energy scale at which this happens is referred to as the QCD scale parameter Λ_{QCD}, and is defined in such way that for an arbitrary scale Q, we have [74]

$$\alpha_s(Q) = \frac{1}{\frac{\beta_0}{4\pi}\ln\frac{Q^2}{\Lambda_{QCD}^2}}, \tag{4.30}$$

which formally means that at Λ_{QCD}, $\alpha_s \to \infty$. The value of Λ_{QCD} depends on the renormalisation scheme as well as on the number of effective flavours that we are considering. Its definition also depends on the number of loops that have been accounted for, when solving the RGE of the coupling constant. The strong scale Λ_{QCD} is determined by comparing experimental data with QCD predictions. Considering terms up to β_3 in the expansion of the β-function (4.26) and using $\alpha_s(M_Z) = 0.1184$, the value of Λ_{QCD} in the $\overline{MS}$ scheme is [15]

$$\Lambda_{\overline{MS}}^{(5)} = (213 \pm 8)\ \text{MeV}. \tag{4.31}$$

Here the superscript denotes the number of active flavours which for example in the case of B-decays is five.

The power of RGEs can be better realised by noticing that in perturbation theory, the running term $(\alpha_s(\mu_0)\ln(\mu_0/\mu))$ is actually the leading radiative correction term. Usually the scale at which renormalisation is performed (μ_0), is of the same order of the typical momentum scale of the process (μ). Hence the argument of the logarithm which is typical to radiative corrections is of order $\mathcal{O}(1)$. Therefore the first few terms of an expansion in α_s are sufficient. However, for a process involving disparate energy scales ($\mu \ll \mu_0$), which is the case of weak decays of hadrons, radiative corrections due to the appearance of large logarithms can be substantial, and a truncation in the expansion of α_s is no longer justified. On the other hand, solving the RGE provides automatic summation of these

large logarithms, and this can be easily seen by expanding (4.29) in powers of α_s

$$\begin{aligned}\alpha_s(\mu) &= \frac{\alpha_s(\mu_0)}{1-\frac{\alpha_s(\mu_0)}{4\pi}\beta_0 \ln\frac{\mu_0^2}{\mu^2}} \\ &= \alpha_s(\mu_0)\left[1+\frac{\beta_0}{4\pi}\alpha_s(\mu_0)\ln\frac{\mu_0^2}{\mu^2}+\left(\frac{\beta_0}{4\pi}\alpha_s(\mu_0)\ln\frac{\mu_0^2}{\mu^2}\right)^2+\ldots\right] \\ &= \alpha_s(\mu_0)\sum_{n=0}\left(\frac{\beta_0}{4\pi}\alpha_s(\mu_0)\ln\frac{\mu_0^2}{\mu^2}\right)^n .\end{aligned} \tag{4.32}$$

Here, the solution of RGE contains all powers of $(\alpha_s(\mu_0)\ln(\mu_0/\mu))$. The RGE gives an improvement of the perturbation theory, and in that sense results in the renormalisation group improved perturbation theory.

To obtain the solution of the coupling constant RGEs we considered only one-loop corrections, a level of accuracy which is called "leading logarithm (LL) approximation". At next-to-leading order (NLO), two-loop corrections must also be considered. Solving the RGE, terms of the form

$$\alpha_s(\mu_0)^n\left(\ln\frac{\mu_0}{\mu}\right)^{n-1}, \tag{4.33}$$

appear, resulting in a summation of next-to-leading logarithm (NLL) approximation. In a similar way, three-loop corrections results in the summation of

$$\alpha_s(\mu_0)^n\left(\ln\frac{\mu_0}{\mu}\right)^{n-2} \tag{4.34}$$

terms in a next-to-next-to-leading logarithm (NNLL) approximation.

4.4 QCD corrections to electroweak processes

In this section we, introduce the QCD corrections from [59, 75] for the sake of being self-contained. QCD corrections have a profound effect on the weak interactions. At order α_s in the full theory the $c \to su\bar{d}$ process receives one-loop QCD corrections from the diagrams of Figure 4.4. In order to calculate the NLO Wilson coefficients of the effective theory, the QCD effects should be computed both for the full and effective theory. Matching the effective and full theory as in Section 4.2 allows to obtain the Wilson coefficients. The inclusion of QCD effects will not only change the value of the Wilson coefficients but it will also introduce new operators.

The contribution of the second diagram in Figure 4.4 to the amplitude (in the Feynman-

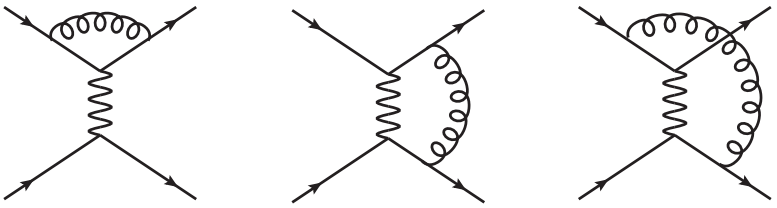

Figure 4.4.: Illustrative examples of QCD contributions in the full theory.

t' Hooft gauge) is [75]

$$\int \frac{d^4k}{(2\pi)^4} V_{cs}^* V_{ud} \frac{4G_F}{\sqrt{2}} \left(\frac{M_W^2}{M_W^2 - k^2}\right) g_s^2 \frac{k^2}{k^6} (\bar{s}\gamma^\nu T^a_{\alpha\beta}\gamma^\lambda\gamma^\mu P_L c)(\bar{u}\gamma_\nu T^a_{\lambda\rho}\gamma_\lambda\gamma_\mu P_L d), \tag{4.35}$$

where the loop momentum k is taken to be much larger than all external momenta. Using Fierz identities, in four dimension we can write

$$(\bar{s}_L\gamma^\nu\gamma^\lambda\gamma^\mu c_L)(\bar{u}_L\gamma_\nu\gamma_\lambda\gamma_\mu d_L) = 16(\bar{s}_L\gamma^\nu P_L c)(\bar{u}\gamma_\nu d_L), \tag{4.36}$$

with $q_{L(R)}$ the left(right)-handed quark.

$$q_{L(R)} = P_{L(R)}q. \tag{4.37}$$

Were it not for the $T^a_{\alpha\beta}T^a_{\lambda\rho}$ term, the above gluon loop would only give a correction to the operator

$$O_2 = (\bar{s}\gamma^\mu P_L c)(\bar{u}\gamma_\mu P_L d) \equiv (\bar{s}_\alpha\gamma^\mu P_L c_\alpha)(\bar{u}_\beta\gamma_\mu P_L d_\beta), \tag{4.38}$$

which was already present in the tree level weak interaction. However, considering the $SU(N)$ generator identity for the $T^a_{\alpha\beta}T^a_{\lambda\rho}$ term we have

$$T^a_{\alpha\beta}T^a_{\lambda\rho} = \frac{1}{2}\delta_{\alpha\rho}\delta_{\lambda\beta} - \frac{1}{2N}\delta_{\alpha\beta}\delta_{\lambda\rho}. \tag{4.39}$$

and it becomes clear that the first term on the right hand side of the above equation will give rise to a new operator

$$O_1 = (\bar{s}_\alpha\gamma^\mu P_L c_\beta)(\bar{u}_\beta\gamma_\mu P_L d_\alpha), \tag{4.40}$$

while the second term on the right hand side of (4.39) results in an operator with the same structure as O_2. Likewise, the third diagram in Figure 4.4 involves both of the operators O_1 and O_2. Let us now bring together all the diagrams contributing to $c \to su\bar{d}$ process: tree-level, as well as the one-loop QCD corrections[3] depicted in Figure 4.4, we find the

[3] The first diagram in Figure 4.4 corresponds to quark field renormalisation. One-loop external quark field renormalisation is the same in both the full and effective theory, therefore they can be omitted

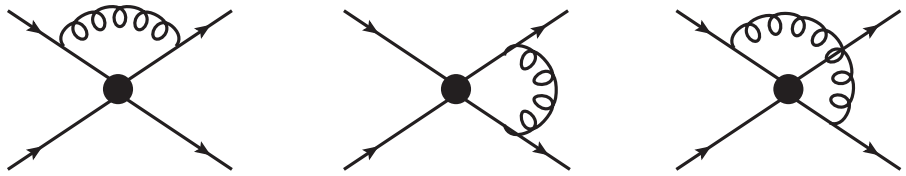

Figure 4.5.: QCD contributions in the effective theory.

following amplitude [75]

$$\mathcal{M}_{full} = \frac{4G_F}{\sqrt{2}} V_{cs}^* V_{ud} \left[1 \times O_2 + \frac{3}{N} \frac{\alpha_s}{4\pi} \ln \frac{M_W^2}{p^2} O_2 - 3 \frac{\alpha_s}{4\pi} \ln \frac{M_W^2}{p^2} O_1 \right], \tag{4.41}$$

where the lower limit of the logarithm (p^2) is set by the external momenta. The coefficient of the first term ($= 1$) corresponds to the tree-level diagram while the second and third terms are the corrections emerging from the one-loop diagrams of Figure 4.4, discussed above.

To perform the matching, the QCD contributions to the effective theory shown in Figure 4.5 should be considered. The effective Hamiltonian should then be generalised to contain both the operators O_1 and O_2

$$\mathcal{H}_{eff} = \frac{4G_F}{\sqrt{2}} V_{cs}^* V_{ud} \left(C_1 O_1 + C_2 O_2 \right). \tag{4.42}$$

Considering (4.35), it can easily be seen that the loop diagrams of the full theory are not divergent. For the effective theory however, since the W-boson propagator is replaced by $1/M_W^2$, the loop diagrams diverge. In this case the $M_W^2/(M_W^2 - k^2)$ term in the integral in (4.35) is replaced by 1 which removes a k^2 factor from the denominator. In order to match the effective theory onto the full theory the divergences should be removed, and this can be achieved by operator renormalisation

$$O_i = Z_{ij} O_j^R, \tag{4.43}$$

where Z_{ij} are the matrix elements of the operator renormalisation constant. The amplitude of the renormalised theory

$$\mathcal{M}_{eff} = \frac{4G_F}{\sqrt{2}} V_{cs}^* V_{ud} \left(C_1 O_1^R + C_2 O_2^R \right), \tag{4.44}$$

in both cases as they will not have any consequence in the matching.

written in terms of the operators O_1 and O_2 is

$$\mathcal{M}_{eff} = -i\frac{4G_F}{\sqrt{2}}\Bigg\{C_1\Bigg[(1+\frac{3}{N}\frac{\alpha_s}{4\pi}\ln\frac{\mu^2}{p^2}O_1) - 3\frac{\alpha_s}{4\pi}\ln\frac{\mu^2}{p^2}O_2\Bigg] \\ +C_2\Bigg[-3\frac{\alpha_s}{4\pi}\ln\frac{\mu^2}{p^2}O_1 + (1+\frac{3}{N}\frac{\alpha_s}{4\pi}\ln\frac{\mu^2}{p^2}O_2)\Bigg]\Bigg\}. \tag{4.45}$$

Matching the above equation to that of (4.41) we finally have the Wilson coefficients

$$C_1 = -3\frac{\alpha_s}{4\pi}\ln\frac{M_W^2}{\mu^2}, \qquad C_2 = 1+\frac{3}{N}\frac{\alpha_s}{4\pi}\ln\frac{M_W^2}{\mu^2}. \tag{4.46}$$

Due to the renormalisation, a scale dependence has appeared in the Wilson coefficients. In the matching the value of μ should be $\mathcal{O}(M_W)$, otherwise the NLO results would be comparable to the LO terms, which would break the validity of the perturbation theory. However, the energy of the decay is of order of the quark masses ($\sim m_c$), and the $\ln\frac{M_W^2}{m_c}$ should be resummed which can be done by RG methods as mentioned in Section 4.3.

4.5 RGE for the Wilson coefficients

The renormalisation procedure of the effective theory in the previous section (performed for the operators) can alternatively be done for the corresponding Wilson coefficients

$$C_i^B = Z_{ij}^C C_j^R. \tag{4.47}$$

Nonetheless, the operator renormalisation constant ($\hat{Z}$) and the Wilson coefficient renormalisation constant ($\hat{Z}^C$) are related. Noting that renormalising C_is or O_is should lead to the same result for the amplitude, we have

$$Z_{ij}^C = Z_{ji}^{-1}. \tag{4.48}$$

To obtain the RGE for the $C_i(\mu)$s, as mentioned in Section 4.3 we use the fact that the bare quantities are μ-independent. From (4.47) we get

$$\frac{dC_i^R}{d\ln\mu} = Z_{ij}^{-1}\frac{dZ_{ij}}{d\ln\mu}C_i, \tag{4.49}$$

and defining the anomalous dimension as

$$\hat{\gamma} = Z^{-1}\frac{d\hat{Z}}{d\ln\mu}, \tag{4.50}$$

the solution to (4.49) is found to be

$$\vec{C}(\mu) = \hat{U}(\mu,\mu_0)\vec{C}(\mu_0), \tag{4.51}$$

where $\hat{U}$ is the evolution matrix from the matching scale μ_0 to the low energy scale of the decay (μ)

$$\hat{U}(\mu,\mu_0) = \exp \int_{g(\mu_0)}^{g(\mu)} dg' \frac{\hat{\gamma}^T(g')}{\beta(g')}. \tag{4.52}$$

The anomalous dimension is in general a matrix which can be perturbatively obtained in g_s

$$\hat{\gamma} = \frac{g^2}{16\pi^2}\hat{\gamma}^{(0)} + (\frac{g^2}{16\pi^2})^2\hat{\gamma}^{(1)} + \ldots, \tag{4.53}$$

with $\gamma^{(0)}$ and$\gamma^{(1)}$ the one and two loop anomalous dimension matrices. In the special case in which γ is a number the lowest order solution for the Wilson coefficient at the scale μ is obtained by using the first term of the γ expansion, as well as the first term of the β expansion (4.26)

$$C(\mu) = \eta^{\frac{\gamma^0}{2\beta_0}}, \tag{4.54}$$

where $\eta \equiv \alpha_s(\mu_0)/\alpha_s(\mu)$. The general case where the anomalous dimension is a matrix is given in Appendix A. The RG running of the Wilson coefficients to low energies is the second step in obtaining the effective low energy weak theory.

4.6 Matrix elements

To obtain physical results for a process we need the decay amplitude, which within the effective theory can be written as

$$\mathcal{A}(i \to f) = \langle f|\mathcal{H}_{eff}|i\rangle \equiv \frac{4G_F}{\sqrt{2}} f(V_{\rm CKM}) \sum_i C_i(\mu)\langle f|O_i(\mu)|i\rangle. \tag{4.55}$$

Here $f(V_{\rm CKM})$ stands for some product of the CKM matrix entries which depends on the process under consideration and $\langle f|O_i(\mu)|i\rangle$ are the matrix elements of O_i. The computation of the matrix elements is the last step within the effective theory.

The matrix elements encode all the long-distance (LD) physics effects from scales lower than μ. This can be understood by considering that loop corrections to the effective four-fermion vertex have integrals that can be cast as

$$\int_p^{M_W} d^4k \frac{1}{k^4} = \int_p^{\mu} d^4k + \frac{1}{k^4}\int_\mu^{M_W} d^4k \frac{1}{k^4}, \tag{4.56}$$

clearly manifesting the separation between the short-distance (SD) and LD contributions through the renormalisation scale (μ), which is present due to dimensional regularisation.

The amplitude obtained from the renormalised effective theory takes the general form

$$\left(1+\alpha_s \ln \frac{M_W^2}{\mu^2}\right)\left(1+\alpha_s \ln \frac{\mu^2}{p^2}\right), \tag{4.57}$$

where the high-energy logarithms ($\ln M_W^2/\mu^2$) enter the Wilson coefficients (e.g. (4.46)) and the low-energy logarithms ($\ln \mu^2/p^2$) are contained in the matrix elements. Thus it is the choice of μ that dictates whether a contribution is encoded in C_i or $\langle O_i \rangle$.

So far, in the matching process and in the running of the Wilson coefficients, the effective theory has been constructed in a perturbative way. However, when there are hadrons in the initial and/or final states, calculations of the matrix elements require non-perturbative methods.

Extracting quark interactions from hadronic interactions is a highly nontrivial task. Thus, in general one can achieve more precise results if less hadrons are involved. One example where there is only one hadron present is the leptonic decay of the π meson. The amplitude of the $\pi^- \to \ell\bar{\nu}$ decay within the effective theory is

$$\mathcal{A} = \langle \ell\nu|\mathcal{H}_{eff}|\pi^-\rangle \equiv \frac{4G_F}{\sqrt{2}} f(V_{\rm CKM}) \sum_i C_i(\mu)\langle \ell\bar{\nu}|O_i(\mu)|\pi\rangle. \tag{4.58}$$

At leading order for this process there is only one relevant operator

$$O = (\bar{u}\gamma^\mu P_L d)(\bar{\ell}\gamma_\mu P_L \nu), \tag{4.59}$$

with Wilson coefficient $C = 1$ and $f(V_{\rm CKM}) = V_{ud}$, which can be easily understood from the previous discussions. At leading order this decay has the same structure of the $c \to su\bar{d}$ process with the c and s quarks replaced with a lepton and an antineutrino. This operator can be factorised into leptonic and hadronic currents as follows

$$O = (\bar{u}\gamma^\mu P_L d)(\bar{\ell}\gamma_\mu P_L \nu) \equiv O_H O_\ell, \tag{4.60}$$

which leads to the factorisation of the matrix elements into leptonic and hadronic parts

$$\mathcal{A} = \frac{4G_F}{\sqrt{2}} V_{ud} \langle \ell\nu|O_\ell|0\rangle\langle 0|O_H|\pi\rangle. \tag{4.61}$$

The leptonic matrix element $\langle O_\ell \rangle$, can be calculated in a straightforward way since ℓ and ν are asymptotic states, whose annihilation and creation operators appear in O_L. On the other hand, the hadronic matrix element requires non-perturbative techniques since the initial and final states are not asymptotic quarks but physical hadrons in the confinement regime of QCD. Writing the hadronic current in terms of a vector and axial vector part we have

$$O_H = \bar{u}\gamma^\mu P_L d = \frac{1}{2}\left[(\bar{u}\gamma^\mu d) - (\bar{u}\gamma^\mu\gamma^5 d)\right]. \tag{4.62}$$

While the hadronic matrix element cannot be calculated from first principles it can

nonetheless be parametrised in terms of a decay constant which is defined via the axial vector current as [76]

$$\langle 0|\bar{u}\gamma^{\mu}\gamma^{5}d|\pi^{-}\rangle = ip^{\mu}f_{\pi}. \tag{4.63}$$

In the above, p^{μ} is the momentum of the π meson (the only available dynamical variable) and its presence is necessary to get the required Lorentz structure. f_{π} is the pion decay constant which encodes all the information relevant for the confinement of the quark-antiquark pair in the meson. The amplitude can thus be written in terms of the pion decay constant as

$$\mathcal{A} = \frac{4G_F}{\sqrt{2}}V_{ud}\left(\frac{ip^{\mu}f_{\pi}}{2}\right)\langle \ell\nu|O_{\ell}|0\rangle. \tag{4.64}$$

The reason why only the axial current part of O_H is relevant for the $\langle 0|O_H|\pi\rangle$ matrix element can be understood by noting that π is a pseudoscalar with odd parity while the vacuum is parity even. Since the vectorial current is a parity even operator, only the axial part of O_H can have a non-vanishing contribution to the amplitude [77]. This type of symmetry argument can be useful when there are various operators of the form $(\bar{u}\,\Gamma\,d)$ giving the same quark transition but each associated to a different Dirac structure $(\,\Gamma\,)$.

In general, one-particle matrix elements are described through decay constants. Moreover, in processes where two hadrons are present, the matrix elements can be parametrised in terms of form factors. The semileptonic decay $\bar{B} \to D^{*+}\bar{\ell}\nu$ is an example where a two particle matrix element ($\langle D^{*+}|O_i|\bar{B}\rangle$) is required.

There are different methods for the evaluation of decay constants and form factors, such as lattice calculations, QCD sum rules, $1/N$ expansion, chiral perturbation theory, heavy quark effective theory, etc. These calculations have some limitations and usually are responsible for the largest part of theoretical uncertainties.

In the one and two particle matrix elements mentioned, the $u \to d$ and $b \to c$ quark level transitions were considered to be exclusive, or in other words, the initial and final states were completely specified. However, decays can also be studied inclusively where either the initial or final state is specified while the other one is a combination of all the hadrons containing a specific quark. For example, the $b \to c$ transition can also be studied via the inclusive decay $B \to X_c\ell\nu$, where X_c stands for any state that contains a c quark. Here one can use the quark-hadron duality principle which states that at high energies, certain inclusive hadronic cross sections which are averaged over an appropriate energy range, can be approximately calculated in the quark-gluon perturbation theory [78]. In other words, this duality indicates that for partial width

$$B \to X_c\ell\nu \approx b \to c\ell\nu, \tag{4.65}$$

where there should be an emphasis on the symbol "$\approx$". For the inclusive modes, non-perturbatively estimated decay constants and form factors are not required, resulting in more precise theoretical predictions. However, the experimental data for inclusive modes are usually less accurate.

The framework described in this Chapter can be applied to FCNC processes. In particular, the effective Hamiltonian for $b \to s$ transitions is given in the next Chapter.

CHAPTER 5

SM predictions for $B \to K^*\ell\ell$ and $B_s \to \ell\ell$ decays

In this chapter we will give the effective Hamiltonian for $b \to s\ell\ell$ transitions within the effective framework introduced in Chapter 4. Later we will apply this framework to the $B \to K^*\ell\ell$ and $B_s \to \ell\ell$ decays along with their associated observables and the Standard Model predictions.

5.1 Effective Hamiltonian of $b \to s\ell\ell$

The effective Hamiltonian describing the $b \to s\ell^+\ell^-$ transitions has the following generic structure[1][2] [79, 80]:

$$\mathcal{H}_{\text{eff}} = -\frac{4G_F}{\sqrt{2}} V_{tb}V_{ts}^* \Big[\sum_{i=1}^{6} C_i(\mu) O_i(\mu) + \sum_{i=7}^{10} \Big(C_i(\mu) O_i(\mu) + C_i'(\mu) O_i'(\mu) \Big) + \sum_{i=1}^{2} \Big(C_{Q_i}(\mu) Q_i(\mu) + C'_{Q_i}(\mu) Q_i'(\mu) \Big) \Big]. \tag{5.1}$$

Physics contributions at scales higher than μ are summarised in the Wilson coefficients $C_{i,Q_i}^{(\prime)}(\mu)$; a typical choice of the scale μ for B decays is $\mu_b = \mathcal{O}(m_b)$. The Wilson coefficients include contributions from all particles heavier than μ_b. In the SM these contributions are the top quark and the electroweak bosons, and beyond standard model (BSM), possible heavy new physics (NP) particles are also accounted for in the Wilson coefficients. On the other hand, the matrix elements of the local operators $O_i^{(\prime)}$ and $Q_i^{(\prime)}$ include the long

[1] The unitarity relation $V_{cb}V_{cs}^* = -V_{tb}V_{ts}^* - V_{ub}V_{us}^*$ has been used and we neglect the GIM and doubly Cabibbo suppressed contributions from $(V_{ub}V_{us}^*)$ terms, which would only bring two new operators like O_1 and O_2

[2] The tensor operators of the form $(\bar{s}\sigma^{\mu\nu}b)(\bar{\ell}\sigma_{\mu\nu}\ell)$ and $(\bar{s}\sigma^{\mu\nu}b)(\bar{\ell}\sigma_{\mu\nu}\gamma_5\ell)$ have negligible effects in the scenarios that we consider. For further discussion on how these operators can be introduced in the MSSM, see [81]. The effects of the tensor operators on B decays can be found in [82–84]

distance contributions from scales lower than μ_b. A choice of independent operators is:

$$O_1 = (\bar{s}\gamma_\mu T^a P_L c)(\bar{c}\gamma^\mu T^a P_L b)\ , \qquad O_2 = (\bar{s}\gamma_\mu P_L c)(\bar{c}\gamma^\mu P_L b)\ , \tag{5.2}$$

$$O_3 = (\bar{s}\gamma_\mu P_L b)\sum_q (\bar{q}\gamma^\mu q)\ , \qquad O_4 = (\bar{s}\gamma_\mu T^a P_L b)\sum_q (\bar{q}\gamma^\mu T^a q)\ , \tag{5.3}$$

$$O_5 = (\bar{s}\gamma_{\mu_1}\gamma_{\mu_2}\gamma_{\mu_3} P_L b)\sum_q (\bar{q}\gamma^{\mu_1}\gamma^{\mu_2}\gamma^{\mu_3} q)\ , \quad O_6 = (\bar{s}\gamma_{\mu_1}\gamma_{\mu_2}\gamma_{\mu_3} T^a P_L b)\sum_q (\bar{q}\gamma^{\mu_1}\gamma^{\mu_2}\gamma^{\mu_3} T^a q)\ ,$$

$$O_7 = \frac{e}{(4\pi)^2} m_b (\bar{s}\sigma^{\mu\nu} P_R b) F_{\mu\nu}\ , \qquad O_8 = \frac{g}{(4\pi)^2} m_b (\bar{s}\sigma^{\mu\nu} T^a P_R b) G^a_{\mu\nu}\ , \tag{5.4}$$

$$O_9 = \frac{e^2}{(4\pi)^2}(\bar{s}\gamma^\mu P_L b)(\bar{\ell}\gamma_\mu \ell)\ , \qquad O_{10} = \frac{e^2}{(4\pi)^2}(\bar{s}\gamma^\mu P_L b)(\bar{\ell}\gamma_\mu\gamma_5 \ell)\ , \tag{5.5}$$

$$Q_1 = \frac{e^2}{(4\pi)^2}(\bar{s} P_R b)(\bar{\ell}\,\ell)\ , \qquad Q_2 = \frac{e^2}{(4\pi)^2}(\bar{s} P_R b)(\bar{\ell}\gamma_5 \ell)\ , \tag{5.6}$$

where four-quark operators O_{1-6} have been taken from [85], the magnetic operators O_{7-8}, as well as the semi-leptonic operators $O_{9,10}$, from [86]. The scalar and pseudo-scalar operators $Q_{1,2}$ are from [87]. The primed operators are chirality flipped versions of the non-primed operators, obtained by exchanging $P_L \leftrightarrow P_R$. In the SM, the primed and (pseudo-) scalar operators are either highly suppressed or absent.

There are several interesting rare decays with $b \to s$ transitions such as $\bar{B} \to X_s\ \gamma$, $\bar{B} \to X_s \ell^+\ell^-$, $B \to\ K^*\ \ell\ \ell$ and $B_s \to \ell\ell$. All of these decays can be studied using the above effective Hamiltonian. In this thesis we focus our attention to the semi-leptonic and leptonic B meson decays of the form

$$B \to K^*\ell\ell, \qquad\qquad B_s \to \ell\ell. \tag{5.7}$$

5.2 $B \to K^*\ell\ell$

Using the effective Hamiltonian and neglecting for the moment the primed operators, the matrix element for the $B \to K^*\ell\ell$ decay can be written as

$$\mathcal{M} = \frac{G_F \alpha_{em}}{\sqrt{2}\pi} V_{tb} V_{ts}^* \Bigg\{ \left[C_9^{eff} \langle K^*|\bar{s}\gamma^\mu P_L b|B\rangle - \frac{2m_b}{q^2} C_7^{eff} \langle K^*|\bar{s} i\sigma^{\mu\nu} q_\nu P_R b|B\rangle \right](\bar{\ell}\gamma_\mu \ell) \tag{5.8}$$

$$+ \left[C_{10}\langle K^*|\bar{s}\gamma^\mu P_L b|B\rangle \right](\bar{\ell}\gamma_\mu\gamma_5\ell) + \left[C_{Q_1}\langle K^*|\bar{s} P_R b|B\rangle \right](\bar{\ell}\ell) + \left[C_{Q_2}\langle K^*|\bar{s} P_R b|B\rangle \right](\bar{\ell}\gamma_5\ell) \Bigg\}.$$

The four-quark operators (O_{1-6}) present in the effective Hamiltonian contribute to the matrix elements via the loops of Figure 5.1. These contributions result in expressions with the same structure as O_7 and O_9 [88, 89]. Hence, instead of explicitly being considered

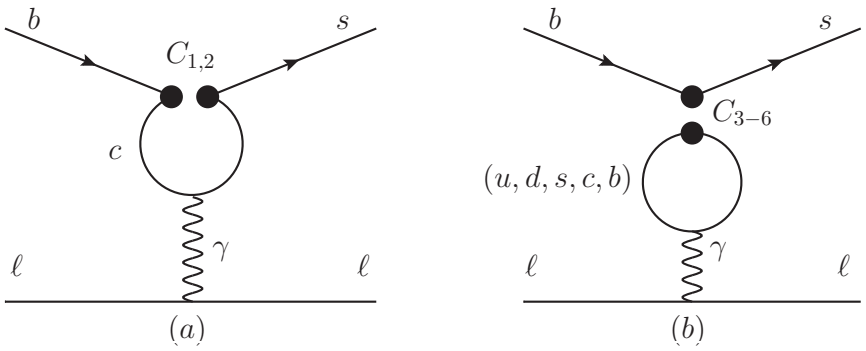

Figure 5.1.: Four-quark operator insertions into penguin diagrams that contribute to the $B \to K^* \ell\ell$ decay. In (a), the bullets "••" denote the insertion of operators $O_{1,2}$ and in (b), the bullets stand for insertion of O_{3-6}.

in (5.8), they are absorbed in the definition of C_7^{eff} and C_9^{eff} [90, 91][3]

$$C_7^{eff} = C_7 - \frac{1}{3}C_3 - \frac{4}{9}C_4 - \frac{20}{3}C_5 - \frac{80}{9}C_6, \tag{5.9}$$

$$C_9^{eff} = C_9 + Y(q^2). \tag{5.10}$$

Here, Y contains the short distance contributions from the four-quark operators [92, 93]

$$\begin{aligned} Y(q^2) = {} & h(q^2, m_c)\left(\frac{4}{3}C_1 + C_2 + 6C_3 + 60C_5\right) \\ & - \frac{1}{2}h(q^2, m_b^{\text{pole}})\left(7C_3 + \frac{4}{3}C_4 + 76C_5 + \frac{64}{3}C_6\right) \\ & - \frac{1}{2}h(q^2, 0)\left(C_3 + \frac{4}{3}C_4 + 16C_5 + \frac{64}{3}C_6\right) \\ & + \frac{4}{3}C_3 + \frac{64}{9}C_5 + \frac{64}{27}C_6. \end{aligned} \tag{5.11}$$

For the function $h(q^2, m_q)$ we have

$$h(q^2, m_q) = -\frac{4}{9}\left(\ln\frac{m_q^2}{\mu^2} - \frac{2}{3} - z\right) - \frac{4}{9}(2+z)\sqrt{|z-1|} \times \begin{cases} \arctan\dfrac{1}{\sqrt{z-1}} & z > 1 \\ \ln\dfrac{1+\sqrt{1-z}}{\sqrt{z}} - \dfrac{i\pi}{2} & z \le 1 \end{cases} \tag{5.12}$$

where $z = 4m_q^2/q^2$. The functions $h(q^2, m_c)$, $h(q^2, m_b)$ and $h(q^2, 0)$ correspond to the internal c, b and massless (u, d, s) quark, respectively [79]. Depending on the operator set,

[3] There is no effective C_{10} since the four-quark loops couple to the lepton pair through the (vectorial) photon.

the definitions of the effective Wilson coefficients can become different. The coefficients $C_{7,9}^{eff}$ can be modified in such a way to include the long-distance contributions as well[4] [93]. In order to calculate (5.8), the following matrix elements are required [94, 95]

$$\langle K^*|V^\mu|B\rangle = i\frac{2V(q^2)}{M_B + M_{K^*}}\epsilon^{\mu\nu\rho\sigma}p^\nu p'^\rho \epsilon^{*\sigma}, \tag{5.13}$$

$$\langle K^*|A^\mu|B\rangle = 2M_{K^*}A_0(q^2)\frac{\epsilon^*\cdot q}{q^2}q^\mu + (M_B + M_{K^*})A_1(q^2)\left[\epsilon^{*\mu} - \frac{\epsilon^*\cdot q}{q^2}q^\mu\right] - A_2(q^2)\frac{\epsilon^*\cdot q}{M_B + M_{K^*}}\left[p^\mu + p'^\mu - \frac{M_B^2 - M_{K^*}^2}{q^2}q^\mu\right], \tag{5.14}$$

$$\langle K^*|T^{\mu\nu}q_\nu|B\rangle = -2T_1(q^2)\epsilon^{\mu\nu\rho\sigma}p^\nu p'^\rho\epsilon^{*\sigma}, \tag{5.15}$$

$$\langle K^*|T_5^{\mu\nu}q_\nu|B\rangle = -iT_2(q^2)\left[(M_B^2 - M_{K^*}^2)\epsilon^{*\mu} - (\epsilon^*\cdot q)(p^\mu + p'^\mu)\right] - iT_3(q^2)(\epsilon^*\cdot q)\left[q^\mu - \frac{q^2}{M_B^2 - M_{K^*}^2}(p^\mu + p'^\mu)\right], \tag{5.16}$$

$$\langle K^*|P|B\rangle = -\frac{1}{m_b + m_s}\langle K^*|i\partial_\mu A^\mu|B\rangle = \frac{2M_{K^*}}{m_b + m_s}(\epsilon^*\cdot q)A_0(q^2), \tag{5.17}$$

$$\langle K^*|S|B\rangle = 0. \tag{5.18}$$

Here, p is the momentum of the B meson and p' and ϵ^μ are the momentum and polarisation vector of the K^* vector mesons, and q^2 is the momentum transfer between the B and K^* mesons or alternatively the dilepton invariant mass

$$q^\mu \equiv p^\mu - p'^\mu = p_{\ell^+}^\mu + p_{\ell^-}^\mu, \tag{5.19}$$

where $p_{\ell^+}^\mu$ and $p_{\ell^-}^\mu$ are the momenta of ℓ^+ and ℓ^-, respectively.
In (5.13–5.18), $S, P, V^\mu, A^\mu, T^{\mu\nu}$ and $T_5^{\mu\nu}$ are respectively the scalar, pseudoscalar, vector, axial, tensor and pseudotensor currents defined as

$$\begin{aligned} S &\equiv \bar{s}b, & V^\mu &\equiv \bar{s}\gamma^\mu b, & T^{\mu\nu} &\equiv \bar{s}\sigma^{\mu\nu}b, \\ P &\equiv \bar{s}\gamma_5 b, & A^\mu &\equiv \bar{s}\gamma^\mu\gamma_5 b, & T_5^{\mu\nu} &\equiv \bar{s}\sigma^{\mu\nu}\gamma_5 b. \end{aligned} \tag{5.20}$$

The matrix elements have been written as the most general linear combination of the available dynamical variables $(p^\mu, p^{\mu\prime}, \epsilon^\mu)$, while respecting the Lorentz structure and discrete symmetries like parity. For instance the matrix elements of the scalar current (5.18) vanishes since there is no combination of $p^\mu, p^{\mu\prime}$ and ϵ^μ that has the correct Lorentz structure while respecting parity. The non-perturbative QCD effects are parametrised in terms of the seven independent Lorentz invariant full form factors (full FF) $V(q^2), A_{0,1,2}(q^2)$ and $T_{1,2,3}(q^2)$. The non-perturbative effects are due to the hadronisation of quarks, where the energy scales are of order Λ_{QCD} and QCD interactions are no longer asymptotically free.

[4] $C_{7,9}^{eff}$ including the long-distance effects for the low and high q^2 region can be found in [96] and [97], respectively.

5.2.1 Differential decay distribution

For the $\bar{B}^0 \to \bar{K}^* \ell^+ \ell^-$ decay, there are only two kinematical variables:

- q^2: the dilepton invariant mass
- $\cos\theta_\ell$: the angle between ℓ^- and the z-direction (defined as the $\bar{B}^0$ flight direction in the dilepton rest frame)

However, the $\bar{K}^*$ itself mostly decays into a π^+ and K^-, providing additional information from the two other kinematical variables:

- $\cos\theta_{K^*}$: the angle between K^- and the z-direction in the K^* rest frame
- ϕ: the angle between the decay planes of $\ell^+\ell^-$ and $K^-\pi^+$ in the $\bar{B}^0$ rest frame

The information obtained from these two variables is sensitive to the polarisation state of K^* meson. The different angles are depicted in figure 5.2 [98].

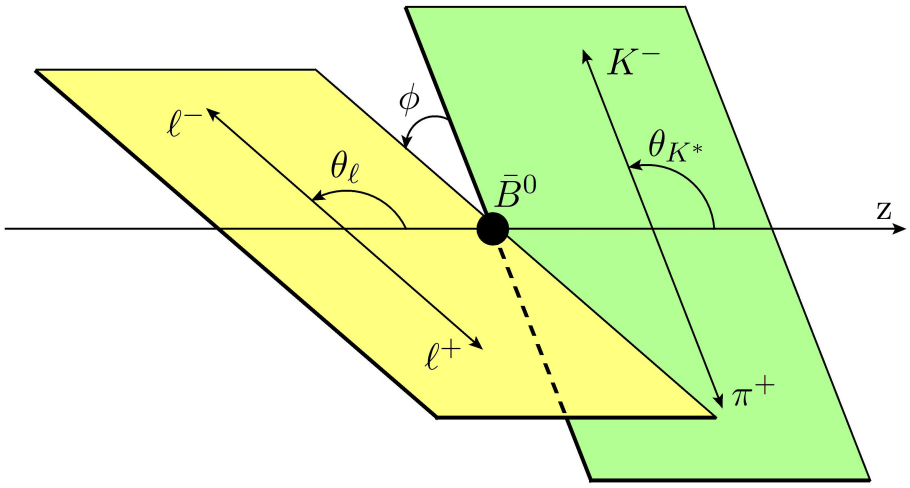

Figure 5.2.: Symbolic representation of the $\bar{B} \to K^-\pi^+\ell\ell$ decay. The plane of the paper is the $\bar{B}^0$ rest frame and the yellow and green planes are the rest frames of the dilepton and $\bar{K}^*$, respectively. The z-direction is defined as the $\bar{B}^0$ flight direction in the dilepton rest frame. $\cos\theta_\ell$ is the angle between ℓ^- and the z-direction, ϕ is the angle between the decay planes of $\ell^+\ell^-$ and $K^-\pi^+$ in the $\bar{B}^0$ rest frame and $\cos\theta_{K^*}$ is the angle between K^- and the z-direction.

Considering the full decay, $\bar{B} \to (\bar{K}^* \to) K^-\pi^+\ell\ell$, the matrix element, can be organised in terms of the Lorentz structure of the hadronic part and the chirality of the leptonic

part

$$\begin{aligned}
\mathcal{M} = \frac{G_F \alpha_{em}}{2\sqrt{2}\pi} V_{tb} V_{ts}^* \Bigg\{ & \Big\langle K^- \pi^+ \ell^+ \ell^- \Big| \\
& \Big[\big((C_9^{eff} + C_9^{eff\prime}) + (C_{10} + C'_{10}) \big) V^\mu - \big((C_9^{eff} - C_9^{eff\prime}) + (C_{10} - C'_{10}) \big) A^\mu \\
& - \frac{2m_b}{q^2} i q_\nu (C_7^{eff} + C_7^{eff\prime}) T^{\mu\nu} - \frac{2m_b}{q^2} i q_\nu (C_7^{eff} - C_7^{eff\prime}) T_5^{\mu\nu} \Big] \times (\bar{\ell} \gamma_\mu P_R \ell) \\
& + \Big[\big((C_9^{eff} + C_9^{eff\prime}) - (C_{10} + C'_{10}) \big) V^\mu - \big((C_9^{eff} - C_9^{eff\prime}) - (C_{10} - C'_{10}) \big) A^\mu \\
& - \frac{2m_b}{q^2} i q_\nu (C_7^{eff} + C_7^{eff\prime}) T^{\mu\nu} - \frac{2m_b}{q^2} i q_\nu (C_7^{eff} - C_7^{eff\prime}) T_5^{\mu\nu} \Big] \times (\bar{\ell} \gamma_\mu P_L \ell) \\
& + \Big[(C_{Q_1} + C'_{Q_1}) S + (C_{Q_1} - C'_{Q_1}) P \Big] \times (\bar{\ell}\ell) \\
& + \Big[(C_{Q_2} + C'_{Q_2}) S + (C_{Q_2} - C'_{Q_2}) P \Big] \times (\bar{\ell} \gamma_5 \ell) \Big| \bar{B} \Big\rangle \Bigg\}.
\end{aligned} \tag{5.21}$$

For the full decay, the following matrix elements would in principle be required

$$\langle K^- \pi^+ | V^\mu | \bar{B} \rangle, \qquad \langle K^- \pi^+ | A^\mu | \bar{B} \rangle, \qquad \langle K^- \pi^+ | T^{\mu\nu} q_\nu | \bar{B} \rangle, \tag{5.22}$$

$$\langle K^- \pi^+ | T_5^{\mu\nu} q_\nu | \bar{B} \rangle, \qquad \langle K^- \pi^+ | P | \bar{B} \rangle, \qquad \langle K^- \pi^+ | S | \bar{B} \rangle. \tag{5.23}$$

These matrix elements can however be written in terms of $B \to K^*$ form factors assuming dominance of the narrow-width approximation [99]. Considering the $\bar{K}^*$ meson to be on-shell and summing over the spins of the final particles, the differential decay distribution of the full decay can be written in terms of the three angles θ_ℓ, θ_{K^*}, ϕ and the invariant dilepton mass (q^2) [94, 98]:

$$d^4\Gamma = \frac{9}{32\pi} J(q^2, \theta_l, \theta_{K^*}, \phi)\, dq^2\, d\cos\theta_l\, d\cos\theta_{K^*}\, d\phi\,, \tag{5.24}$$

with the physical region of phase space bounded by

$$4m_\ell^2 \leqslant q^2 \leqslant (M_B - M_{K^*})^2, \quad -1 \leqslant \cos\theta_\ell \leqslant 1, \quad -1 \leqslant \cos\theta_{K^*} \leqslant 1, \quad 0 \leqslant \phi \leqslant 2\pi. \tag{5.25}$$

The angular dependence of $J(q^2, \theta_l, \theta_{K^*}, \phi)$ can be decomposed as

$$\begin{aligned}
J(q^2, \theta_\ell, \theta_{K^*}, \phi) = {} & J_1^s \sin^2\theta_{K^*} + J_1^c \cos^2\theta_{K^*} + (J_2^s \sin^2\theta_{K^*} + J_2^c \cos^2\theta_{K^*}) \cos 2\theta_\ell \\
& + J_3 \sin^2\theta_{K^*} \sin^2\theta_\ell \cos 2\phi + J_4 \sin 2\theta_{K^*} \sin 2\theta_\ell \cos\phi + J_5 \sin 2\theta_{K^*} \sin\theta_\ell \cos\phi \\
& + (J_6^s \sin^2\theta_{K^*} + J_6^c \cos^2\theta_{K^*}) \cos\theta_\ell + J_7 \sin 2\theta_{K^*} \sin\theta_\ell \sin\phi \\
& + J_8 \sin 2\theta_{K^*} \sin 2\theta_\ell \sin\phi + J_9 \sin^2\theta_{K^*} \sin^2\theta_\ell \sin 2\phi\,.
\end{aligned} \tag{5.26}$$

The angular coefficients J_i, are functions of q^2 and can be described in terms of eight transversity amplitudes[5] [94]

$$J_1^s = \frac{(2+\beta_\ell^2)}{4}\left[|A_\perp^L|^2 + |A_\parallel^L|^2 + (L \to R)\right] + \frac{4m_\ell^2}{q^2}\mathrm{Re}\left(A_\perp^L A_\perp^{R*} + A_\parallel^L A_\parallel^{R*}\right) , \tag{5.27a}$$

$$J_1^c = |A_0^L|^2 + |A_0^R|^2 + \frac{4m_\ell^2}{q^2}\left[|A_t|^2 + 2\mathrm{Re}(A_0^L A_0^{R*})\right] + \beta_\ell^2 |A_S|^2 , \tag{5.27b}$$

$$J_2^s = \frac{\beta_\ell^2}{4}\left[|A_\perp^L|^2 + |A_\parallel^L|^2 + (L \to R)\right] , \tag{5.27c}$$

$$J_2^c = -\beta_\ell^2\left[|A_0^L|^2 + (L \to R)\right] , \tag{5.27d}$$

$$J_3 = \frac{1}{2}\beta_\ell^2\left[|A_\perp^L|^2 - |A_\parallel^L|^2 + (L \to R)\right] , \tag{5.27e}$$

$$J_4 = \frac{1}{\sqrt{2}}\beta_\ell^2\left[\mathrm{Re}(A_0^L A_\parallel^{L*}) + (L \to R)\right] , \tag{5.27f}$$

$$J_5 = \sqrt{2}\beta_\ell\left[\mathrm{Re}(A_0^L A_\perp^{L*}) - (L \to R) - \frac{m_\ell}{\sqrt{q^2}}\mathrm{Re}(A_\parallel^L A_S^* + A_\parallel^R A_S^*)\right] , \tag{5.27g}$$

$$J_6^s = 2\beta_\ell\left[\mathrm{Re}(A_\parallel^L A_\perp^{L*}) - (L \to R)\right] , \tag{5.27h}$$

$$J_6^c = 4\beta_\ell\frac{m_\ell}{\sqrt{q^2}}\mathrm{Re}\left[A_0^L A_S^* + (L \to R)\right] , \tag{5.27i}$$

$$J_7 = \sqrt{2}\beta_\ell\left[\mathrm{Im}(A_0^L A_\parallel^{L*}) - (L \to R) + \frac{m_\ell}{\sqrt{q^2}}\mathrm{Im}(A_\perp^L A_S^* + A_\perp^R A_S^*)\right] , \tag{5.27j}$$

$$J_8 = \frac{1}{\sqrt{2}}\beta_\ell^2\left[\mathrm{Im}(A_0^L A_\perp^{L*}) + (L \to R)\right] , \tag{5.27k}$$

$$J_9 = \beta_\ell^2\left[\mathrm{Im}(A_\parallel^{L*} A_\perp^L) + (L \to R)\right] , \tag{5.27l}$$

with $J_i \equiv 2J_i^s + J_i^c$ (for $i = 1, 2, 6$), and β_ℓ is the lepton velocity in the B rest frame [100]

$$\beta_\ell = \sqrt{1 - \frac{4m_\ell^2}{q^2}} . \tag{5.28}$$

[5] Referring to the linear or longitudinal polarisations of K^* ($A_{\perp,\parallel}$ or A_0) and to the temporal or scalar components of the dilepton pair (A_t or A_S).

The transversity or spin amplitudes are in turn expressed in terms of the form factors[6] [94]:

$$A_\perp^{L,R} = N\sqrt{2}\lambda^{1/2}\Bigg[\Big[(C_9^{eff} + C_9^{eff\prime}) \mp (C_{10} + C'_{10})\Big] \frac{V(q^2)}{M_B + m_{K^*}} + \frac{2m_b}{q^2}(C_7^{eff} + C_7^{eff\prime})T_1(q^2)\Bigg], \tag{5.29a}$$

$$A_\parallel^{L,R} = -N\sqrt{2}(M_B^2 - m_{K^*}^2)\Bigg[\Big[(C_9^{eff} - C_9^{eff\prime}) \mp (C_{10} - C'_{10})\Big] \frac{A_1(q^2)}{M_B - m_{K^*}} + \frac{2m_b}{q^2}(C_7^{eff} - C_7^{eff\prime})T_2(q^2)\Bigg], \tag{5.29b}$$

$$A_0^{L,R} = -\frac{N}{2m_{K^*}\sqrt{q^2}}\Bigg\{ \Big[(C_9^{eff} - C_9^{eff\prime}) \mp (C_{10} - C'_{10})\Big] \times \Big[(M_B^2 - m_{K^*}^2 - q^2)(M_B + m_{K^*})A_1(q^2) - \lambda\frac{A_2(q^2)}{M_B + m_{K^*}}\Big] + 2m_b(C_7^{eff} - C_7^{eff\prime})\Big[(M_B^2 + 3m_{K^*}^2 - q^2)T_2(q^2) - \frac{\lambda}{M_B^2 - m_{K^*}^2}T_3(q^2)\Big]\Bigg\}, \tag{5.29c}$$

$$A_t = \frac{N}{\sqrt{q^2}}\lambda^{1/2}\left[2(C_{10} - C'_{10}) + \frac{q^2}{m_\ell m_b}(C_{Q_2} - C'_{Q_2})\right] A_0(q^2), \tag{5.29d}$$

$$A_S = -\frac{2N\lambda^{1/2}}{m_b}(C_{Q_1} - C'_{Q_1})A_0(q^2). \tag{5.29e}$$

The above equations share a common pre-factor

$$N = V_{tb}V_{ts}^*\left[\frac{G_F^2\alpha_{em}^2}{3\cdot 2^9\,\pi^5 M_B^2}q^2\,|\boldsymbol{P}_{K^*}|\,\beta_l\right]^{1/2}, \tag{5.30}$$

where $|\boldsymbol{P}_{K^*}| = \sqrt{\lambda}/2M_B$ is the value of the 3-momentum of the K^* meson in the B rest frame [100], and λ is the triangle function

$$\lambda = M_B^4 + m_{K^*}^4 + q^4 - 2(M_B^2 m_{K^*}^2 + m_{K^*}^2 q^2 + M_B^2 q^2). \tag{5.31}$$

The $\perp$, $\parallel$ and 0 in $A_\perp^{L,R}, A_\parallel^{L,R}$ and $A_0^{L,R}$ are related to different combination of the K^* helicity amplitudes[7] by [98]

$$A_{\perp,\parallel} = (H_{+1} \mp H_{-1})/\sqrt{2}, \qquad A_0 = H_0. \tag{5.32}$$

The L and R in $A_\perp^{L,R}, A_\parallel^{L,R}$ and $A_0^{L,R}$ refer to the chirality of the leptonic current. The t in A_t refers to the time-like polarisation vector of the virtual gauge boson that produces

[6] Here, the mass of the s-quark has been neglected.

[7] The three helicity amplitudes can be associated with the three polarisation states of the on-shell K^* meson's polarisation vector [100].

the lepton pair and the S in A_S refers to the scalar coupling to the lepton pair [94]. The specific combination of the Wilson coefficients in (5.29) are due to the arrangement of the operators based on their Lorentz structure for the hadronic matrix elements which can be seen in (5.21).
For the differential distribution of the CP conjugate decay $B^0 \to K^*(\to K^+\pi^-)\ell^+\ell^-$, keeping the definition of θ_ℓ, replacing K^- with K^+ for the definition of θ_{K^*} and considering ϕ to be the angle between the normals of the $\ell^+\ell^-$ plane and the $K^+\pi^-$ in the B^0 rest frame, we can use (5.24) where J is replaced with $\bar{J}$. The function $\bar{J}(q^2, \theta_\ell, \theta_{K^*}, \phi)$ is obtained from (5.26) by the replacements [99]

$$J_{1,2}^{(c,s)} \to \bar{J}_{1,2}^{(c,s)}, \qquad J_6^{(c,s)} \to -\bar{J}_6^{(c,s)}, \tag{5.33}$$

$$J_{3,4,7} \to \bar{J}_{3,4,7}, \qquad J_{5,8,9} \to -\bar{J}_{5,8,9}, \tag{5.34}$$

where $\bar{J}$ is equal to J with all the weak phases conjugated. The change of sign for $J_{5,6,8,9}$ can be understood by considering that the CP conjugate decay leads to the transformations $\theta_l \to \pi - \theta_l$ and $\phi \to -\phi$ in (5.26).

5.2.2 Observables

Integrating (5.24) over all angles, the dilepton mass distribution can be written in terms of the angular coefficients [94, 101]:

$$\frac{d\Gamma}{dq^2} = \frac{3}{4}\left(J_1 - \frac{J_2}{3}\right). \tag{5.35}$$

For the normalised forward-backward asymmetry A_{FB} we use [94, 101]:

$$A_{\rm FB}(q^2) \equiv \left[\int_{-1}^{0} - \int_{0}^{1}\right] d\cos\theta_l \, \frac{d^2\Gamma}{dq^2\, d\cos\theta_l} \Bigg/ \frac{d\Gamma}{dq^2} = -\frac{3}{8} J_6 \Bigg/ \frac{d\Gamma}{dq^2}\,. \tag{5.36}$$

Considering A_{FB}, another observable known as the zero-crossing (q_0^2) can be obtained. q_0^2 denotes the value of the dilepton invariant mass at which A_{FB} becomes zero.
The longitudinal polarisation fraction F_L can be constructed as the ratios of the transversity amplitudes and therefore contains less theoretical uncertainty from the form factors. For the longitudinal polarisation, F_L we have [94, 98]:

$$F_L(q^2) = \frac{-J_2^c}{d\Gamma/dq^2}. \tag{5.37}$$

Another observable which is rather independent of hadronic input parameters is the isospin asymmetry which arises from non-factorisable effects. The non-factorisable effects depend on the charge of the spectator quark, and hence depending on whether the decaying B meson is charged or neutral, there will be a difference in the contribution of these effects to the decay width which can cause an isospin asymmetry. The (CP

averaged) isospin asymmetry is defined as [102]

$$\frac{dA_I}{dq^2} = \frac{d\Gamma[B^0 \to K^{*0}\ell^+\ell^-]/dq^2 - d\Gamma[B^\pm \to K^{*\pm}\ell^+\ell^-]/dq^2}{d\Gamma[B^0 \to K^{*0}\ell^+\ell^-]/dq^2 + d\Gamma[B^\pm \to K^{*\pm}\ell^+\ell^-]/dq^2} \,. \tag{5.38}$$

In the SM, dA_I/dq^2 is less than 1% [102, 103], the smallness of the isospin asymmetry makes it sensitive to isospin-violating NP effects.

Other observables of interest are the transverse asymmetries which have a small dependence on the form factors and/or a large sensitivity to right-handed currents via C_7'. They are defined as [94, 98, 104, 105]

$$A_T^{(2)}(q^2) = \frac{J_3}{2\,J_2^s} \,, \tag{5.39}$$

$$A_T^{(3)}(q^2) = \left(\frac{4(J_4)^2 + \beta_\ell^2 (J_7)^2}{-2J_2^c\,(2J_2^s + J_3)}\right)^{1/2} \,, \tag{5.40}$$

$$A_T^{(4)}(q^2) = \left(\frac{\beta_\ell^2 (J_5)^2 + 4(J_8)^2}{4(J_4)^2 + \beta_\ell^2 (J_7)^2}\right)^{1/2} \,, \tag{5.41}$$

as well as

$$A_{Im}(s) = \frac{J_9}{d\Gamma/dq^2} \,, \tag{5.42}$$

which is sensitive to the complex phases, but very small ($\mathcal{O}(10^{-3})$) in the SM.

All the observables can also be expressed in terms of the CP averaged angular coefficients S_i [94]. In particular, S_3, which has recently been measured by LHCb, can be related to F_L and $A_T^{(2)}$ by

$$S_3 = \frac{1}{2}(1 - F_L) A_T^{(2)} \,. \tag{5.43}$$

A very interesting observable which only involves the amplitudes $A_\parallel$ and $A_\perp$ has been proposed by [106]

$$A_T^{(\mathrm{re})}(q^2) = \frac{\beta_\ell}{4} \frac{J_6^s(q^2)}{J_2^s(q^2)}. \tag{5.44}$$

Furthermore, for the low recoil region, other observables have been proposed by [107]

$$H_T^{(1)} = \frac{\sqrt{2} J_4}{\sqrt{-J_2^c \left(2 J_2^s - J_3\right)}} , \tag{5.45}$$

$$H_T^{(2)} = \frac{\beta_l J_5}{\sqrt{-2 J_2^c \left(2 J_2^s + J_3\right)}} , \tag{5.46}$$

$$H_T^{(3)} = \frac{\beta_l J_6}{2\sqrt{(2 J_2^s)^2 - (J_3)^2}} . \tag{5.47}$$

5.2.3 Difference between high and low recoil

Considering the relations for the transversity amplitudes, any observable that is considered depends on several form factors which are independent of each other. To obtain quantitative results for the form factors, methods such as sum rules and lattice simulations are applied but they suffer from large theoretical uncertainties. However, when dealing with form factors that describe current matrix elements of heavy mesons or baryons, Heavy Quark Effective Theory (HQET) [108, 109] is applicable. HQET provides a systematic framework where the matrix elements are expanded in inverse powers of the heavy quark mass ($1/m_Q$). Within HQET, symmetries that are not apparent in QCD are brought to light. By exploring the new symmetries, relations can be obtained among the different matrix elements. These relations reduce the number of independent form factors and thereby provide significant simplifications in the theoretical description of the relevant process. The relations that are obtained between the $B \to K^*$ form factors depend on the energy of the outgoing K^* meson[8]

$$E_{K^*} = \frac{M_B^2 + M_{K^*}^2 - q^2}{2 M_B}. \tag{5.48}$$

Moreover, besides the short-distance contributions that are included in the Wilson coefficients, the four-quark loops have long-distance effects from the real intermediate states $u\bar{u}$ and $c\bar{c}$ (Figure 5.3), where the relevant process are $B \to K^*(c\bar{c} \to)\ell\ell$ or $B \to K^*(u\bar{u} \to)\ell\ell$.

The long-distance effects depend on the kinematics of the dilepton invariant mass. While the $u\bar{u}$ intermediate states can be safely neglected due to their small CKM factors, the $c\bar{c}$ resonances such as J/ψ and ψ' have large contributions. These large effects can be eliminated by putting cuts in the dilepton invariant mass (q^2), for regions that are close to these resonances ($q^2 = m_{J/\psi}^2 \simeq 9.6$ GeV^2 and $q^2 = m_{\psi'}^2 \simeq 13.6$ GeV^2). While for q^2 below the pronounced J/ψ and ψ' resonances, there are no other charmonium contributions, for the high q^2 region ($q^2 \gtrsim 14$ GeV^2) there are long-distance effects from the wide resonances of the heavier $c\bar{c}$ bound states of $\psi(3770), \psi(4040), \psi(4160)$ and $\psi(4415)$ [93, 97].
The $B \to K^* \ell^+\ell^-$ decay is hence usually studied distinctly for low q^2 ($\lesssim 6$ GeV^2) and high q^2 ($\gtrsim 14$ GeV^2). The high q^2 region coincides with the low recoil of the K^* meson

[8] The energy of the K^* meson is given in the B meson rest frame.

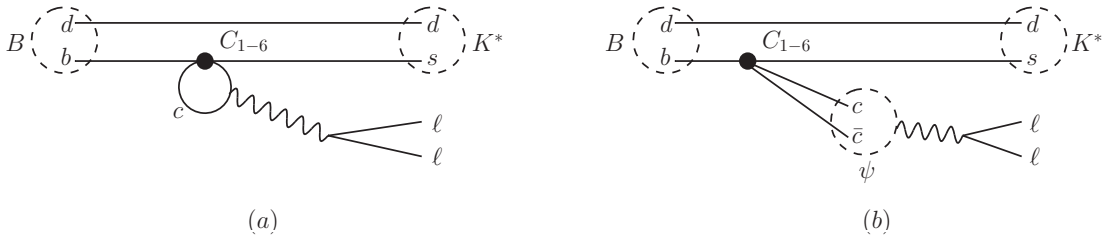

Figure 5.3.: Illustrative diagrams of the short- and long-distance contributions of the four-quark operators on the $B \to K^* \ell\ell$ decay, respectively in (a) and (b).

and the low q^2 region with the high recoil of the K^* meson. In the intermediate q^2 region, the narrow $\bar{c}c$ resonance background from J/ψ and ψ' are two orders of magnitude larger than the short distance effects [110]. Hence the intermediate region is of no interest in studying New Physis effects.

In our work we will mostly concentrate on the high (large) recoil region.

5.2.4 $B \to K^* \ell^+ \ell^-$ at large recoil

In the limit where the K^* meson has a large recoil energy, the form factors are calculated using light cone sum rule methods (LCSR). These form factors suffer from large uncertainties, but even if they were known precisely, the $\bar{B}^0 \to \bar{K}^* \ell^+ \ell^-$ decay would still need corrections emerging from non-factorisable effects which are related to the current-current operators O_1 and O_2, the QCD penguin operators O_3-O_6 and the chromomagnetic operator O_8 [91]. The non-factorisable corrections contribute to the decay amplitude by producing a virtual photon which decays into a lepton pair. When the $\bar{K}^*$ has a large energy (q^2 is small) and the decaying hadron ($\bar{B}^0$) is heavy, the non-factorisable corrections can be computed in the QCD factorisation (QCDf) framework [91, 103] and its field theoretical formulation, Soft Collinear Effective Theory (SCET) [111].

Transversity amplitudes at LO

Using the Large Energy Effective Theory (LEET) [112], Charles et al. [95] have shown that in the kinematic region of large recoil of the K^* meson, OPE can be used where the small parameter is $(1/E_{K^*})$. Simultaneously, HQET is applicable and a heavy quark expansion in $1/m_b$ can be done. By exploring symmetries and making an expansion in $(1/E_{K^*})$ and $(1/m_b)$ at leading order in $1/m_b$ and α_s, the seven form factors reduce to

two universal soft form factors $\xi_\perp$ and $\xi_\parallel$ [95, 98, 113]:

$$A_1(s) = \frac{2E_{K^*}}{M_B + M_{K^*}} \xi_\perp(E_{K^*}), \tag{5.49a}$$

$$A_2(s) = \frac{M_B}{M_B - M_{K^*}} \Big[\xi_\perp(E_{K^*}) - \xi_\parallel(E_{K^*}) \Big], \tag{5.49b}$$

$$A_0(s) = \frac{E_{K^*}}{M_{K^*}} \xi_\parallel(E_{K^*}), \tag{5.49c}$$

$$V(s) = \frac{m_B + m_{K^*}}{M_B} \xi_\perp(E_{K^*}), \tag{5.49d}$$

$$T_1(s) = \xi_\perp(E_{K^*}), \tag{5.49e}$$

$$T_2(s) = \frac{2E_{K^*}}{M_B} \xi_\perp(E_{K^*}), \tag{5.49f}$$

$$T_3(s) = \xi_\perp(E_{K^*}) - \xi_\parallel(E_{K^*}). \tag{5.49g}$$

where $\perp$ and $\parallel$ in $\xi_\perp$ and $\xi_\parallel$, correspond to the transverse and longitudinal polarisation of K^*.

Using the above relations, the transversity amplitudes can be expressed in a very simple form[9] [94, 98]:

$$A_\perp^{L,R} = \sqrt{2} N M_B (1 - \hat{s}) \Big[(C_9^{eff} + C_9^{eff\prime}) \mp (C_{10} + C'_{10}) + \frac{2\hat{m}_b}{\hat{s}} (C_7^{eff} + C_7^{eff\prime}) \Big] \xi_\perp(E_{K^*}) \tag{5.50a}$$

$$A_\parallel^{L,R} = -\sqrt{2} N M_B (1 - \hat{s}) \Big[(C_9^{eff} - C_9^{eff\prime}) \mp (C_{10} - C'_{10}) + \frac{2\hat{m}_b}{\hat{s}} (C_7^{eff} - C_7^{eff\prime}) \Big] \xi_\perp(E_{K^*}) \tag{5.50b}$$

$$A_0^{L,R} = -\frac{N M_B}{2\hat{M}_{K^*}\sqrt{\hat{s}}} (1 - \hat{s})^2 \Big[(C_9^{eff} - C_9^{eff\prime}) \mp (C_{10} - C'_{10}) + 2\hat{m}_b (C_7^{eff} - C_7^{eff\prime}) \Big] \xi_\parallel(E_{K^*}) \tag{5.50c}$$

$$A_t = \frac{N M_B}{2\hat{M}_{K^*}\sqrt{\hat{s}}} (1 - \hat{s})^2 \Big[2(C_{10} - C'_{10}) + \frac{\hat{s} M_B}{\hat{m}_b} (C_{Q_2} - C'_{Q_2}) \Big] \xi_\parallel(E_{K^*}) \tag{5.50d}$$

$$A_S = -\frac{N(1 - \hat{s})^2}{\hat{M}_{K^*}} \frac{M_B}{\hat{m}_b} (C_{Q_1} - C'_{Q_1}) \xi_\parallel(E_{K^*}), \tag{5.50e}$$

with $\hat{s} = q^2/M_B^2$, $\hat{m}_b = m_b/M_B$ and $\hat{M}_{K^*} = M_{K^*}/M_B$.

The LO relations for the transversity amplitude are useful for the construction of various observables by different combinations of the angular coefficients where there are either a small or no dependence on the form factors. For instance, the relation for the zero-crossing

[9] Here terms of $\mathcal{O}$ $(M_{K^*}^2/M_B^2$) have been neglected.

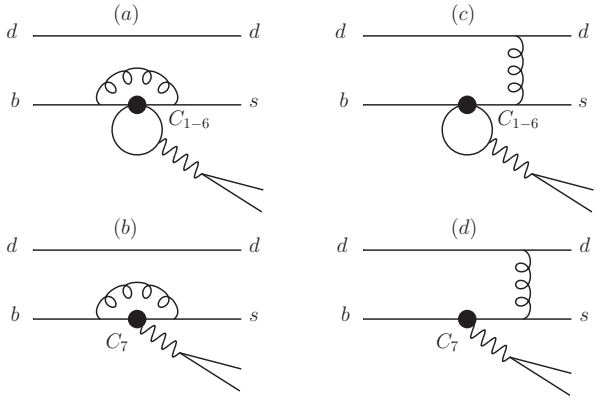

Figure 5.4.: Factorisable corrections to the soft form factors. Diagrams (a) and (b) correspond to vertex corrections, and diagrams (c) and (d) correspond to spectator scattering.

of the Forward-Backward asymmetry at LO becomes

$$q_0^2 = -\frac{2m_b C_7^{eff}}{C_9 + Y(q_0)}, \tag{5.51}$$

which is completely independent of form factors.

Transversity amplitudes at NLO

In expressing the seven form factors in terms of $\xi_\perp$ and $\xi_\parallel$ (5.49), there are symmetry breaking terms proportional to α_s and $1/m_b$ that have been neglected. The $1/m_b$ corrections appear due to the finiteness of m_b, since the used symmetry relations only hold exactly in the heavy quark limit ($m_b \to \infty$). Another type of corrections arise from hard gluon exchanges where there is either a gluon exchange in the $b \to s$ vertex (Figure 5.4.a, b) or a gluon exchange between the $b \to s$ current and the spectator quark (Figure 5.4.c, d). While there is no clear calculation of the $1/m_b$ corrections, gluon exchange symmetry breaking contributions have been calculated to $\mathcal{O}(\alpha_s)$ [113]. These are known as factorisable corrections and are shown in Figure 5.4. Moreover, there are non-factorisable contributions (Figure 5.5) that are not included in the definition of the full form factors. These contributions, similar to the factorisable ones, are either hard vertex corrections (Figure 5.5.a, b) or spectator scatterings (Figure 5.5.$c - e$). These effects have been calculated in the QCDf [91,103,113] framework. Including the factorisable as well as non-factorisable contributions in QCDf, the form factors can schematically be expressed as [91]

$$\mathcal{T}_a \propto C_a \xi_a + \Phi_B \otimes T_a \otimes \Phi_{K^*,a}, \tag{5.52}$$

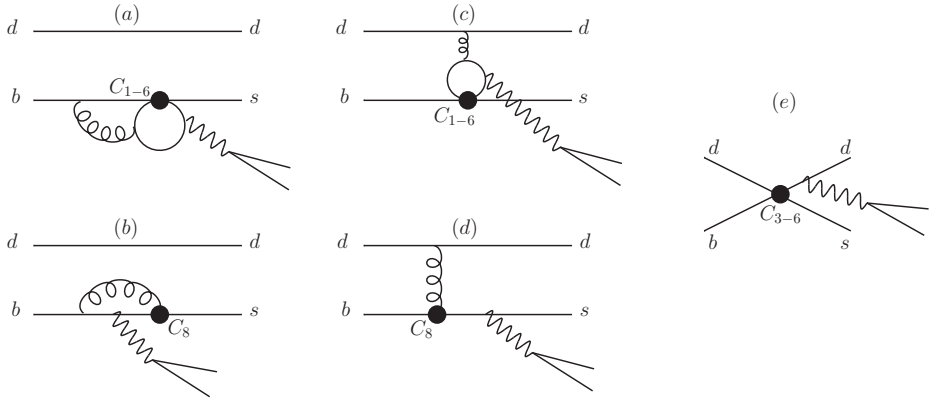

Figure 5.5.: Non-factorisable corrections to the soft form factors (not included in the definition of Full form factors). Diagrams (a) and (b) correspond to vertex corrections included in C_a, and diagrams $(c-e)$ correspond to hard spectator scattering kernel T_a. The diagram in (e) is the only leading order non-factorisable correction.

where $a = \|, \perp$ corresponds to longitudinal and transverse polarisation of K^*, respectively. Here the non-perturbative hadronic quantities include the meson Light Cone Distribution Amplitudes (LCDA) Φ_B, Φ_{K^*}, and the soft form facotors $\xi_{\perp,\|}$. The factors C_a (Appendix B.2) and T_a (Appendix B.3) contain the perturbatively calculable hard vertex and spectator scattering contributions, respectively.

These contributions can be included in the transversity amplitudes by the following replacements [98, 101]:

$$(C_7^{\text{eff}} + C_7')T_i(q^2) \to \mathcal{T}_i^+, \qquad (C_7^{\text{eff}} - C_7')T_i(q^2) \to \mathcal{T}_i^-, \qquad C_9^{\text{eff}}(q^2) \to C_9, \tag{5.53}$$

where

$$\mathcal{T}_1^\pm = \mathcal{T}_\perp^\pm, \qquad \mathcal{T}_2^- = \frac{2E}{M_B}\mathcal{T}_\perp^-, \qquad \mathcal{T}_3^- = \mathcal{T}_\perp^- + \mathcal{T}_\|^-, \tag{5.54}$$

and $\mathcal{T}_{\perp,\|}^\pm$ are given in Appendix B.

Neglecting $1/m_b$ corrections, the transversity amplitudes at NLO in α_s in the large recoil

limit are[10] [94, 98, 101]:

$$A_\perp^{L,R} = N\sqrt{2}\sqrt{\lambda}\Bigg[[(C_9 + C_9') \mp (C_{10} + C_{10}')] \frac{V(q^2)}{M_B + m_{K^*}} + \frac{2m_b}{q^2}\mathcal{T}_\perp^+ \Bigg] , \tag{5.55a}$$

$$A_\parallel^{L,R} = -N\sqrt{2}(M_B^2 - m_{K^*}^2)\Bigg[[(C_9 - C_9') \mp (C_{10} - C_{10}')] \frac{A_1(q^2)}{M_B - m_{K^*}} + \frac{4m_b}{M_B}\frac{E_{K^*}}{q^2}\mathcal{T}_\perp^- \Bigg] , \tag{5.55b}$$

$$A_0^{L,R} = -\frac{N}{2m_{K^*}\sqrt{q^2}}\Bigg\{ [(C_9 - C_9') \mp (C_{10} - C_{10}')] \times \Bigg[(M_B^2 - m_{K^*}^2 - q^2)(M_B + m_{K^*})A_1(q^2) - \lambda \frac{A_2(q^2)}{M_B + m_{K^*}} \Bigg] + 2m_b \Bigg[\frac{2E_{K^*}}{M_B}(M_B^2 + 3m_{K^*}^2 - q^2)\mathcal{T}_\perp^- - \frac{\lambda}{M_B^2 - m_{K^*}^2}\Big(\mathcal{T}_\perp^- + \mathcal{T}_\parallel^- \Big) \Bigg] \Bigg\} \tag{5.55c}$$

$$A_t = \frac{N}{\sqrt{q^2}}\sqrt{\lambda}\left[2(C_{10} - C_{10}') + \frac{q^2}{m_\ell m_b}(C_{Q_2} - C_{Q_2}') \right] \frac{E_{K^*}}{m_{K^*}} \xi_\parallel(q^2), \tag{5.55d}$$

$$A_S = -\frac{2N}{m_b}\sqrt{\lambda}(C_{Q_1} - C_{Q_1}')\frac{E_{K^*}}{m_{K^*}}\xi_\parallel(q^2). \tag{5.55e}$$

A few comments are in order here as to why we have kept A_1, A_2 and V in the above relations. Depending on the renormalisation convention for the soft form factors (or the factorisation scheme), $\xi_\perp$ and $\xi_\parallel$ are obtained via two full form factors A_0 and V [91], or through three full form factors A_1, A_2 and V [103]. For the soft form factors we follow [103]

$$\xi_\perp(q^2) = \frac{M_B}{M_B + M_{K^*}} V(q^2) , \tag{5.56}$$

$$\xi_\parallel(q^2) = \frac{M_B + M_{K^*}}{2E_{K^*}} A_1(q^2) - \frac{M_B - M_{K^*}}{M_B} A_2(q^2) . \tag{5.57}$$

By using soft form factors instead of full form factors, factorisable corrections in α_s and $1/m_b$ are introduced. However, by convention, (5.56) and (5.57) hold for all orders of α_s. Hence there are no α_s corrections from expressing V in terms of $\xi_\perp$. At leading order there is no α_s correction from describing A_1 in terms of $\xi_\perp$ either. So there is no over counting when using V and A_1. On the other hand there is a negligible α_s correction included in $\mathcal{T}_\parallel$ from rewriting A_2 in terms of $\xi_\perp$ and $\xi_\parallel$. However we prefer to keep A_1, A_2 and V since the additional $1/m_b$ uncertainty that emerges from describing the full form factors in terms of the soft ones are eliminated. A thorough discussion about this issue can be found in [94].

[10] For A_t and A_S, the α_s correction which emerges from describing A_0 in terms of $\xi_\parallel$ is very small and has been neglected.

$m_B = 5.27950$ GeV	[115]	$m_{B_s} = 5.3663$ GeV	[115]
$m_{K^*} = 0.89594$ GeV	[115]	$\lvert V_{tb}V_{ts}^*\rvert = 0.0403^{+0.0011}_{-0.0007}$	[115]
$m_b^{\overline{MS}}(m_b) = 4.19^{+0.18}_{-0.06}$ GeV	[115]	$m_c^{\overline{MS}}(m_c) = 1.29^{+0.05}_{-0.11}$ GeV	[115]
$m_t^{pole} = 172.9 \pm 0.6 \pm 0.9$ GeV	[115]	$m_\mu = 0.105658$ GeV	[115]
$\alpha_s(M_Z) = 0.1184 \pm 0.0007$	[115]	$\hat{\alpha}_{em}(M_Z) = 1/127.916$	[115]
$\alpha_s(\mu_b) = 0.2161$		$\hat{\alpha}_{em}(m_b) = 1/133$	
$\sin^2\hat{\theta}_W(M_Z) = 0.23116(13)$	[115]	$G_F/(\hbar c)^3 = 1.16637(1) \times 10^{-5}$ GeV^{-2}	[115]
$f_B = 194 \pm 10$ MeV	Table 5.5	$\tau_B = 1.519 \pm 0.007$ ps	[115]
$f_{B_s} = 234 \pm 10$MeV	Table 5.5	$\tau_{B_s} = 1.472 \pm 0.026$ ps	[115]
$f_{K^*,\perp}(1\text{ GeV}) = 0.185 \pm 0.009$ GeV	[116]	$f_{K^*,\parallel} = 0.220 \pm 0.005$ GeV	[116]
$a_{1,\perp}(1\text{ GeV}) = 0.10 \pm 0.07$	[114]	$a_{1,\parallel}(1\text{ GeV}) = 0.10 \pm 0.07$	[114]
$a_{2,\perp}(1\text{ GeV}) = 0.13 \pm 0.08$	[114]	$a_{2,\parallel}(1\text{ GeV}) = 0.09 \pm 0.05$	[114]
$V^{B_q\to K^*}(0) = 0.411 \pm 0.046$	[114]	$A_1^{B_q\to K^*}(0) = 0.292 \pm 0.038$	[114]
$\lambda_{B,+}(1\text{ GeV}) = 0.46 \pm 0.11$ GeV	[117]	$A_2^{B_q\to K^*}(0) = 0.259 \pm 0.036$	[114]
$\mu_b = m_b^{pole}$		$\mu_0 = 2M_W$	
$\mu_f = \sqrt{0.5 \times \mu_b}$ GeV	[103]		

Table 5.1.: Input parameters used in this work. Table taken from [118].

$C_1(\mu_b)$	$C_2(\mu_b)$	$C_3(\mu_b)$	$C_4(\mu_b)$	$C_5(\mu_b)$	$C_6(\mu_b)$	$C_7^{\text{eff}}(\mu_b)$	$C_8^{\text{eff}}(\mu_b)$	$C_9(\mu_b)$	$C_{10}(\mu_b)$
-0.2610	1.0076	-0.0052	-0.0795	0.0004	0.0009	-0.2974	-0.1614	4.2297	-4.2068

Table 5.2.: SM Wilson coefficients at $\mu_b = m_b^{\text{pole}}$ and $\mu_0 = 2M_W$ to NNLO accuracy in α_s.Table taken from [118].

Standard Model values and theoretical uncertainties

For our numerical analysis we have used the NLO relations for the transversity amplitudes in the ($1 < q^2 < 6$ GeV^2) region, where we are sufficiently below the charm resonance threshold ($q^2 = 4m_c^2$) and far enough from the kinematic minimum where the decay amplitude is dominated by the photon pole. The input parameters can be found in Table 5.1 and the SM Wilson coefficients are given in Table 5.2. Further explanation on what we use for $\xi_{\perp,\parallel}$, $A_{1,2}$ and V is given in Appendix C. The available experimental values are given for q^2 bins which can be shown as $\langle\text{observable}\rangle_{[q^2_{min},q^2_{max}]}$, in other words the dq^2 integration is over the $[q^2_{min}, q^2_{max}]$ range. For normalised quantities like A_{FB} and F_L, the numerator and denominator are integrated separately [98, 107]:

$$\langle A_{FB}\rangle_{[q^2_{min},q^2_{max}]} = -\frac{3}{8}\frac{\langle J_6\rangle_{[q^2_{min},q^2_{max}]}}{\langle d\Gamma/dq^2\rangle_{[q^2_{min},q^2_{max}]}}, \tag{5.58}$$

$$\langle F_L\rangle_{[q^2_{min},q^2_{max}]} = \frac{\langle -J_2^c\rangle_{[q^2_{min},q^2_{max}]}}{\langle d\Gamma/dq^2\rangle_{[q^2_{min},q^2_{max}]}}. \tag{5.59}$$

We estimate the theoretical uncertainties for the SM values in the low q^2 region considering five different sources of uncertainty: (i) the errors from the form factors (FF) have

Observable	SM prediction	(FF)	(SL)	(QM)	(CKM)	(Scale)
$10^7 \times BR(B \to K^* \mu^+ \mu^-)_{[1,6]}$	2.32	± 1.34	± 0.04	$^{+0.04}_{-0.03}$	$^{+0.08}_{-0.13}$	$^{+0.09}_{-0.05}$
$\langle A_{FB}(B \to K^* \mu^+ \mu^-) \rangle_{[1,6]}$	-0.06	± 0.04	± 0.02	± 0.01	—	—
$\langle F_L(B \to K^* \mu^+ \mu^-) \rangle_{[1,6]}$	0.71	± 0.13	± 0.01	± 0.01	—	—
$q_0^2(B \to K^* \mu^+ \mu^-)/\text{GeV}^2$	4.26	± 0.30	± 0.15	$^{+0.14}_{-0.04}$	—	$^{+0.02}_{-0.04}$

Table 5.3.: SM predictions and errors for the high recoil region. Table taken from [118].

been calculated by adding in quadrature the uncertainties due to V, A_1 and A_2 (11%, 13% and 14%, respectively [114]); (ii) for the unknown $1/m_b$ sub-leading corrections (SL), we have assumed 7% corrections to the $\mathcal{T}_{\perp,\parallel}$ terms in the transversity amplitudes[11], and these corrections have been added in quadrature; (iii) errors from the quark mass uncertainties (QM) have been estimated by separately varying m_t^{pole}, $m_b^{\overline{MS}}$ and $m_c^{\overline{MS}}$ according to Table 5.1 and also added in quadrature; (iv) errors also come from the uncertainty in the CKM matrix element combination $|V_{tb}V_{ts}^*|$ (CKM) which has been computed by considering the uncertainty given in Table 5.1; (v) the last source of error considered is the scale dependence (Scale) which we estimate by varying μ_b between $\mu_b/2$ and $2\mu_b$ (with $\mu_b = m_b^{pole}$). These five groups of errors for BR, A_{FB}, F_L and q_0^2 in the SM have been summarised in Table 5.3. For the Standard Model predictions the primed coefficients (C'_{i,Q_1,Q_2}) as well as the scalar coefficients ($C_{Q_{1,2}}$) have been put to zero.

5.2.5 $B \to K^* \ell^+ \ell^-$ at low recoil

For the low recoil of the K^* meson, the definitions for the angular coefficients (5.27) are the same as for the high recoil region. While the transversity amplitudes are also the same (5.29), the relations that are used among the form factors no longer hold in the low recoil region. Furthermore, the application of QCD factorisation is not justified near the endpoint of the q^2 spectrum ($q^2 \approx q_{max} = (M_B - M_K)^2$). In order to reduce the number of independent form factors appearing in the transversity amplitudes, HQET combined with an OPE is used.

Using HQET, Isgur and Wise obtained certain relations among the different full form factors ($V(q^2)$, $A_{0,1,2}(q^2)$ and $T_{1,2,3}(q^2)$) [119]. These relations, which result in a reduction in the number of independent form factors, lead to significant simplifications for the transversity amplitudes (similar to (5.50) in Section 5.2.4). However, in the same spirit of what was discussed for the high recoil region, there are several sources of uncertainty associated with this approach. One source of uncertainty is the $1/m_b$ symmetry breaking corrections from the higher order operators in HQET, which require further hadronic matrix elements, not calculable in perturbation theory [120]. On the other hand, corrections emerging from hard gluon exchanges between the flavour changing currents and the spectator quarks are calculable perturbatively and have been computed to $\mathcal{O}(\alpha_s)$ in [121],

[11] If for the (SL) error a 10% correction to the $\mathcal{T}_{\perp,\parallel}$ is considered the overall uncertainties will not have a significant change since they are dominated by the (FF) uncertainties.

resulting in improved Isgur-Wise relations.

The first step in obtaining the improved Isgur-Wise relations is the application of the QCD equation of motion for quark fields ($i\not{D}q = m_q q$) from where we have the following operator identity[12]

$$i\partial^\nu(\bar{s}i\sigma_{\mu\nu}b) = -m_b\bar{s}\gamma_\mu b + i\partial\mu(\bar{s}b) - 2\bar{s}i\overleftarrow{D}_\mu b. \tag{5.60}$$

The $\bar{s}i\overleftarrow{D}_\mu b$ term can be expanded in $1/m_b$ and matched onto HQET

$$\bar{s}i\overleftarrow{D}_\mu b = D_0^{(v)}(\mu)m_b\bar{s}\gamma_\mu h_v + D_1^{(v)}(\mu)m_b v_\mu \bar{s}h_v + \cdots, \tag{5.61}$$

where h_v is the HQET b-quark field. The quark currents $\bar{s}\gamma_\mu b$ and $\bar{s}b$ can also be expressed in terms of HQET currents

$$\bar{s}\gamma_\mu b = C_0^{(v)}(\mu)\bar{s}\gamma_\mu h_v + C_1^{(v)}(\mu)v_\mu\bar{s}h_v + \cdots, \tag{5.62}$$

$$\bar{s}b = C_0^{(v)}(\mu)\bar{s}h_v + \cdots. \tag{5.63}$$

The matrix element of $\bar{s}i\overleftarrow{D}_\mu b$ can hence be written in terms of the matrix element of $\bar{s}\gamma_\mu b$

$$\langle K^*|\bar{s}i\overleftarrow{D}_\mu b|B\rangle = \frac{m_b D_0^{(v)}(\mu)}{C_0^{(v)}(\mu)}(\mu)\langle K^*|\bar{s}\gamma_\mu b|B\rangle + \cdots. \tag{5.64}$$

In the above relations $C_i^{(v)}$ and $D_i^{(v)}$ are HQET Wilson coefficients [122]. Taking the matrix element of (5.60) and using the (5.64), the improved Isgur-Wise relation among V and T_1 is obtained [107]

$$T_1(q^2) = \kappa V(q^2), \tag{5.65}$$

with

$$\kappa = \left(1 + 2\frac{D_0^{(v)}(\mu)}{C_0^{(v)}(\mu)}\right)\frac{m_b(\mu)}{M_B}. \tag{5.66}$$

Up to NLO in α_s

$$\kappa = 1 - 2\frac{\alpha_s}{3\pi}\ln\left(\frac{\mu}{m_b}\right). \tag{5.67}$$

Considering the relevant formulae for the axial currents two other relations among the

[12]Here the s-quark has been considered to be massless.

Observable	SM prediction
$10^7 \times BR(B \to K^* \mu^+ \mu^-)_{[14.18,16]}$	1.27 ± 0.35
$\langle A_{FB}(B \to K^* \mu^+ \mu^-) \rangle_{[14.18,16]}$	0.44 ± 0.07
$\langle F_L(B \to K^* \mu^+ \mu^-) \rangle_{[14.18,16]}$	0.36 ± 0.05
$10^7 \times BR(B \to K^* \mu^+ \mu^-)_{[16,19.21]}$	1.50 ± 0.46
$\langle A_{FB}(B \to K^* \mu^+ \mu^-) \rangle_{[16,19.21]}$	0.38 ± 0.07
$\langle F_L(B \to K^* \mu^+ \mu^-) \rangle_{[16,19.21]}$	0.34 ± 0.05

Table 5.4.: SM predictions for the low recoil region using SuperIso v3.3. The theoretical errors have been estimated adapting the relative errors of [107] to our central values.

form factors can be obtained [107]

$$T_2(q^2) = \kappa A_1(q^2), \qquad T_3(q^2) = \kappa A_2(q^2) \frac{M_B^2}{q^2}. \tag{5.68}$$

An important source of uncertainty that appears in the low recoil region is due to long distance effects from $c\bar{c}$ loops. Grinstein and Pirjol implemented these long distance contributions as short distance effects, using HQET combined with OPE in $1/m_Q$ with $Q = \{m_b, \sqrt{q^2}\}$ [122] [13]. These effects are then absorbed into the redefinition of C_7^{eff} and C_9^{eff} [14]. It should be noted that in the low recoil region power corrections unlike the high recoil region enter with parametric suppression.
To apply the improved Isgur-Wise relations, and include the long distance contributions to the $B \to K^* \ell^+ \ell^-$ decay we have followed [107]. In the SM, using the input parameters of Table 5.1, the numerical results for the observables BR, A_{FB} and F_L are obtained as summarised in Table 5.4. These observables are defined in the same way as done for the low q^2 region.

[13] A somewhat different approach where HQET is not applied, has been used for the calculation of the long distance effects in [123].

[14] The definitions used for C_7^{eff} and C_9^{eff} in the low recoil region are not the same as for the high recoil region and can be found in [107, 122].

5.3 $B_s \to \bar{\ell}\ell$

5.3.1 Theoretical framework

Considering the effective Hamiltonian for $b \to s$ transitions (5.1), the matrix element for the $\bar{B}_s \to \bar{\ell}\ell$ decay can be written in the same way as what was previously done for the $B \to K^*\ell\ell$ decay (5.8). For the amplitude of $\bar{B}_s \to \ell\ell$ we have

$$\begin{aligned}\mathcal{M} = \frac{G_F \alpha_{em}}{2\sqrt{2}\pi} V_{tb} V_{ts}^* \Bigg\{ \Bigg\langle \ell^+\ell^- \Bigg| & \left[C_7^{eff}(T^{\mu\nu} + T_5^{\mu\nu}) + C_7^{eff\prime}(T^{\mu\nu} - T_5^{\mu\nu}) \right] \times \frac{m_b}{e} F_{\mu\nu} \\ & + \left[C_9^{eff}(V^\mu - A^\mu) + C_9^{eff\prime}(V^\mu + A^\mu) \right] \times (\bar{\ell}\gamma_\mu \ell) \\ & + \left[C_{10}(V^\mu - A^\mu) + C'_{10}(V^\mu + A^\mu) \right] \times (\bar{\ell}\gamma_\mu\gamma_5 \ell) \\ & + \left[C_{Q_1}(S + P) + C'_{Q_1}(S - P) \right] \times (\bar{\ell}\ell) \\ & + \left[C_{Q_2}(S + P) + C'_{Q_2}(S - P) \right] \times (\bar{\ell}\gamma_5 \ell) \Big| \bar{B}_s \Bigg\rangle \Bigg\},\end{aligned} \tag{5.69}$$

where $S, P, V^\mu, A^\mu, T^{\mu\nu}$ and $T_5^{\mu\nu}$ are defined in (5.20). Upon factorising the hadronic and leptonic parts, the following hadronic matrix elements are required

$$\begin{aligned} &\langle 0|A^\mu|\bar{B}\rangle, \quad && \langle 0|P|\bar{B}\rangle, \\ &\langle 0|V^\mu|\bar{B}\rangle, \quad && \langle 0|S|\bar{B}\rangle, \quad && \langle 0|T^{\mu\nu}|\bar{B}\rangle, \quad && \langle 0|T_5^{\mu\nu}|\bar{B}\rangle. \end{aligned} \tag{5.70}$$

The decay constant f_{B_s} is defined via the matrix element of the axial vector current

$$\langle 0|A^\mu|\bar{B}_s\rangle = ip^\mu f_{B_s}, \tag{5.71}$$

where p^μ is the momentum of the $\bar{B}_s$ meson. Using the equations of motion after contracting both sides of the above equation with $i\partial^\mu$, the pseudo scalar matrix element can be obtained [124]

$$\langle 0|P|\bar{B}_s\rangle = -i\frac{M_{B_s}^2}{m_b + m_s} f_{B_s}, \tag{5.72}$$

where M_{B_s} is the B_s meson mass.

The other matrix elements appearing in the second line of (5.70) all vanish [125]. The scalar and vector current matrix elements vanish since S and V^μ are parity even while $\bar{B}_s$ is a pseudo-scalar meson with odd parity. The tensor currents $T^{\mu\nu}$ and $T_5^{\mu\nu}$ also vanish since they are antisymmetric under a $\mu \leftrightarrow \nu$ interchange and it is not possible to construct an antisymmetric combination with p^μ as the only available dynamical variable. Hence the operator O_7 does not contribute to the $\bar{B}_s \to \ell\ell$ decay. Even though the O_9 operator

consists of an axial vector piece in the quark current, it doesn't contribute to the decay either. The axial vector current is $\langle 0|A^\mu|\bar{B}\rangle \propto p^\mu = p^\mu_{\ell^+} + p^\mu_{\ell^-}$, which upon contraction with the leptonic vector current part of O_9 vanishes. Hence, only the operators $Q^{(\prime)}_{1,2}$ and $O^{(\prime)}_{10}$ contribute to this decay. The transition amplitude can be written as

$$\mathcal{M} = \frac{-iG_F\alpha_{em}}{2\sqrt{2}\pi}V_{tb}V^*_{ts}\frac{f_{B_s}}{M_{B_s}}\Bigg\{\left[\frac{2m_\ell}{M_{B_s}}(C_{10}-C'_{10}) + \frac{M_{B_s}}{m_s+m_b}(C_{Q_2}-C'_{Q_2})\right]\times\langle\bar{\ell}\ell|\bar{\ell}\gamma_5\ell|0\rangle \\ + \left[\frac{M_{B_s}}{m_s+m_b}(C_{Q_1}-C'_{Q_1})\right]\times\langle\bar{\ell}\ell|\bar{\ell}\ell|0\rangle\Bigg\}, \tag{5.73}$$

where m_ℓ is the lepton mass. Squaring the amplitude and summing over the lepton spins, the decay width is obtained, from where the branching ratio is [124, 126]:

$$BR(B_s\to\ell^+\ell^-) = \frac{G_F^2\alpha_{em}^2}{64\pi^3}f_{B_s}^2M_{B_s}^3|V_{tb}V^*_{ts}|^2\tau_{B_s}\sqrt{1-\frac{4m_\ell^2}{M_{B_s}^2}}\Bigg\{\left(1-\frac{4m_\ell^2}{M_{B_s}^2}\right) \\ \times\left|\left(\frac{M_{B_s}}{m_b+m_s}\right)(C_{Q_1}-C'_{Q_1})\right|^2 + \left|\left(\frac{M_{B_s}}{m_b+m_s}\right)(C_{Q_2}-C'_{Q_2}) + \frac{2m_\mu}{M_{B_s}}(C_{10}-C'_{10})\right|^2\Bigg\}. \tag{5.74}$$

The branching ratio of $B_s \to \ell^+\ell^-$ described above is CP-averaged. For the $B_s \to \mu^+\mu^-$ however, the experimental value is untagged. Taking into account the precise measurement [127] of the fractional decay width difference between the B_s heavy and light mass eigenstates, $y_s \equiv \Delta\Gamma_{B_s}/(2\Gamma_{B_s}) = 0.088 \pm 0.014$, the untagged branching ratio is related to the CP-averaged one by [128]:

$$BR^{\text{untag}}(B_s\to\mu^+\mu^-) = \left[\frac{1+\mathcal{A}_{\Delta\Gamma}y_s}{1-y_s^2}\right]BR(B_s\to\mu^+\mu^-), \tag{5.75}$$

where

$$\mathcal{A}_{\Delta\Gamma} = \frac{|P|^2\cos(2\phi_P) - |S|^2\cos(2\phi_S)}{|P|^2+|S|^2}, \tag{5.76}$$

with

$$S \equiv \sqrt{1-\frac{4m_\mu^2}{M_{B_s}^2}}\frac{M_{B_s}}{2m_\mu}\frac{M_{B_s}}{(m_b+m_s)}\frac{(C_{Q_1}-C'_{Q_1})}{C_{10}^{SM}}, \tag{5.77}$$

$$P \equiv \frac{C_{10}-C'_{10}}{C_{10}^{SM}} + \frac{M_{B_s}}{2m_\mu}\frac{M_{B_s}}{(m_b+m_s)}\frac{(C_{Q_2}-C'_{Q_2})}{C_{10}^{SM}}, \tag{5.78}$$

Lattice QCD Group	Ref.	f_{B_s}	f_B
ETMC-11	[129]	232 ± 10 MeV	195 ± 12 MeV
Fermilab-MILC-11	[130, 131]	242 ± 9.5 MeV	197 ± 9 MeV
HPQCD-12	[132]	227 ± 10 MeV	191 ± 9 MeV
Our choice		234 ± 10 MeV	194 ± 10 MeV

Table 5.5.: Average of lattice QCD results used as input in our work.

and

$$\phi_S = \arg(S), \qquad \phi_P = \arg(P), \tag{5.79}$$

are the CP-violating phases.

5.3.2 Standard Model values and theoretical uncertainties

In the Standard Model, only C_{10} is non-vanishing and its largest contributions arise from a Z penguin top loop (75%), and from a charmed box diagram (24%) . With the inputs of Table 5.1, $C_{10} = -4.21$, from which $BR(B_s \to \mu^+\mu^-)|_{SM} = (3.53 \pm 0.38) \times 10^{-9}$. The latest experimental results thus severely constrain the room for new physics, and its proximity with the 2σ upper value calls for a discussion of the uncertainties in this SM prediction.

The main uncertainty comes from the B_s decay constant f_{B_s}, which has recently been re-evaluated by independent lattice QCD groups (see Table 5.5). Their 4.3% uncertainties agree, as do their results within these uncertainties, so that we have chosen an average of these three results in what follows. This implies a 8.7% uncertainty on the branching ratio.

Notice this range covers the recently published result $f_{B_s} = 225 \pm 4\,\text{MeV}$ of McNeile et al. [133], whose lower value and striking precision dominates any weighted average including it, like the one in [134] (227 ± 4 MeV) proposed by one of the authors of [133], or the one in [135]: 227 ± 6 MeV. The smallness of the extrapolation error in this work raises a number of new questions, and we prefer to keep our naive but more conservative average. This choice has however little effect on the new physics applications we have in mind, as these depend mostly on the lower end of the 2σ range: $214 = 234 - 20 \simeq 215 = 227 - 12$.

Another potential source of uncertainty comes from the choice of scale at which the fine structure constant is used in (5.74): there is a non-negligible 4% difference between the running $\overline{MS}$ couplings $\hat{\alpha}(m_b) = 1/133$ and $\hat{\alpha}(m_Z) = 1/128$. If the first choice may seem natural, the weak couplings involved in the top Z-penguin (or charmed box) are closer to the weak scale, and do not run below it, as discussed in Ref. [136]. We thus take that last value, as well as $\sin^2\hat{\theta}_W(m_Z) = 0.2312$ in the expression of (5.74). This may seem at odds with the conclusion of [136], which states that choosing $\hat{\alpha}(m_b)$ minimises the EW corrections to $B \to K^*\ell^+\ell^-$. However, the EW corrections to $C_{7,9}$, which dominate the low q^2_{ll} region of this last process, are opposite to the EW corrections for C_{10}, which

controls $B_s \to \mu^+\mu^-$. Having made this choice for the EM-coupling, we expect EW corrections to mostly absorb the remaining scale dependence in $\hat{\alpha}_{EM}(\mu)$, leaving a small, 2% uncertainty in the branching ratio.
The remaining theoretical uncertainties are smaller owing to the NNLO treatment of QCD corrections: increasing the low scale μ_b (or the matching scale μ_W) by a factor of 2 induces a 1.4% (or respectively 2%) effect.
Finally, parametric uncertainties from the top mass (1.3%), from the B_s lifetime (1.8%) and from the CKM element V_{ts} (5%), are expected to be reduced in the future. Adding all these (small) errors in quadrature, we thus get a Standard Model prediction assorted with an 11% uncertainty:

$$BR(B_s \to \mu^+\mu^-) = (3.53 \pm 0.38) \times 10^{-9} \; . \tag{5.80}$$

This value is compatible with recent SM predictions for this observable, i.e. by the CKMfitter group [137], for which the uncertainties are reduced by the use of other flavour information.
The lower $(3.23 \pm 0.15 \pm 0.32)\times 10^{-9}$ value in [138] mostly comes from a lower choice of f_{B_s}, which accounts for 6% out of the 9% difference. Another source of discrepancy is the $\overline{MS}$ value of the top mass $m_t(m_t)$ used in the Inami-Lim function for $C_{10}(m_t) \sim m_t^{3.0}$: for a given pole mass, the one-loop $\overline{MS}$ mass is 2.5 GeV higher than the 3 or 4-loop mass, more than twice the current experimental error. We used the 1-loop results, as normally suited for NLO-corrected results, whereas [138] used the 4-loop result.

CHAPTER 6

Constraints on SUSY

In this chapter we will first present recent experimental result for the $B_s \to \mu^+\mu^-$ and $B \to K^*\mu^+\mu^-$ decays, and then proceed to consider the supersymmetric effects on the Wilson coefficients. In the absence of any significant deviation of the experimental values for $B_s \to \mu^+\mu^-$ and $B \to K^*\mu^+\mu^-$ observables from the SM predictions (as presented in the previous chapter), we will discuss the constraining power of these observables on the parameter space of chosen minimal flavour violating (MFV) scenarios.

6.1 Experimental results

6.1.1 $B_s \to \mu^+\mu^-$

Experimental searches for the rare $B_s \to \mu^+\mu^-$ decay have been carried out for more than a quarter of a decade [139]. Recently, in the Autumn of 2012, the first evidence of $B_s \to \mu^+\mu^-$ decay was presented by the LHCb collaboration [140]:

$$\mathrm{BR}(B_s \to \mu^+\mu^-) = (3.2^{+1.5}_{-1.2}) \times 10^{-9} \,, \qquad \text{at } 95\% \text{ C.L.} \tag{6.1}$$

Prior to that, there were only upper limits available, the best having been published by the LHCb collaboration in the spring of the same year [141]:

$$\mathrm{BR}(B_s \to \mu^+\mu^-) < 4.5 \times 10^{-9} \,, \qquad \text{at } 95\% \text{ C.L.} \tag{6.2}$$

This upper limit was followed by the result from CMS [142]:

$$\mathrm{BR}(B_s \to \mu^+\mu^-) < 7.7 \times 10^{-9} \,. \qquad \text{at } 95\% \text{ C.L.} \tag{6.3}$$

Further independent bounds were provided by the CDF collaboration with a weaker upper limit [143]:

$$\mathrm{BR}(B_s \to \mu^+\mu^-) < 3.4 \times 10^{-8} \,, \tag{6.4}$$

together with a one standard deviation interval

$$\mathrm{BR}(B_s \to \mu^+\mu^-) = (1.3^{+0.9}_{-0.7}) \times 10^{-8} \,, \tag{6.5}$$

arising from an observed excess over the expected background.

For the purpose of our subsequent numerical studies, we adopt the Spring 2012 LHCb limit[1] and, accounting for 11% theoretical uncertainty (as explained in Section 5.3), we impose the following upper limit at 95% C.L.[2]

$$\mathrm{BR}(B_s \to \mu^+\mu^-) < 5.0 \times 10^{-9} \,. \tag{6.6}$$

The lower limit does not provide any constraint for the models that we have considered.

6.1.2 $B \to K^*\mu^+\mu^-$

For $B \to K^*\mu^+\mu^-$ related observables, we will use the latest LHCb results which correspond to an integrated luminosity of 1 fb^{-1} [144]. These results are summarised in Table 6.1 where the experimental uncertainties are statistical and systematic. For comparison, the different SM predictions with the corresponding theoretical errors (from the five sources of errors mentioned in Table 5.3, added in quadrature) are also provided.

Observable	SM prediction	Experiment
$10^7\mathrm{GeV}^2 \times \langle dBR/dq^2\,(B \to K^*\mu^+\mu^-)\rangle_{[1,6]}$	0.47 ± 0.27	$0.42 \pm 0.04 \pm 0.04$
$\langle A_{FB}(B \to K^*\mu^+\mu^-)\rangle_{[1,6]}$	-0.06 ± 0.05	$-0.18^{+0.06+0.01}_{-0.06-0.01}$
$\langle F_L(B \to K^*\mu^+\mu^-)\rangle_{[1,6]}$	0.71 ± 0.13	$0.66^{+0.06+0.04}_{-0.06-0.03}$
$10^7\mathrm{GeV}^2 \times \langle dBR/dq^2\,(B \to K^*\mu^+\mu^-)\rangle_{[14.18,16]}$	0.70 ± 0.19	$0.59 \pm 0.07 \pm 0.04$
$\langle A_{FB}(B \to K^*\mu^+\mu^-)\rangle_{[14.18,16]}$	0.44 ± 0.07	$0.49^{+0.04+0.02}_{-0.06-0.05}$
$\langle F_L(B \to K^*\mu^+\mu^-)\rangle_{[14.18,16]}$	0.36 ± 0.05	$0.35^{+0.07+0.07}_{-0.06-0.02}$
$q_0^2(B \to K^*\mu^+\mu^-)/\mathrm{GeV}^2$	$4.26^{+0.36}_{-0.34}$	$4.9^{+1.1}_{-1.3}$

Table 6.1.: Experimental values and SM predictions (the theoretical errors are from adding in quadrature the different errors in Table 5.3).

In addition to the observables listed in Table 6.1, three other observables have also been measured using 1 fb^{-1} of LHCb data, namely S_3 and A_{Im} [144] as well as the isospin

[1] The upper limit of the Autumn 2012 LHCb result is 4.7×10^{-9}; when compared to the 4.5×10^{-9} upper limit of Spring 2012 it is clear that such a small discrepancy should have no significant effect in the constraints obtained in Section 6.3.2.

[2] To be fully accurate [128], we should multiply this number by a factor $(1+y_s)/(1+\mathcal{A}_{\Delta\Gamma}y_s)$ and compute the asymmetry $\mathcal{A}_{\Delta\Gamma}$ for the particular SUSY models studied. However, for most of the models passing this constraint, this factor provides less than a 2% correction.

asymmetry, A_I [145]. The reported results are:

$$\langle 2\, S_3(B \to K^* \mu^+ \mu^-) \rangle_{[1,6]} = 0.10^{+0.15+0.02}_{-0.16-0.01} , \quad (6.7)$$

$$\langle A_{Im}(B \to K^* \mu^+ \mu^-) \rangle_{[1,6]} = 0.07^{+0.07+0.02}_{-0.07-0.01} , \quad (6.8)$$

$$\langle A_I(B \to K^* \mu^+ \mu^-) \rangle_{[1,6]} = -0.15 \pm 0.16 . \quad (6.9)$$

However, with the current experimental accuracy, these observables are not sensitive enough to probe SUSY parameters.

For all $B_s \to \mu^+\mu^-$ and $B \to K^*\mu^+\mu^-$ observables, the experimental results are in very good agreement with the SM prediction. This implies that these observables will allow to severely constrain any contribution from new physics models.

6.2 SUSY contributions in the MSSM

The effective theory formalism of weak B-decays allows for a convenient inclusion of the effects of new physics (NP). NP contributions to $b \to s\ell\ell$ processes can be reabsorbed into the Wilson coefficients of the effective Hamiltonian, presented in Chapter 5

$$C_i(\mu_0) = C_i^{SM}(\mu_0) + C_i^{NP}(\mu_0), \quad (6.10)$$

where $C_i(\mu_0)$ contain all the contributions from both SM and NP particles at the electroweak ($\mu_0 \sim M_W$) and higher scales. The Wilson coefficients are then evolved down to the scale at which the B-decay takes place ($\mu_b \sim m_b$) through renormalisation group equations (RGEs) (see Appendix A). When the considered NP scenario is the minimal supersymmetric standard model (MSSM) with R-parity conservation, the new particles only contribute through loops. As mentioned in Chapter 3, besides the $W^\pm$ and up-type quark contributions, which are already present in the SM, in the MSSM there are additional contributions from: *a*) charged Higgs; *b*) up-type squarks and charginos; *c*) down-type squarks and gluinos; *d*) down-type squarks and neutralino loops. The latter loops can correspond to either box diagrams or penguins, mediated by either a photon, Z-boson or neutral Higgs subsequently decaying into a lepton pair.
In our work we have considered constrained MSSM scenarios with MFV. We have mostly focused on the CMSSM and briefly on models with non-universal Higgs masses (NUHM), both assuming SUSY breaking mediated by gravity (thus flavour blind) and invoking universal boundary conditions at a very high scale $m_{\rm GUT}$.

For these scenarios, flavour changing contributions from neutralino and gluino loops are negligible compared to the chargino loops, since the flavour mixing among the third and the two other generations of the down-squarks are comparatively small [146–148]. Alternatively it can be said that, to a good approximation the down squark mass-squared matrix is flavour diagonal [40]. Hence the flavour changing contributions from neutralino and gluino interactions can be neglected. In the MSSM, the chargino and charged Higgs contributions to the most relevant Wilson coefficients for $B_s \to \mu^+\mu^-$ and $B \to K^*\mu^+\mu^-$

($C^{(\prime)}_{7,\ldots,10,Q_{1,2}}$) have been calculated by various authors [40, 41, 86, 87, 124, 146, 149]. In order to compare the relative deviation of the Wilson coefficients from their SM value we introduce the following quantity,

$$\delta C_i = \frac{C_i^{MSSM} - C_i^{SM}}{C_i^{SM}}. \tag{6.11}$$

A detailed list of all the relevant MSSM contributions to the Wilson coefficients considered in this work can be found in [150].

6.3 CMSSM

The first model that we consider is the CMSSM, characterised by the set of parameters $\{m_0, m_{1/2}, A_0, \tan\beta, \mathrm{sgn}(\mu)\}$. Here m_0 is the universal scalar mass, $m_{1/2}$ the universal gaugino mass, A_0 the universal trilinear coupling, and $\tan\beta$ the ratio of the vacuum expectation values of the Higgs doublets. The analysis described here corresponds to the study of [118]. Despite being disfavoured by the recent evidence for a ∼125 GeV Higgs [151, 152], the CMSSM offers an illustrative and controllable prototype of MFV SUSY scenarios.

6.3.1 Wilson coefficients in the CMSSM

When all new contributions are included, one can find significant deviations from the SM values of the Wilson coefficients. To numerically evaluate the effect of SUSY contributions in the CMSSM, we performed a scan over the following ranges for the relevant parameters: $m_0 \in [100, 3000]$ GeV, $m_{1/2} \in [100, 3000]$ GeV, $A_0 \in [-5000, 2000]$ GeV and $\tan\beta \in [1, 60]$, with $\mu > 0$. For each of the $\simeq$ 500000 points generated, we computed the SUSY spectrum and couplings using SOFTSUSY 3.2.4 [153]. The contributions of the SUSY particles to the Wilson coefficients were then computed and run down to the μ_b scale, using SuperIso v3.3 [126, 154]. For this Ph.D, soft form factors, non-factorisable corrections, additional angular $B \to K^+\ell\ell$ observables as well as C_9 running were added to this software package.

The full variation of the Wilson coefficients in such a CMSSM scan is presented in Figure 6.1, ignoring existing constraints on SUSY parameters and/or Wilson coefficients. As can be seen, C_7 and C_8 can have both signs and their correlation is visible in the figure. C_9, exhibits hardly any change while C_{10} can have a larger spread. This feature can be understood once we notice that box diagrams are suppressed with respect to Higgs- or Z-penguin diagrams, giving $\delta C_9/\delta C_{10} \sim (g_V/g_A)_\mu \sim 1 - 4\sin^2\theta_W$.
On the other hand (pseudo-) scalar coefficients ($C_{Q_{1,2}}$) can receive the largest SUSY contributions, owing to the scalar penguin enhancement proportional to $\tan^3\beta$ at large $\tan\beta$ regime. The primed coefficients ($C'_{7,\ldots,10,Q_{1,2}}$) are suppressed in the CMSSM and have negligible effects. The relative deviation of the most relevant non-primed Wilson

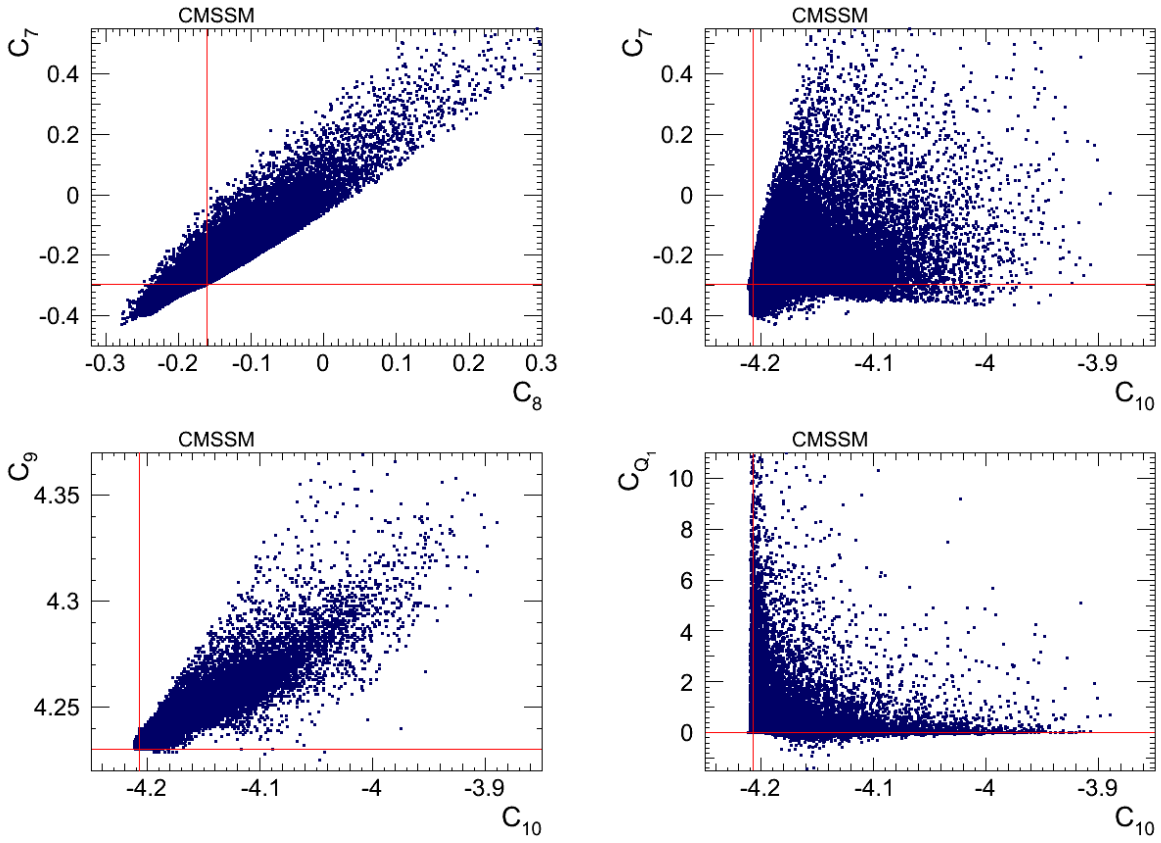

Figure 6.1.: Variation of the Wilson coefficients in the CMSSM with all the parameters varied in the ranges given in the text. The red lines correspond to the SM predictions.

coefficients in the CMSSM thus obey the following hierarchy at large $\tan\beta$

$$\left|\delta C_{Q_{1,2}}\right| \gg |\delta C_7| > |\delta C_{10}| > |\delta C_9|\,. \tag{6.12}$$

Moreover, while the scalar and pseudoscalar coefficients ($C_{Q_{1,2}}$) have the same absolute value, they have opposite signs.

The observables associated with $B_s \to \mu^+\mu^-$ and $B \to K^*\mu^+\mu^-$ are sensitive to different Wilson coefficients as given in Table 6.2.

Observable	C_7	C_9	C_{10}	C_{Q_1}	C_{Q_2}
$\mathrm{BR}(B_s \to \mu^+\mu^-)$	✗	✗	✓	✓	✓
$\mathrm{BR}(B \to K^*\mu^+\mu^-)$	✓	✓	✓	✓	✓
$A_{FB}(B \to K^*\mu^+\mu^-)$	✓	✓	✓	✓	✓
$F_L(B \to K^*\mu^+\mu^-)$	✓	✓	✓	✓	✓
$q_0^2(B \to K^*\mu^+\mu^-)$	✓	✓	✓	✓	✗
$A_T^{(2)}(B \to K^*\mu^+\mu^-)$	✓	✓	✓	✗	✗
$A_T^{(3)}(B \to K^*\mu^+\mu^-)$	✓	✓	✓	✗	✗
$A_T^{(4)}(B \to K^*\mu^+\mu^-)$	✓	✓	✓	✓	✗

Table 6.2.: Dependence of the $B_s \to \mu^+\mu^-$ and $B \to K^*\mu^+\mu^-$ observables to the different Wilson coefficients, ✓(✗) denoting the (lack of) dependence for a given observable.

6.3.2 CMSSM constraints

We now proceed to display the impact of the SUSY contributions to BR($B_s \to \mu^+\mu^-$). This will allow to derive constraints on the SUSY spectrum that was specified. As mentioned before, in the absence of any significant deviation of the experimental results from the SM predicted value for BR($B_s \to \mu^+\mu^-$), the flavour observable can be used to put constraints on the CMSSM parameter space. The constraints are shown in Figure 6.2 in the ($M_{\tilde{t}_1}$, $\tan\beta$) and ($M_{H^\pm}$, $\tan\beta$) planes, where $M_{\tilde{t}_1}$ and $M_{H^\pm}$ are the masses of the lightest stop and charged Higgs, respectively. It is clear that the large values of $\tan\beta$ above 50 are strongly constrained except for a few fine-tuned points with light charged Higgs H^+. Contributions can still happen for low enough $\tilde{t}_1$ (or H^+) masses, but not necessarily when other parameters are varied.

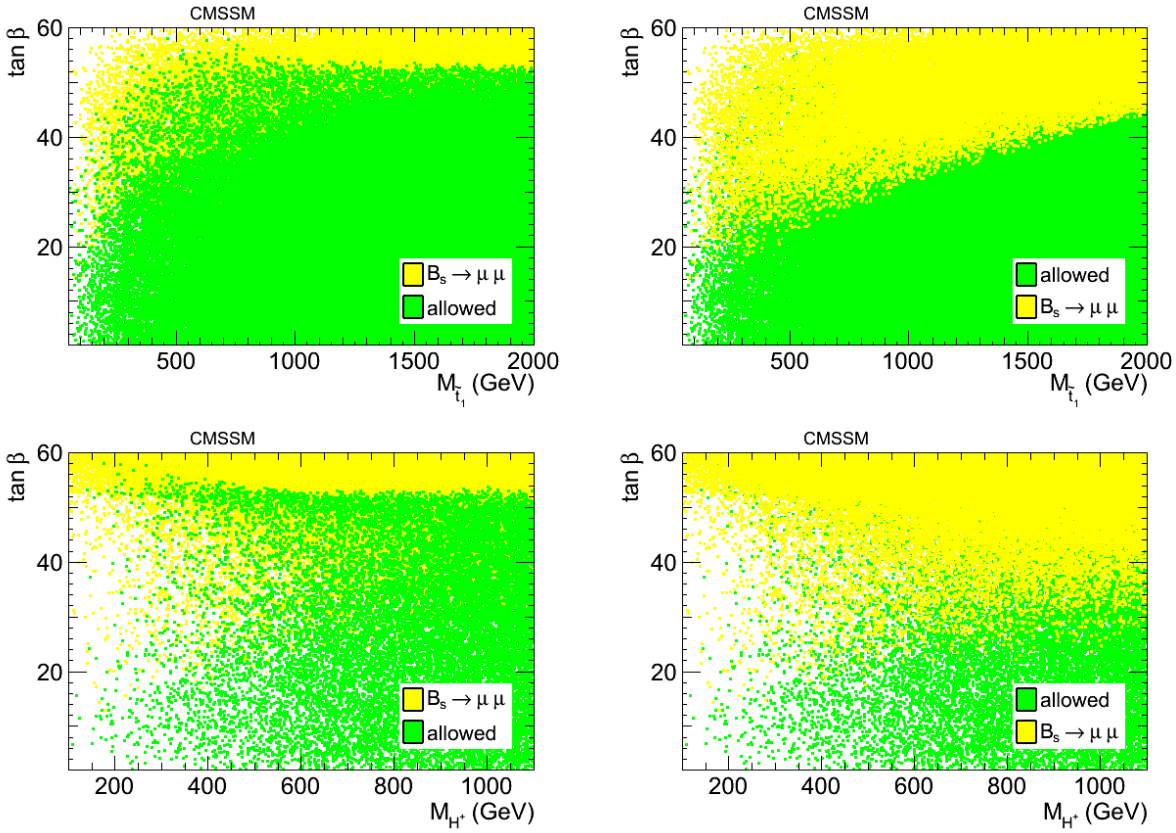

Figure 6.2.: CMSSM constraints from BR($B_s \to \mu^+\mu^-$) on the ($M_{\tilde{t}_1}$, $\tan\beta$) plane (upper panel) and on the ($M_{H^\pm}$, $\tan\beta$) plane (lower panel). The allowed points are displayed in the foreground on the left and in the background on the right.

Next we address the constraints from $B \to K^*\mu^+\mu^-$ observables. In order to maximise the SUSY effects, we consider the large $\tan\beta$ regime, $\tan\beta = 50$, also displaying for completeness the results for $\tan\beta = 30$. We further investigate the sensitivity of the SUSY contributions to the lightest stop. We start with the averaged differential branching ratio as defined in Table 5.3. The results in the CMSSM are displayed in Figure 6.3 for the low q^2 region and in Figure 6.4 for the high q^2 region, the solid red lines correspond to the LHCb central value, while the dashed and dotted lines represent the 1 and 2σ bounds respectively, including both theoretical and experimental errors (added in quadrature).

At low q^2, this branching ratio excludes $M_{\tilde{t}_1}$ below $\sim$ 250 GeV for $\tan\beta$=50 and $\sim$ 150 GeV for $\tan\beta$=30. In the high q^2 region, the constraints from BR($B \to K^*\mu^+\mu^-$) have a milder impact, as the $M_{\tilde{t}_1}$ below $\sim$ 300 GeV and $\sim$ 200 GeV are excluded for $\tan\beta$=50 and $\tan\beta$=30 respectively. As this light stop region is already excluded by the direct

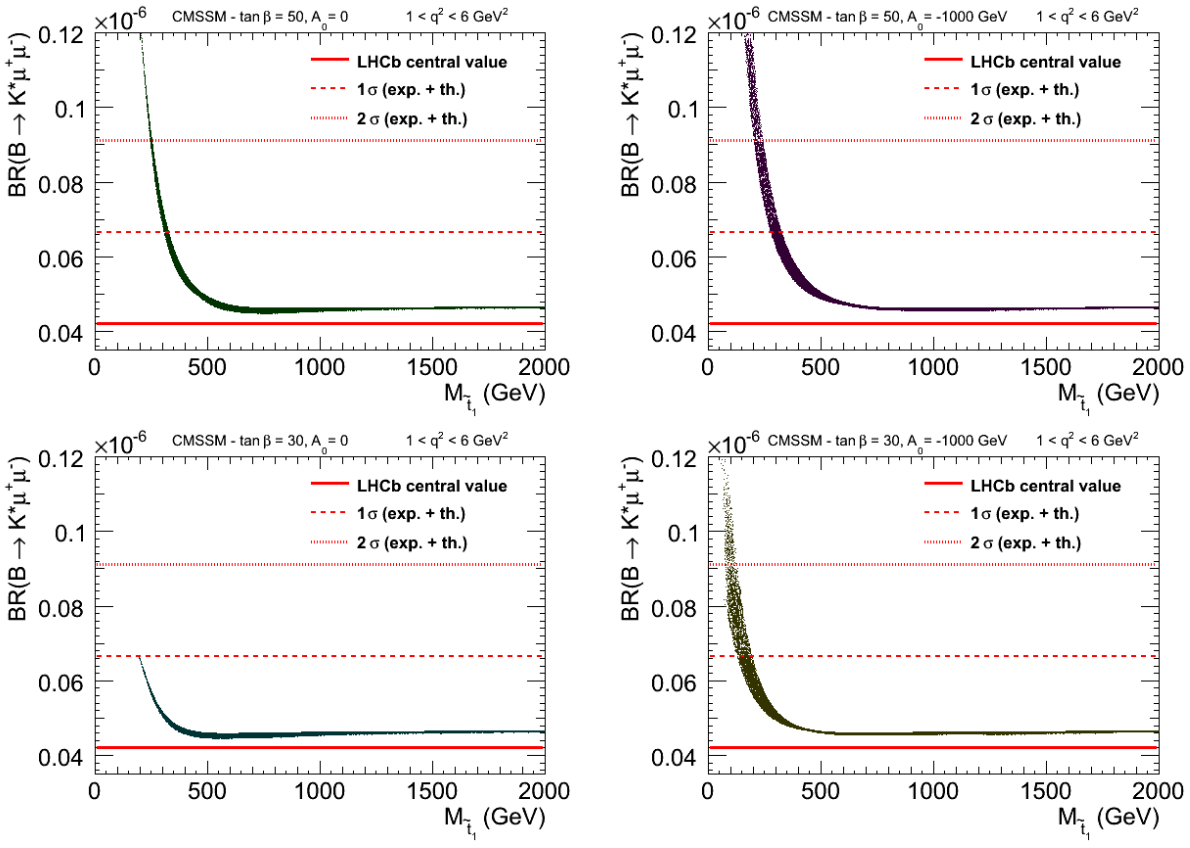

Figure 6.3.: Full SUSY + SM contributions to the averaged BR($B \to K^*\mu^+\mu^-$) at low q^2 as a function of the lightest stop mass, for $\tan\beta$=50 (upper panel) and $\tan\beta$=30 (lower panel). On the left we set $A_0 = 0$ while on the right $A_0 = -1000$ GeV. The solid red line corresponds to the LHCb central value, while the dashed and dotted lines represent the 1 and 2σ bounds respectively, including both theoretical and experimental errors (added in quadrature).

SUSY searches for the same scenario, BR($B \to K^*\mu^+\mu^-$) does not provide additional information. It is worth stressing that the main reason behind the limited constraining power of the branching ratio is the large theoretical uncertainties (mainly due to form factors) from which this observable is suffering. The results are shown for two values of A_0 (=0 and -1000 GeV) for comparison. As can be seen from the figures, the constraints for the more negative values of A_0 are slightly stronger.

Contrary to the BR($B \to K^*\mu^+\mu^-$), angular distributions, in which the theoretical uncertainties are reduced, can in principle provide more robust constraints on the SUSY parameter space. In particular, in our work we have considered the forward-backward asymmetry A_{FB}, the zero-crossing q_0^2 of A_{FB}, F_L, as well as S_3 and A_{Im} for which the LHCb results with 1 fb^{-1} of data are available (see Section 6.1). The two latter observables do not provide any relevant constraint with the current results and accuracy. The SUSY spreads as a function of the stop mass, for A_{FB}, q_0^2 and F_L are presented in Figures 6.5–6.7. As can be seen, A_{FB} provides the most stringent constraints among these observables, and excludes $M_{\tilde{t}_1} \lesssim 800$ GeV and $\lesssim 600$ GeV at tan β=50 and tan β=30, respectively. On the other, hand q_0^2 excludes $M_{\tilde{t}_1} \lesssim 550$ GeV (for tan β=50) and $\lesssim 400$ GeV

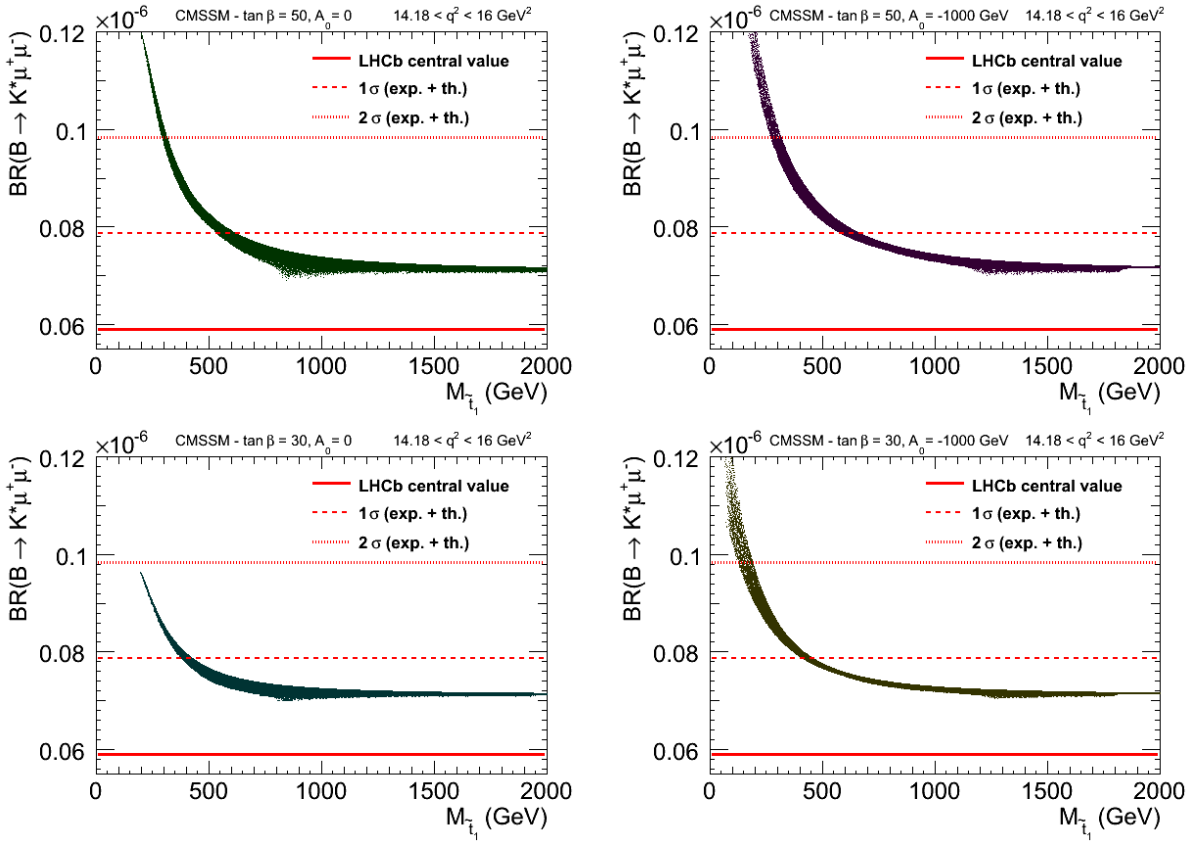

Figure 6.4.: Full SUSY + SM contributions to the averaged BR($B \to K^*\mu^+\mu^-$) at high q^2. Parameters and line/colour code as in Figure 6.3.

(for $\tan\beta$=30), while F_L only disfavours $M_{\tilde{t}_1} \lesssim 200$ GeV (for $\tan\beta$=50) and $\lesssim 150$ GeV (for $\tan\beta$=30). The impressive constraining power of A_{FB} is mainly due to the facts that the reported experimental errors are more than twice smaller than the previous results, and the measured central value is more than 1σ away from the SM, and that SUSY contributions increase this tension. The same observables at high q^2 have less impact on the SUSY parameters and therefore their results are not reproduced here.

To illustrate the sensitivity of the observables to other SUSY parameters, in Figure 6.8 we present the variation of A_{FB} (which has the largest impact as we have shown) with respect to the pseudo scalar Higgs and the gluino masses (although gluino loops are negligible, a small gluino mass implies a low $m_{1/2}$ which allows for a small $\tilde{t}_1$ and $\tilde{\chi}^{\pm}$). Notice the CMSSM correlation between M_A and $M_{\tilde{t}_1}$ when comparing Figure 6.8 (left) and Figure 6.5 (upper left).

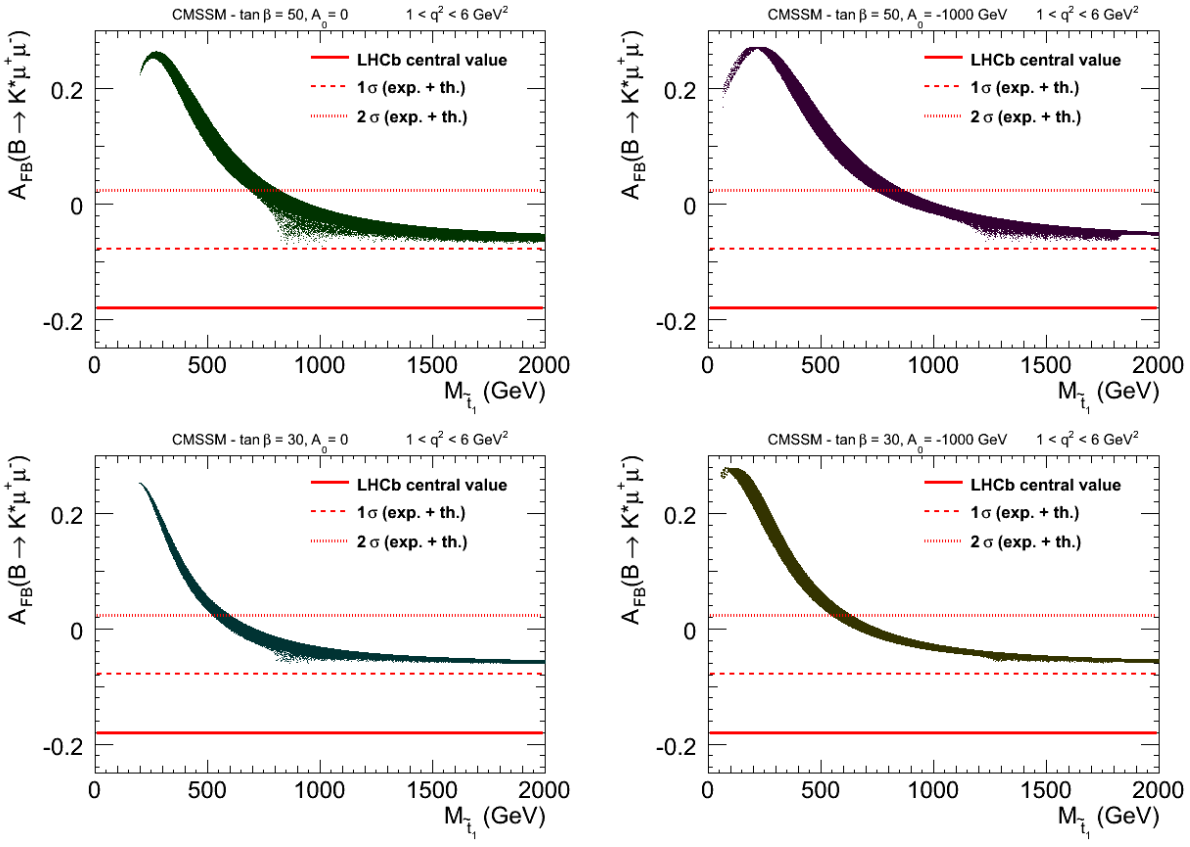

Figure 6.5.: Full SUSY + SM contributions to the $A_{FB}(B \to K^*\mu^+\mu^-)$ at low q^2 as a function of the lightest stop mass. Parameters and line/colour code as in Figure 6.3.

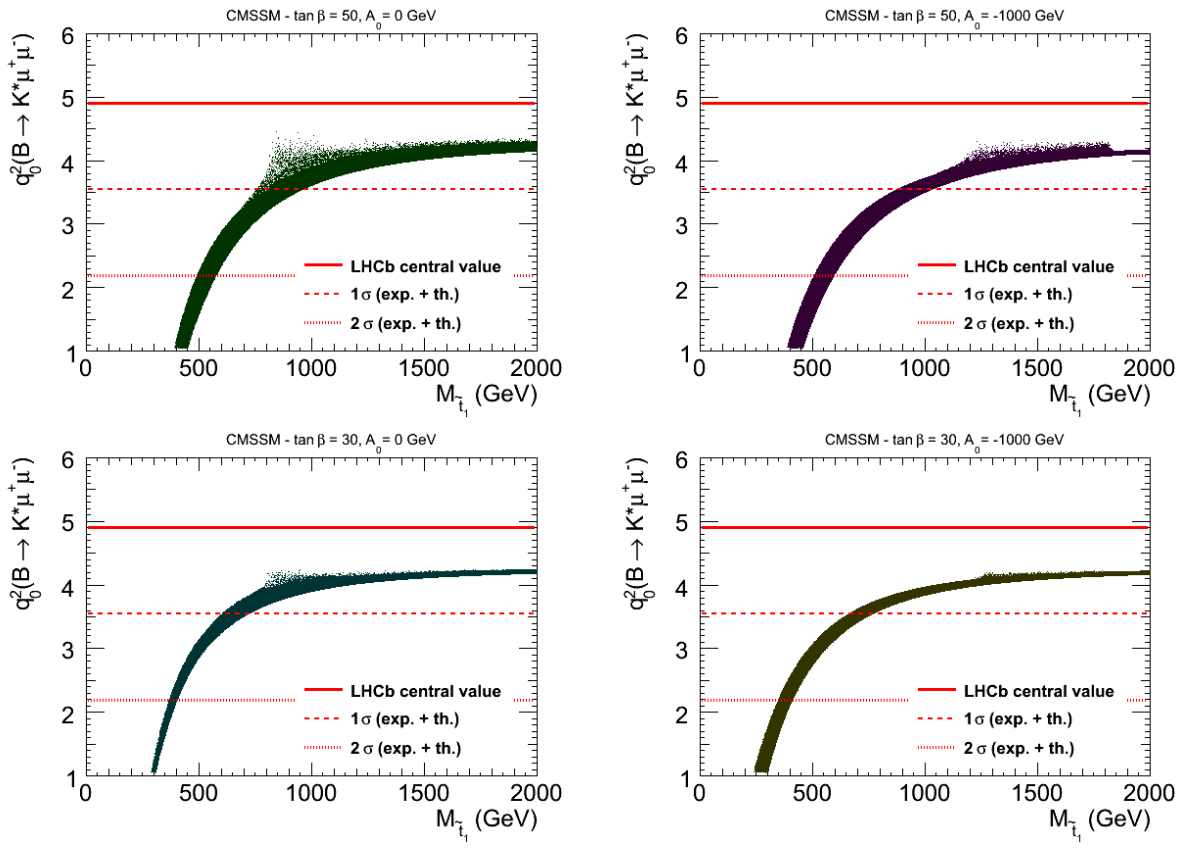

Figure 6.6.: Full SUSY + SM contributions to the $A_{FB}(B \to K^*\mu^+\mu^-)$ zero–crossing q_0^2. Parameters and line/colour code as in Figure 6.3.

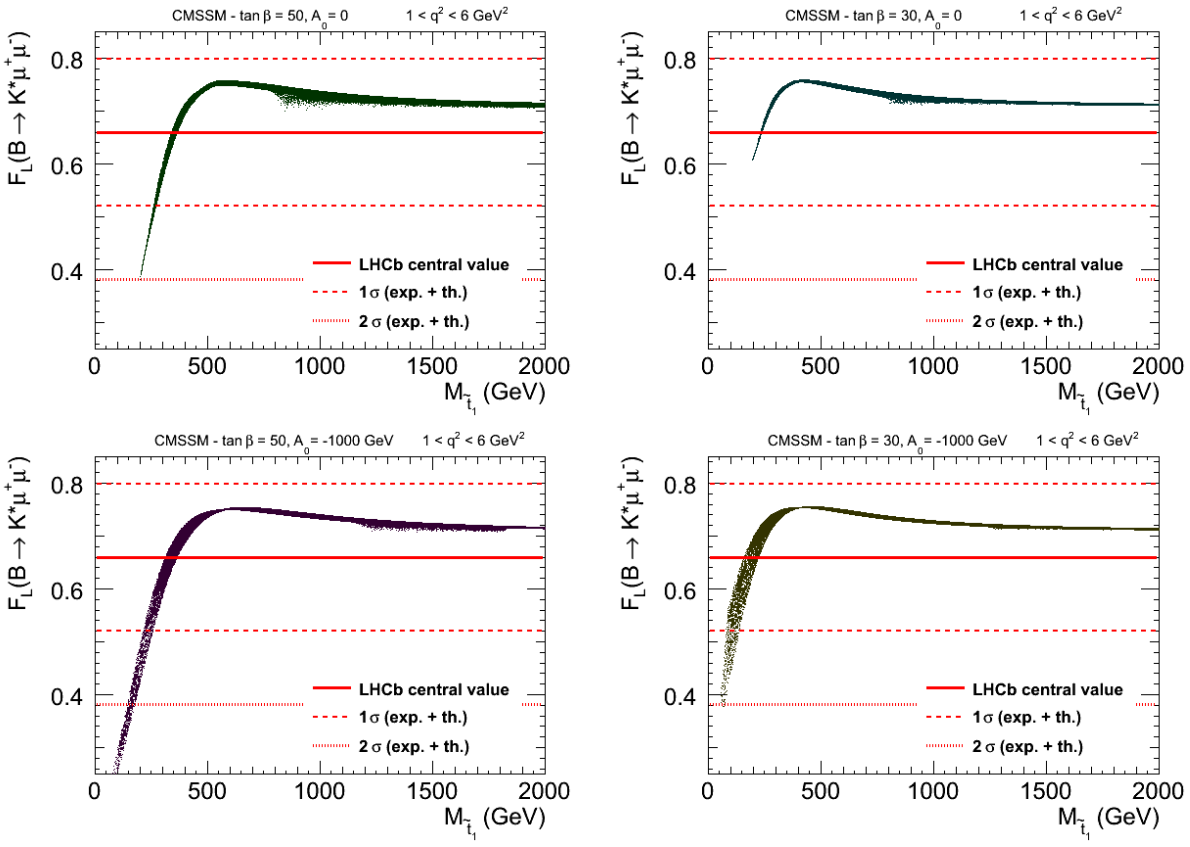

Figure 6.7.: Full SUSY + SM contributions to $F_L(B \to K^*\mu^+\mu^-)$ at low q^2 as a function of the lightest stop mass. Parameters and line/colour code as in Figure 6.3.

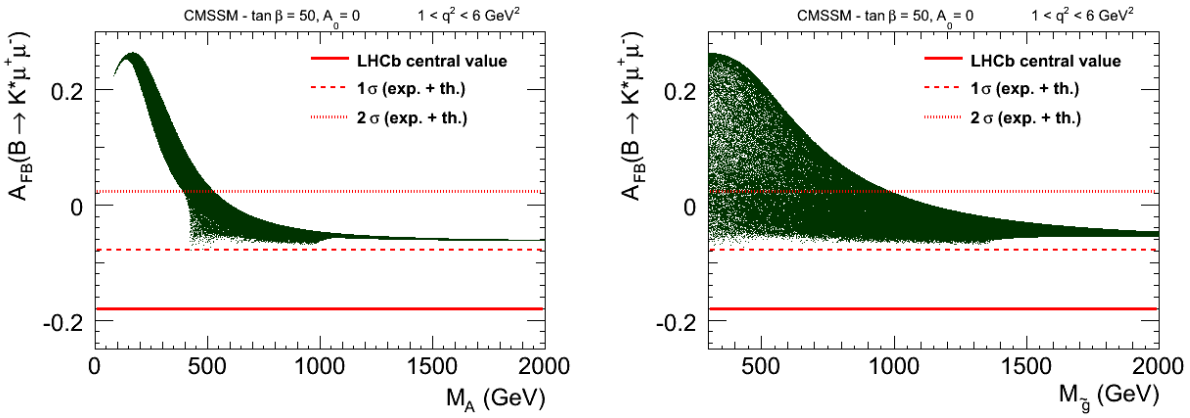

Figure 6.8.: Full SUSY + SM contributions to the $A_{FB}(B \to K^*\mu^+\mu^-)$ at low q^2 as a function of the pseudo scalar Higgs mass (left) and of the gluino mass (right), for $\tan\beta$=50 and $A_0 = 0$.

Another observable of interest for which LHCb has recently announced a measurement for [145] is the isospin asymmetry A_I, defined in (5.38). Figure 6.9 illustrates the SUSY spread of A_I as a function of $M_{\tilde{t}_1}$. Since the experimental measurement (6.9) has an error larger than the SUSY spread, the current result does not provide any relevant information on the SUSY parameters.
In Figure 6.10, we show the SUSY spread as a function of the lightest stop mass, for $A_T^{(2)}$, $A_T^{(3)}$, $A_T^{(4)}$ (as defined in (5.39)–(5.41)) which have not yet not been measured by LHCb. Large deviations from the Standard Model can be found for small values of $M_{\tilde{t}_1}$, depending on the upcoming experimental measurements, these observables could prove to be of interest in constraining the SUSY parameters.

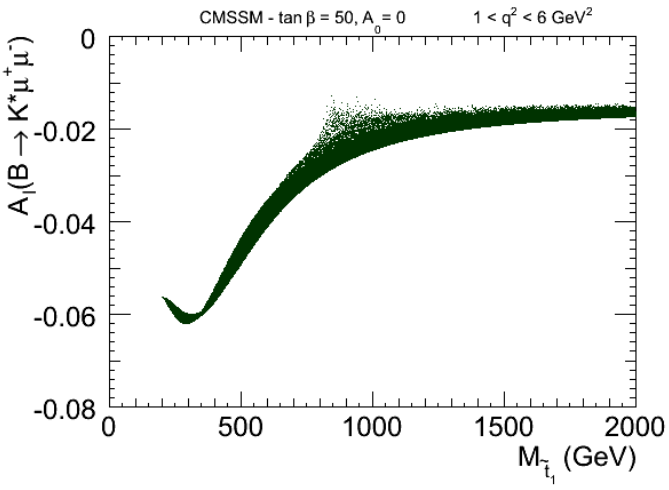

Figure 6.9.: Full SUSY + SM contributions to the isospin asymmetry ($B \to K^* \mu^+ \mu^-$) at low q^2 as a function of the lightest stop mass, for $\tan\beta$=50 and $A_0 = 0$.

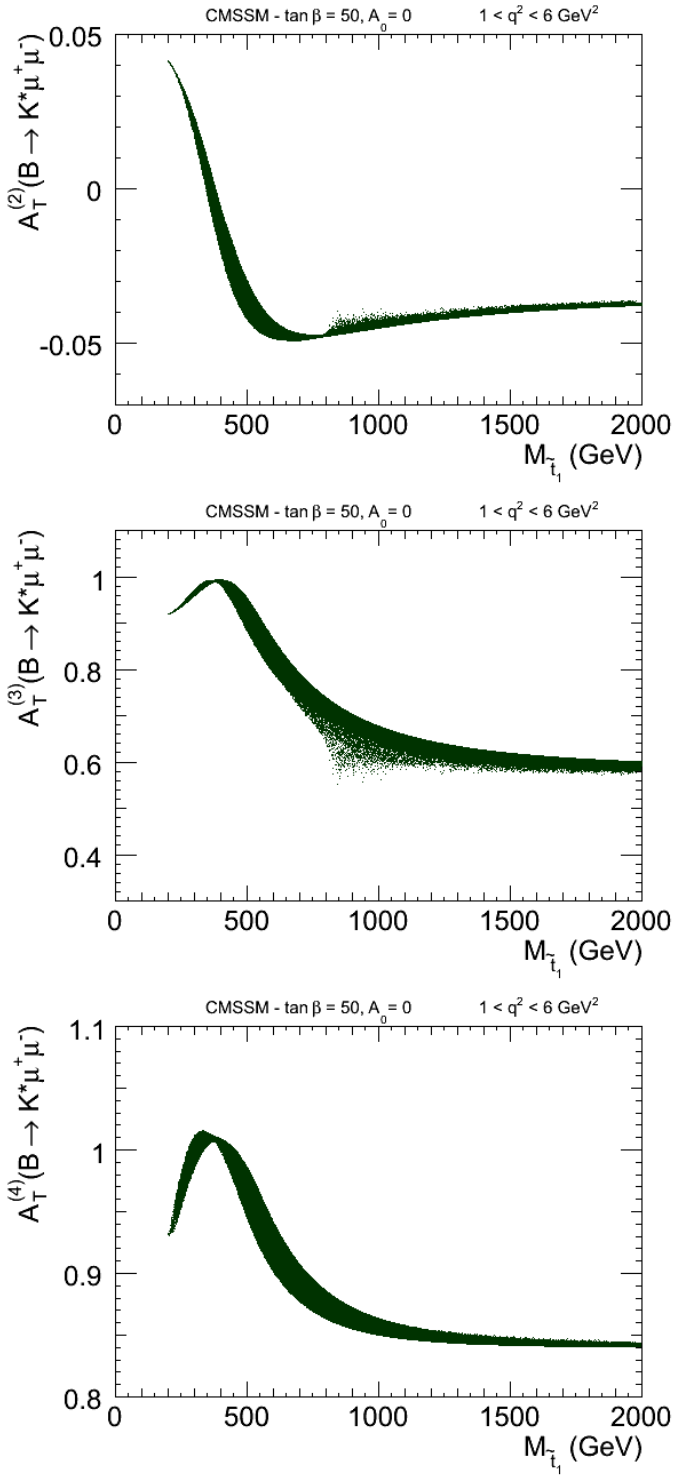

Figure 6.10.: Full SUSY + SM contributions to $A_T^{(2)}$, $A_T^{(3)}$ and $A_T^{(4)}$ at low q^2 as a function of the lightest stop mass, for $\tan\beta$=50 and $A_0 = 0$.

A comparison between the constraining power of these observables in the $(m_{1/2}, m_0)$ plane is provided in Figure 6.11. As expected, A_{FB} is the most constraining observable also in this plane. All the observables show more sensitivity at larger $\tan\beta$ and smaller A_0.

The limits on the various observables, allow to derive bounds on the Wilson coefficients (see for example [94,101,107,155,156]). For instance, information can be obtained on the sign of C_7 by considering the zero–crossing of A_{FB} since it depends on the relative sign of C_7 and C_9. The positive sign of C_7 can thus be excluded (Figure 6.12).

Finally, in Figure 6.13 we show the correlations of $\mathrm{BR}(B \to X_s\gamma)$ with $\mathrm{BR}(B \to K^*\mu^+\mu^-)$ and $A_{FB}(B \to K^*\mu^+\mu^-)$. In the SM, $\mathrm{BR}(B \to X_s\gamma)$ is dominated by contributions from C_7. The SM prediction for this branching ratio is $(3.08 \pm 0.22) \times 10^{-4}$ [126, 157, 158] while the latest combined experimental value from HFAG is $(3.55 \pm 0.24 \pm 0.09) \times 10^{-4}$ [159]. As expected, there are strong correlations between $B \to X_s\gamma$ and the $B \to K^*\mu^+\mu^-$ branching ratios and the forward backward asymmetry, especially for small and intermediate values of $\tan\beta$, where the scalar and pseudo scalar contributions have a limited effect.

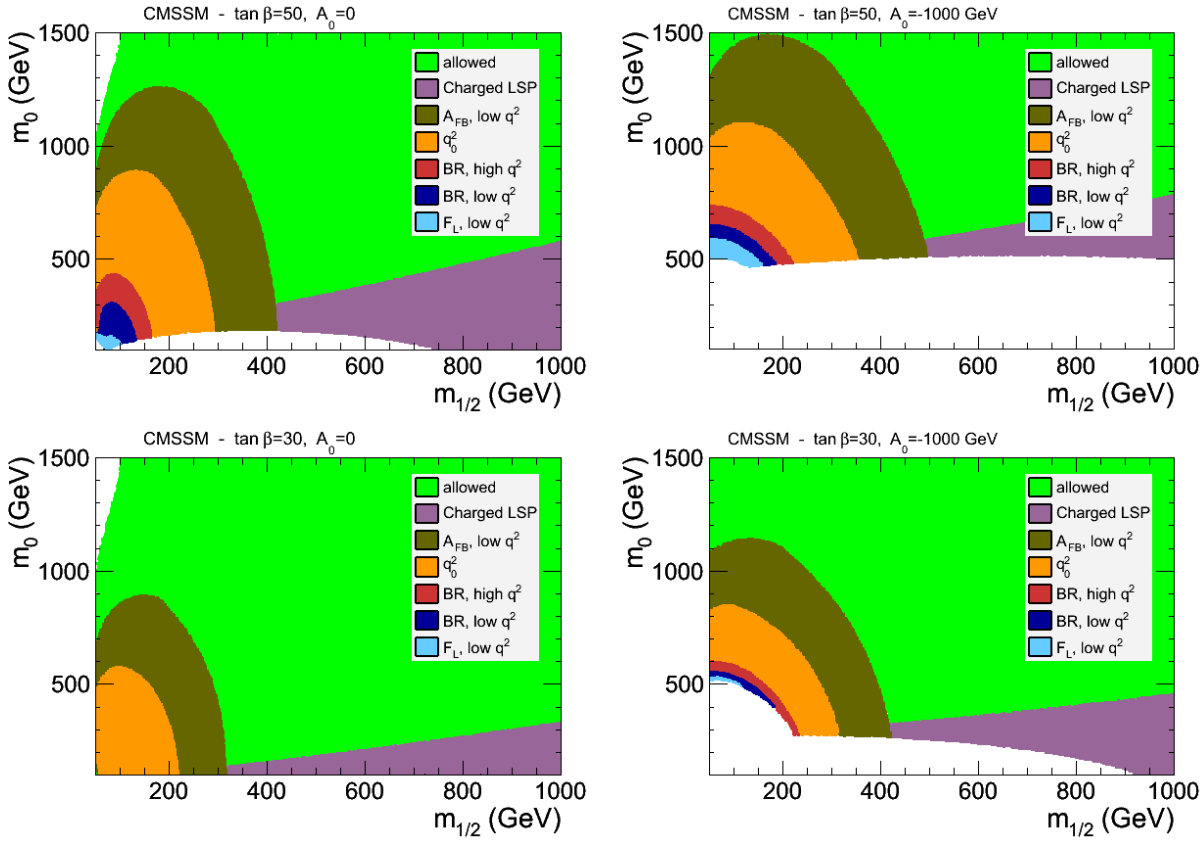

Figure 6.11.: Constraining power of the different $B \to K^*\mu^+\mu^-$ observables in the $(m_{1/2}, m_0)$ plane, for $\tan\beta$=50 (upper panel) and $\tan\beta$=30 (lower panel), in the left for $A_0 = 0$ and in the right for $A_0 = -1000$ GeV.

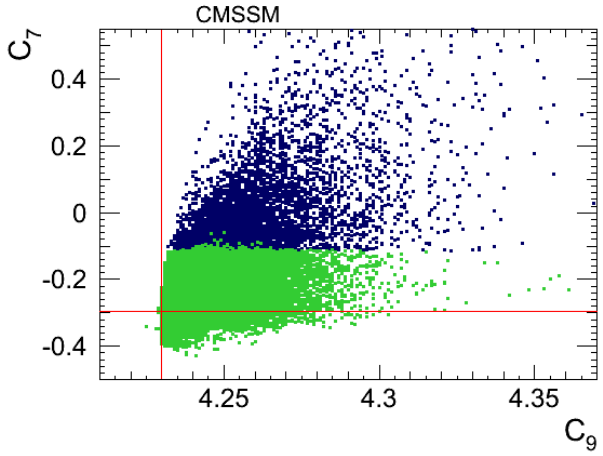

Figure 6.12.: Variation of C_7 and C_9 in the CMSSM with all the parameters varied in the ranges given in the text. Only the green points are allowed by the zero–crossing of A_{FB}. The red lines correspond to the SM predictions.

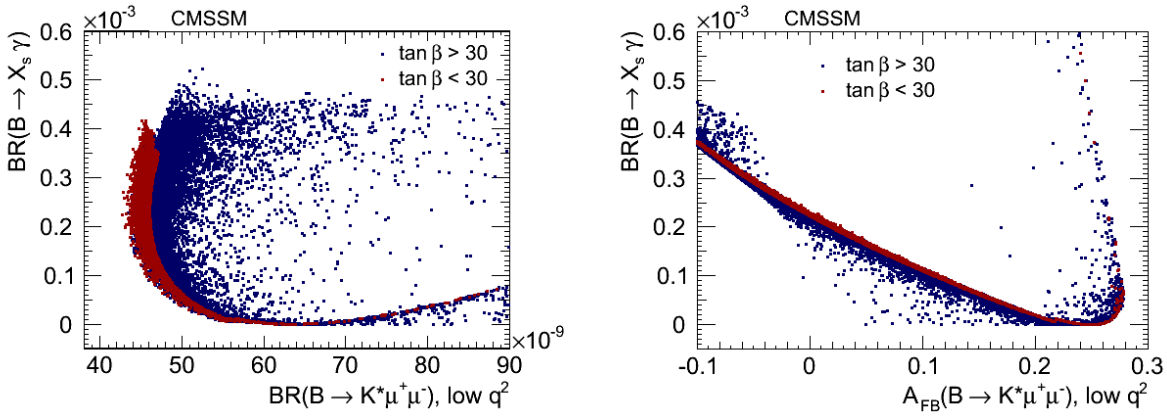

Figure 6.13.: The correlation between BR($B \to X_s\gamma$) and averaged BR($B \to K^*\mu^+\mu^-$) in the left, and between BR($B \to X_s\gamma$) and $A_{FB}(B \to K^*\mu^+\mu^-)$ in the right.

In the CMSSM, the impact of the observed Higgs mass ($\sim 123 - 127$) strongly limits the variation of the Wilson coefficients, as evident by comparing Figure 6.14, where the bounds from the Higgs mass has been imposed, with Figure 6.1.
In Figure 6.15 we have shown the variation of Wilson coefficients considering only the bounds from $B \to K^* \ell^+ \ell^-$ observables. Comparing Figures 6.14 and 6.15, it can be seen that the constraints from the observed Higgs mass supersedes almost all the constraints from $B \to K^* \ell^+ \ell^-$ observables.

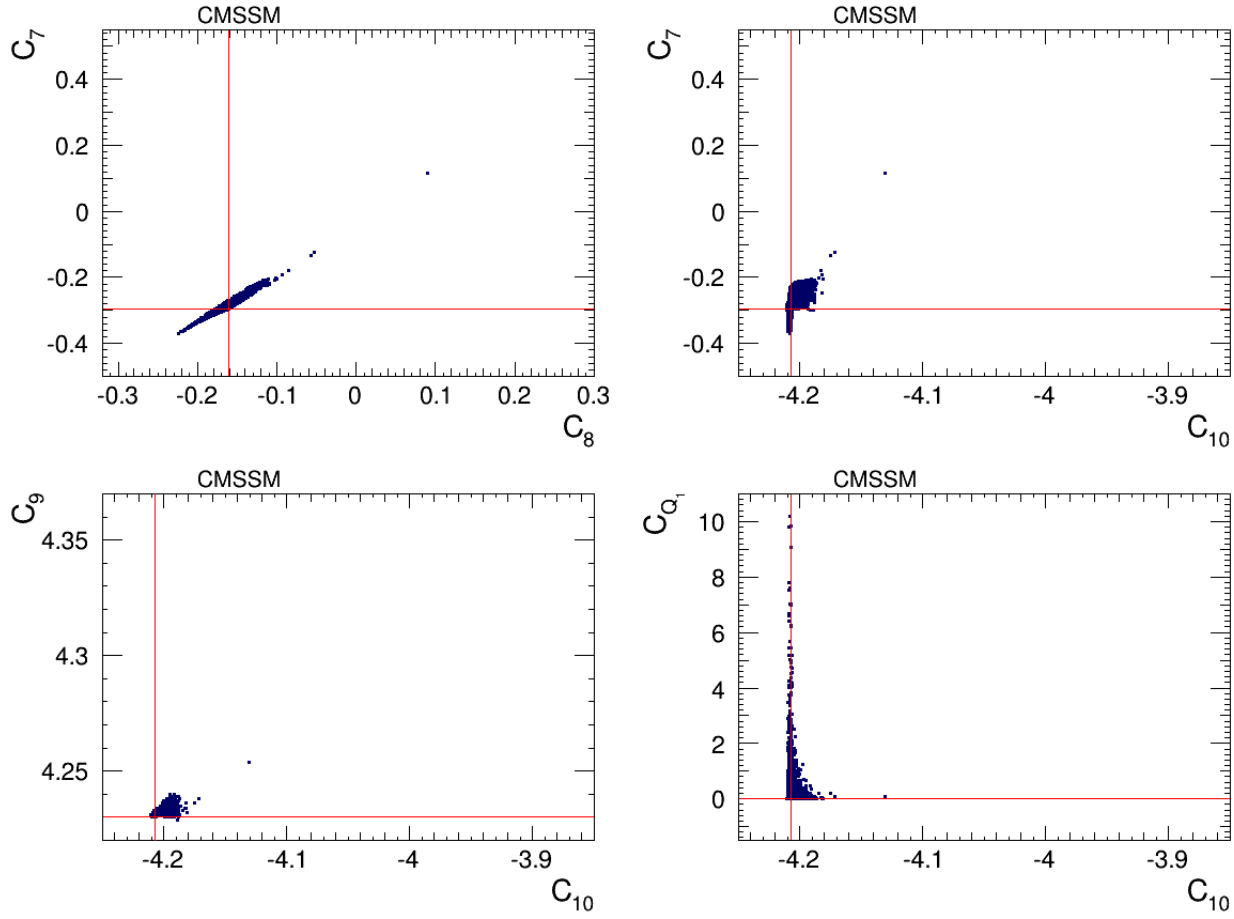

Figure 6.14.: Variation of the Wilson coefficients in the CMSSM imposing the Higgs mass range $123 < m_{h^0} < 127$ GeV. Line/colour code are the same as in Figure 6.1.

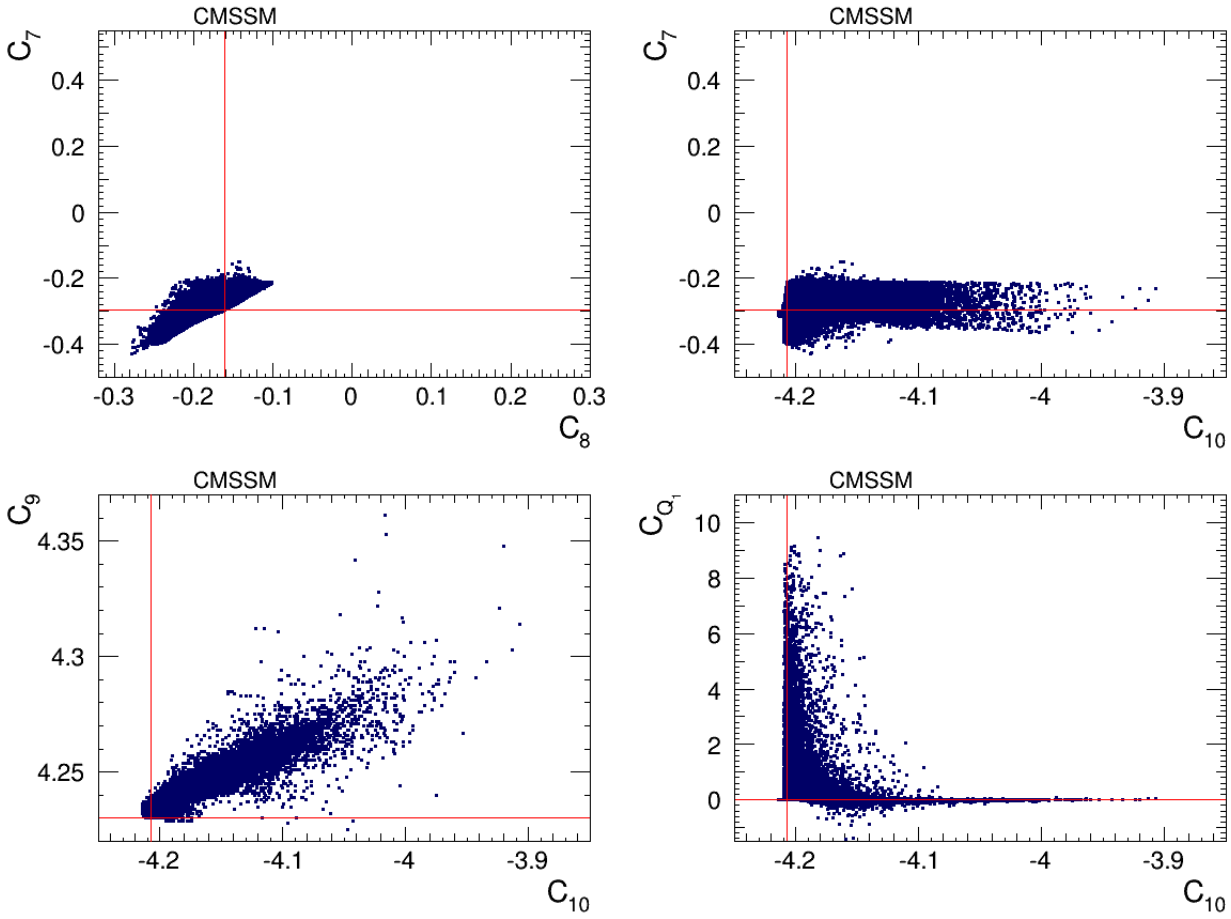

Figure 6.15.: Variation of the Wilson coefficients in the CMSSM considering only the bounds from $B \to K^* \ell^+ \ell^-$ observables (BR, A_{FB}, q_0^2 and F_L). Line/colour code are the same as in Figure 6.1.

6.4 NUHM

The second model we consider involves non-universal Higgs masses (NUHM). This model generalises the CMSSM, allowing for non-universal Higgs masses at the GUT scale (i.e. $m^2_{H^1} \neq m^2_{H^2} \neq m^2_0$). For the purpose of phenomenological analysis, it is convenient to trade these two additional degrees of freedom by low-scale parameters, in general μ and M_A (the CP-odd Higgs boson mass). This implies that the charged Higgs boson mass can be treated as a free parameter, contrary to the CMSSM.

The numerical analysis of the NUHM scenario is done in a similar way to the CMSSM, varying in addition $\mu \in [-2000, 2000]$ GeV and $M_A \in [50, 1100]$ GeV. The contributions of the SUSY particles on the Wilson coefficients are presented in Figure 6.16. Here, the correlations that appeared among the Wilson coefficients in the CMSSM are relaxed. In particular, C_9 and C_{10} are no longer strongly correlated in NUHM. Moreover, while CMSSM contributions could only increase the value of a certain Wilson coefficient, the NUHM contributions can also have a decreasing effect.

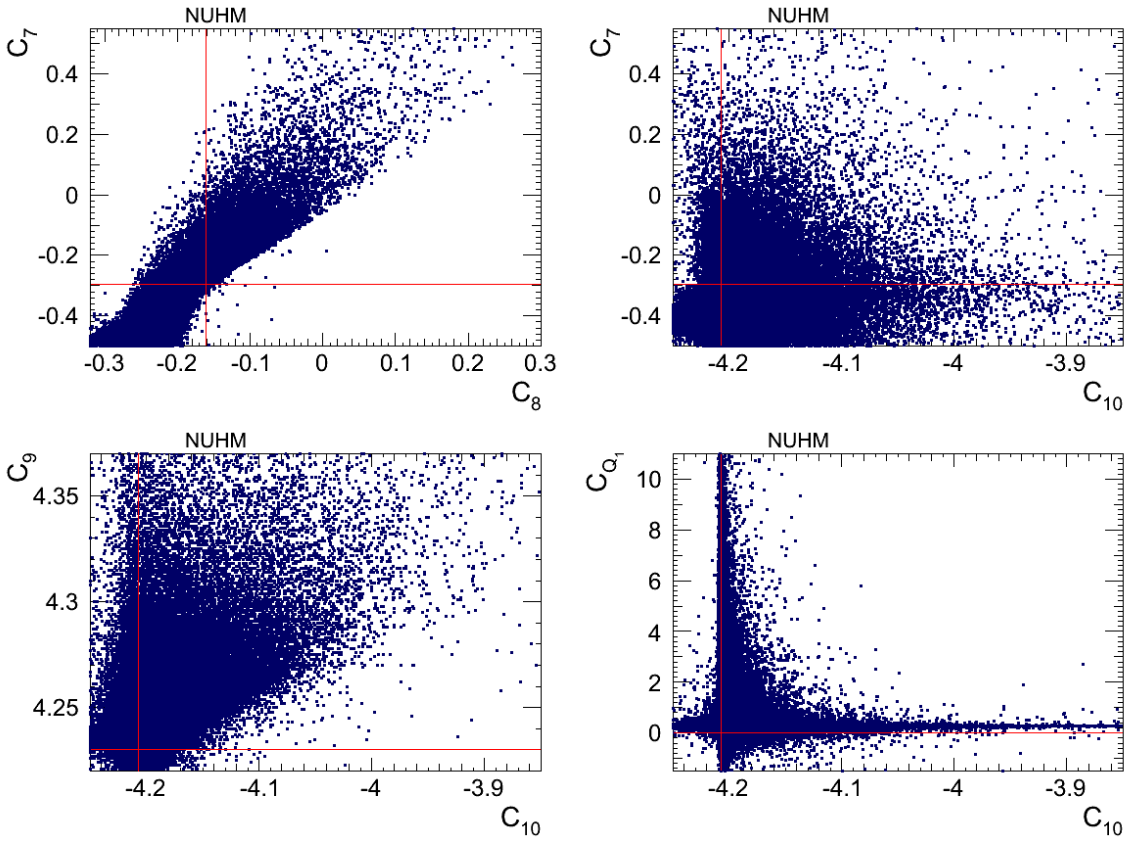

Figure 6.16.: Variation of the Wilson coefficients in NUHM with all the parameters varied in the ranges given in the text. The red lines correspond to the SM predictions.

The corresponding impact of SUSY contributions on the BR($B_s \to \mu^+\mu^-$) are shown in Figure 6.17. Since there are two additional degrees of freedom in NUHM as compared to the CMSSM, it is easier for a model point to evade the constraint, as can be seen by comparing left panels of Figures 6.2 and 6.17, where the allowed points are displayed on the foreground. On the other hand, since $M_{\tilde{t}_1}$ and $M_{H^\pm}$ are discorrelated in NUHM, it is possible for any $M_{\tilde{t}_1}$ to find excluded models with small $M_{H^\pm}$ even for low $\tan\beta$, as can be seen from the plot with the allowed points in the background.

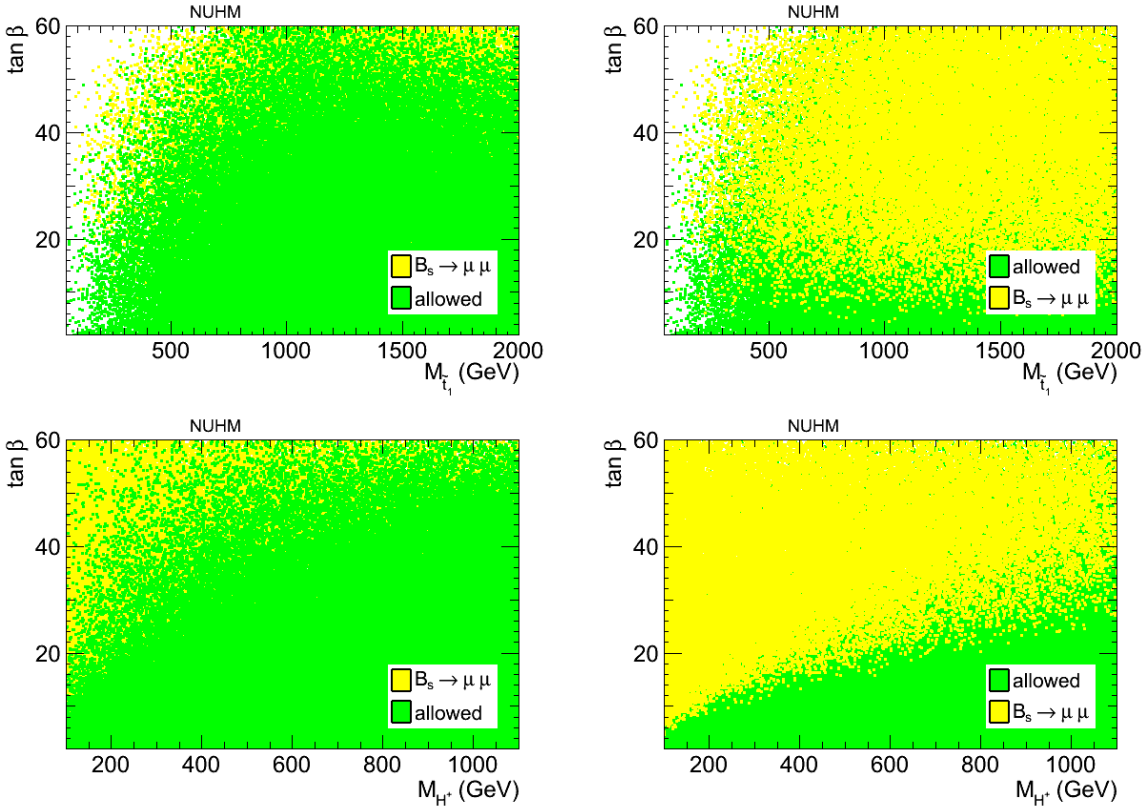

Figure 6.17.: Constraint from BR($B_s \to \mu^+\mu^-$) in the NUHM plane ($M_{\tilde{t}_1}$, $\tan\beta$) in the upper panel and ($M_{H^\pm}$, $\tan\beta$) in the lower panel, with the allowed points displayed in the foreground on the left and in the background on the right.

In the NUHM, the bounds from the observed Higgs mass is less constraining than in the CMSSM. The effect of the observed Higgs mass on the possible variation of the Wilson coefficients in the NUHM is shown in Figure 6.18. Comparing Figures 6.18 and 6.14, it can be seen that while the observed Higgs mass does limit the variation of the Wilson coefficients, the bounds are less constraining than in the case of CMSSM. The bounds of $B \to K^*\ell^+\ell^-$ observables on the Wilson coefficients in NUHM can be seen in Figure 6.19. In NUHM the constraining power of $B \to K^*\ell^+\ell^-$ observables supersedes the bounds from the Higgs mass as can be seen by comparing Figures 6.18 and 6.19.

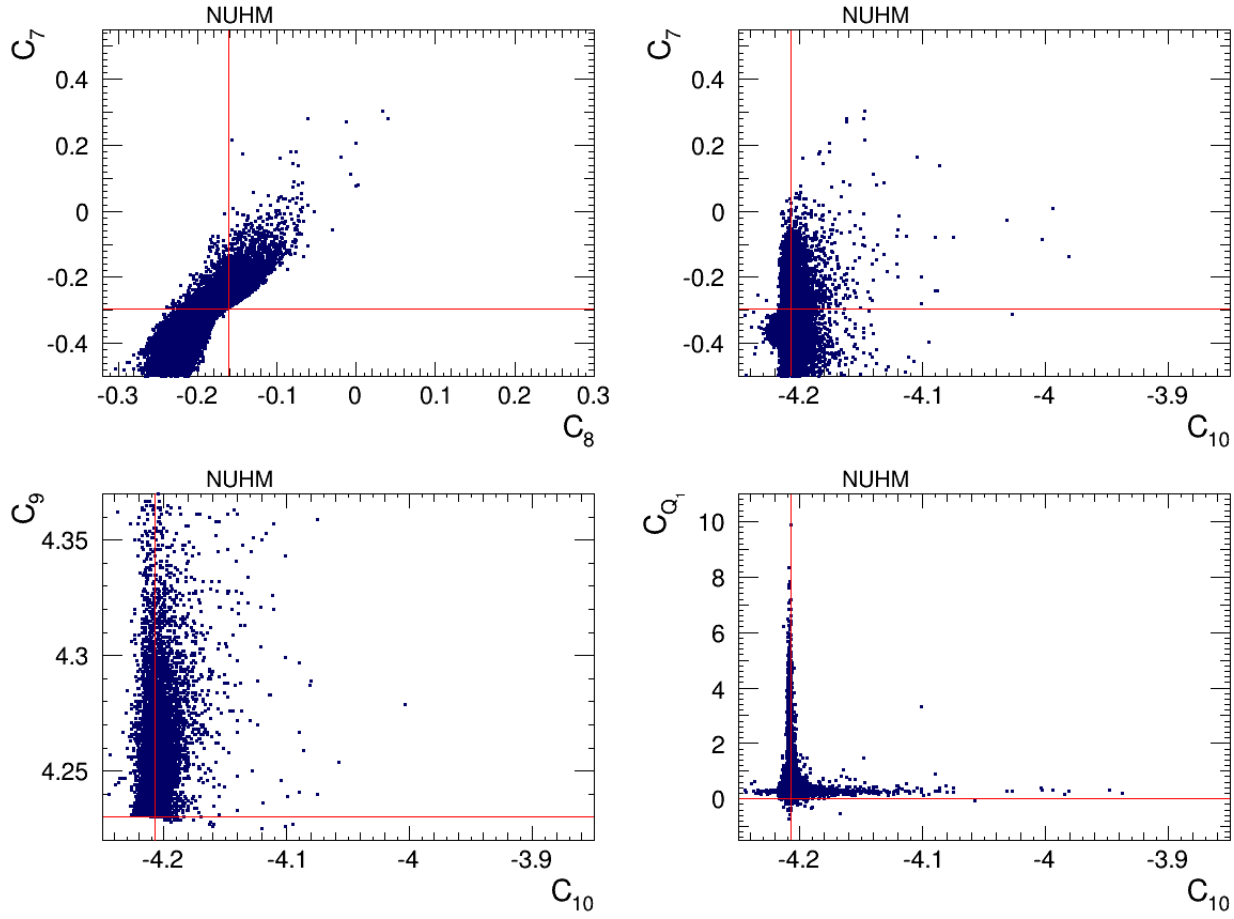

Figure 6.18.: Variation of the Wilson coefficients in the NUHM imposing the Higgs mass range $123 < m_{h^0} < 127$ GeV. Line/colour code are the same as in Figure 6.1.

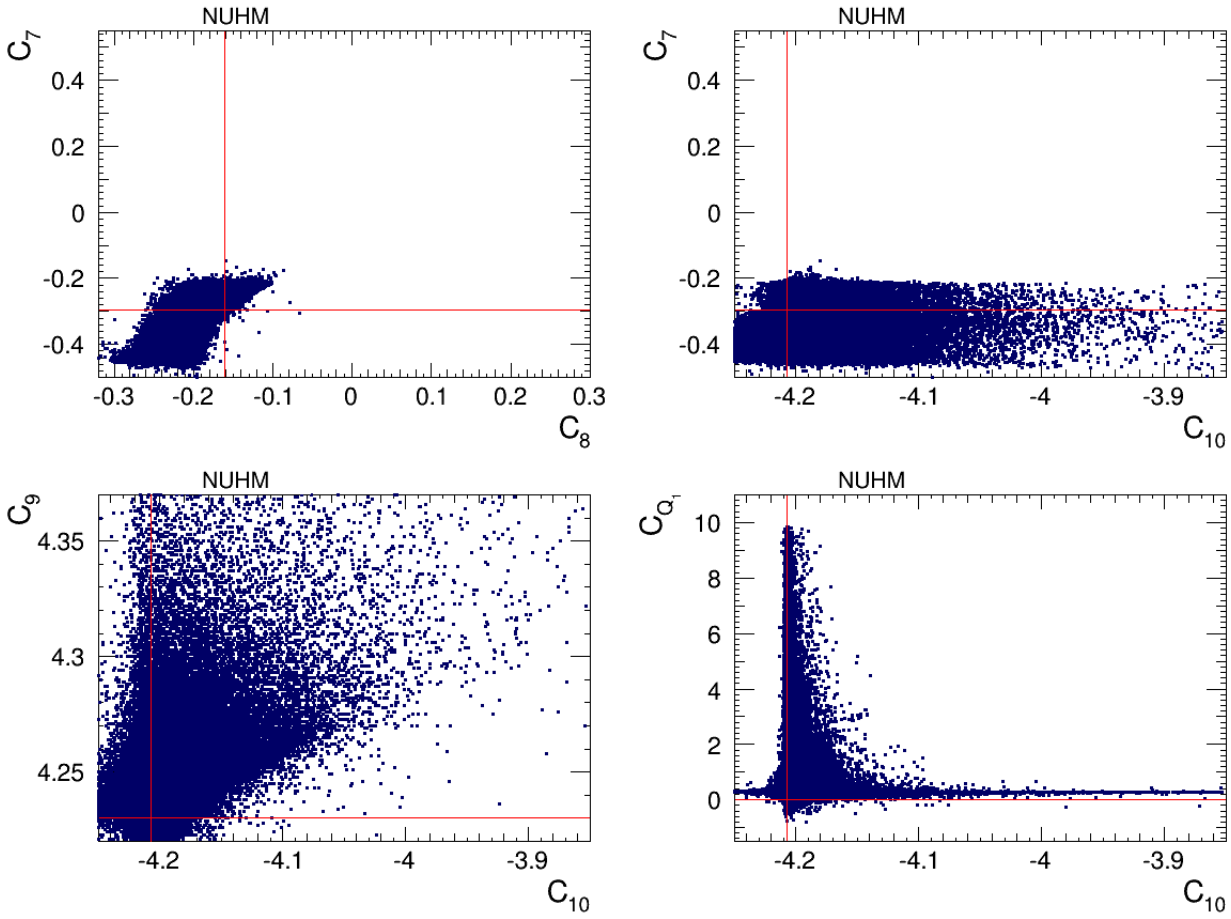

Figure 6.19.: Variation of the Wilson coefficients in the NUHM considering only the bounds from $B \to K^* \ell^+ \ell^-$ observables (BR, A_{FB}, q_0^2 and F_L). Line/colour code are the same as in Figure 6.1.

CHAPTER 7

Conclusions

The rare decays $B_s \to \ell^+\ell^-$ and $B \to K^*\ell^+\ell^-$ are sensitive probes of possible extensions of the Standard Model (SM). The measurements of these decays provide important constraints on the masses of new particles, as for example those arising in the framework of SUSY models. In the latter case, and in the large $\tan\beta$ regime, the new supersymmetric contributions to the $B_s \to \ell^+\ell^-$ decay are dominated by the exchange of neutral Higgs bosons. As emphasised in many related works, this decay receives large enhancements, and thus very restrictive constraints can be obtained on the supersymmetric parameters. On the other hand, the $B \to K^*\ell^+\ell^-$ decay provides a variety of complementary observables, as it gives access to angular distributions in addition to the differential branching ratio.

Experimentally, the exclusive $B \to K^*\ell^+\ell^-$ decay is easier to measure compared to the (theoretically cleaner) inclusive mode $B \to X_s\ell^+\ell^-$. However, from a theoretical point of view, in the exclusive mode there are large uncertainties, which are mostly due to the $B \to K$ form factors. Within the QCD factorisation, simplifications can be made on the description of hadronic matrix elements, and by considering the rich phenomenology of the various kinematic distributions, observables that have smaller dependency on the form factors can be constructed. These observables prove to be important tools in the study of extensions of the SM, and they can provide valuable information on different sectors of the model. The full determination of the angular distributions of $B \to K^*\ell^+\ell^-$ constitutes a worthwhile challenge to the present and future generation of experiments. Several angular observables have already been measured by Belle, BaBar, CDF and LHCb. The most precise measurements are from the recent LHCb analyses with 1 fb^{-1} of integrated luminosity.

In this thesis, we have explored the power of BR($B_s \to \mu^+\mu^-$) and several $B \to K^*\mu^+\mu^-$ observables in constraining two minimal flavour violating (MFV) supersymmetric scenarios, the CMSSM and NUHM. We have demonstrated the effect of SUSY contributions on $B \to K^*\mu^+\mu^-$ observables i.e. BR, A_{FB}, q_0^2, F_L, $A_T^{(2,3,4)}$ and A_I, mostly focusing on the low q^2 region. Considering recent LHCb results for BR, A_{FB}, q_0^2 and F_L, we have

shown that these observables can provide information which is competitive to direct SUSY searches in the large $\tan\beta$ regime of the CMSSM. In particular, the forward backward asymmetry is a very powerful observable. The constraining power of other observables, like the isospin asymmetry (whose measurement is still under way), have been displayed in order to demonstrate their significance in the framework of MFV models for which the CMSSM provides an interesting prototype. We have also presented an update of the bounds on two constrained MSSM scenarios, CMSSM and NUHM, from the inclusion of the LHCb Spring 2012 data on BR($B_s \to \mu^+\mu^-$).

To investigate the origin of the rare B-decay constraints in the CMSSM, we have also explored the possible values and correlations between the Wilson coefficients. Among them, the Wilson coefficient C_9 is a parameter for which the $B \to K^*\ell^+\ell^-$ angular observables provide a unique probe. However, we have shown that the sensitivity of C_9 to CMSSM effects is suppressed by the muon vector coupling, since these decays proceed mainly through a Z penguin diagram.

Although the recent discovery of SM-like Higgs boson at the LHC has already excluded vast regions of CMSSM parameter space, the framework and theoretical tools presented in this thesis can be applied to a variety of less constrained supersymmetric models (namely those where the Higgs mass can be more easily accommodated by minimal deviations from strict universality at the GUT scale). In such scenarios, the observables discussed here will have a significant impact in constraining the allowed parameter space. In this sense, the analyses presented here for the CMSSM can be seen as a valuable illustrative example, which allows to identify interesting regimes and behaviours which otherwise would have been missed.

The exclusion bounds on sparticle masses derived here (via rare B-decays) might appear redundant when compared to recent LHC limits from negative searches. Some redundancy is however valuable, and can turn into complementarity as soon as applied to less constrained versions of the MSSM.

For the decays analysed in this work, significant improvements are still possible on the theoretical and experimental side. It is worth recalling that for our analyses only 2011 LHCb data was available. It is thus only natural to expect that when we include the new LHCb data in our analyses, stronger bounds on sparticle masses will be obtained. The constraining effect of the improved experimental results on the lightest stop mass can readily be applied to our study by modifying (adding) the experimental bounds for BR, q_0^2, A_{FB} and F_L ($A^{(2,3,4)}$ and A_I). Moreover, lattice results for the hadronic parameters can improve the theoretical predictions of both decays, since hadronic uncertainties are the major source of theoretical error.

APPENDIX A

Renormalisation group equations

A.1 RGE for $C_1 - C_9$

To obtain the evolved Wilson coefficients from the matching scale (μ_0) to μ_b, the renormalisation group equation (RGE) for $\vec{\tilde{C}}$ has to be solved:

$$\mu \frac{d}{d\mu} \vec{\tilde{C}}(\mu) = \hat{\gamma}^T(g) \vec{\tilde{C}}(\mu) \,, \tag{A.1}$$

where $\hat{\gamma}$ is the Anomalous Dimension Matrix (ADM). The general solution for the RGE is

$$\vec{\tilde{C}}(\mu_b) = \hat{U}(\mu_b, \mu_0) \vec{\tilde{C}}(\mu_0) \,, \tag{A.2}$$

where $\hat{U}$ is the evolution matrix

$$\hat{U}(\mu_b, \mu_0) = T_g \exp \int_{g(\mu_0)}^{g(\mu_b)} dg' \frac{(\hat{\gamma}^T(g'))}{\beta(g')} \,. \tag{A.3}$$

T_g is the $g(=\sqrt{4\pi\alpha_s})$-ordering operator such that the coupling constants increase from right to left. $\hat{\gamma}$ and β can be expanded in g as mentioned in (4.53) and (4.26)

$$\hat{\gamma}(g) = \frac{g^2}{16\pi^2}\hat{\gamma}^{(0)} + \left(\frac{g^2}{16\pi^2}\right)^2 \hat{\gamma}^{(1)} + \left(\frac{g^2}{16\pi^2}\right)^3 \hat{\gamma}^{(2)} + \cdots \,, \tag{A.4}$$

$$\beta(g) = -\frac{g^3}{16\pi^2}\beta_0 - \frac{g^5}{(16\pi^2)^2}\beta_1 - \frac{g^7}{(16\pi^2)^4}\beta_2 + \cdots \,. \tag{A.5}$$

The Wilson coefficients and the evolution matrix expanded in α_s are

$$\hat{U}(\mu_b, \mu_0) = \sum_{n \geqslant 0} \left(\frac{\alpha_s(\mu_0)}{4\pi} \right)^{(n)} \hat{U}^{(n)}, \tag{A.6}$$

$$\vec{\tilde{C}}_i(\mu) = \sum_{n \geqslant 0} \left(\frac{\alpha_s(\mu)}{4\pi} \right)^{(n)} \vec{\tilde{C}}_i^{(n)}(\mu). \tag{A.7}$$

Following the conventions used in [160], the evolution matrix can be written as

$$U_{kl}^{(n)} = \sum_{j=0}^{n} \sum_{i=1}^{9} m_{kli}^{(nj)} \eta^{a_i - j} \quad , \tag{A.8}$$

with

$$\eta = \alpha_s(\mu_0)/\alpha_s(\mu_b). \tag{A.9}$$

Using the above relations for the different orders of $C_k(\mu_b)$ we have

$$\tilde{C}_k^{(0)}(\mu_b) = \sum_{l=1}^{k} U_{kl}^{(0)} \tilde{C}_l^{(0)}(\mu_0) \tag{A.10}$$

$$\tilde{C}_k^{(1)}(\mu_b) = \eta \left[\sum_{l=1}^{k} U_{kl}^{(0)} \tilde{C}_l^{(1)}(\mu_0) + \sum_{l=1}^{k} U_{kl}^{(1)} \tilde{C}_l^{(0)}(\mu_0) \right] \tag{A.11}$$

$$\tilde{C}_k^{(2)}(\mu_b) = \eta^2 \left[\sum_{l=1}^{k} U_{kl}^{(0)} \tilde{C}_l^{(2)}(\mu_0) + \sum_{l=1}^{k} U_{kl}^{(1)} \tilde{C}_l^{(1)}(\mu_0) + \sum_{l=1}^{k} U_{kl}^{(2)} \tilde{C}_l^{(0)}(\mu_0) \right]. \tag{A.12}$$

To obtain the evolution matrix we have followed [161] and [162], the details of the calculations are given in Appendix A.4. Taking $\hat{\gamma}^{(0)}$, $\hat{\gamma}^{(1)}$ and $\hat{\gamma}^{(2)}$ from [160] and [163], we have produced the necessary "magic numbers" ($m_{kli}^{(nj)}$) for the evaluation of U_{kl}. The a_i's are given in Table A.1, and $m_{kli}^{(nj)}$ can be found in Tables A.2-A.20. Since not all Wilson coefficients mix with each other many of the magic numbers are zero:

$$m_{kli}^{(nj)} = 0 \quad \text{for all } n, j \text{ and } i \quad \text{when} \begin{cases} k = 1, 2 & \& \quad l = 3 - 9 \\ k = 3 - 6 & \& \quad l = 7 - 9 \\ k = 7, 8 & \& \quad l = 9 \\ k = 9 & \& \quad l = 7, 8 \end{cases} \tag{A.13}$$

Besides $m_{9li}^{(nj)}$, all of the magic numbers that are relevant in the SM for the running of the non-vanishing Wilson coefficients can be found in [160]. For completeness we have reproduced all of them here, including those that are irrelevant for SM vanishing Wilson coefficients, since these coefficients may receive BSM contributions.

In the above formulas, the SM values for $\tilde{C}_i(\mu_0)$ for $(i = 1 - 6, 9)$ can be found in Section 2

of [90], where to get our $\tilde{C}_i^{(n)}(\mu_0)$ we use $\tilde{C}_i^{(n)}(\mu_0) = C_i^{t(n)}(\mu_0) - C_i^{c(n)}(\mu_0)$. Due to the different normalisation used for O_9 in [90], to obtain C_9 based on our choice of operators we have

$$C_9(\mu_b) = \frac{4\pi}{\alpha_s(\mu_b)}\tilde{C}_9(\mu_b), \tag{A.14}$$

while $\tilde{C}_i(\mu_b)$ for $(i = 1-6)$ coincides with the Wilson coefficients used in this work. On the other hand $\tilde{C}_{7,8}$ are in fact C_7^{eff} and C_8^{eff} as defined in (5.9) and (B.26), respectively. The SM values for C_7 and C_8 can also be found in [90], where $C_{7,8}^{Q(n)}$ given there are combined to our $C_{7,8}^{(n)}(\mu_0)$ according to $C_{7,8}^{(n)}(\mu_0) = C_{7,8}^{t(n)}(\mu_0) - C_{7,8}^{c(n)}(\mu_0)$.[1]

A.2 RGE for C_{10}

There is no mixing between O_{10} and the other operators. However, there is a scale dependency in C_{10} which comes from $\alpha_s(\mu)$. Hence for C_{10} we have

$$C_{10}^{(0)}(\mu_b) = C_{10}^{(0)}(\mu_0), \qquad C_{10}^{(1)}(\mu_b) = \eta C_{10}^{(0)}(\mu_0). \tag{A.15}$$

A.3 RGE for C_{Q_1,Q_2}

The operators $O_i(i = 1, \cdots, 10)$ do not mix into Q_1 and Q_2 and also there is no mixing between Q_1 and Q_2. Therefore, the evolution of C_{Q_1}, C_{Q_2} is controlled by the anomalous dimensions of Q_1, Q_2 respectively.

$$C_{Q_i}(m_b) = \eta^{\gamma_Q/\beta_0} C_{Q_i}(m_W), \quad i = 1, 2, \tag{A.16}$$

where $\gamma_Q = -4$ is the anomalous dimension of $\bar{s}_L b_R$ [164].

A.4 Detailed calculations of the evolution matrix

We first calculate $\hat{U}^{(0)}$, taking the first terms of the expansions of $\hat{\gamma}$ (A.4) and β (A.5)

$$\hat{U}^{(0)}(\mu_b, \mu_0) = \exp\left(\int_{g(\mu_0)}^{g(\mu_b)} \frac{g^2 \hat{\gamma}^{(0)T}}{-g^3\beta_0} dg'\right) \tag{A.17}$$

$$= \exp\left(\int_{\alpha_s(\mu_0)}^{\alpha_s(\mu_b)} \frac{\hat{\gamma}^{(0)T}}{-2\beta_0} d\ln(\alpha_s(\mu))\right) = \eta^{\left(\frac{\hat{\gamma}^{(0)T}}{2\beta_0}\right)}, \tag{A.18}$$

[1] This rather bizarre recipe for the different Wilson coefficients is due to the fact ADMs given in [90] and [160] are given for different normalisation of the operators. Also for $(i, j = 7, 8)$ the ADM entries $(\gamma_{i,j}^{(n)})$ are given for the effective coefficients while for $(i, j = 1-6, 9)$ the ADM entries are given for the non-effective coefficients.

with η defined in (A.9). It should be noted that $\hat{U}^{(0)}$ given in the above equation is a function of a matrix. In general for any diagonalisable matrix A there is a matrix V, such that

$$A_D = V^{-1}AV = \begin{pmatrix} d_1 & 0 & \cdots & 0 \\ 0 & d_2 & \cdots & 0 \\ \vdots & \vdots & \ddots & \vdots \\ 0 & 0 & \cdots & d_n \end{pmatrix} \tag{A.19}$$

is diagonal. Any function of this matrix, $f(A)$, can then be written as

$$f(A) = V \begin{pmatrix} f(d_1) & 0 & \cdots & 0 \\ 0 & f(d_2) & \cdots & 0 \\ \vdots & \vdots & \ddots & \vdots \\ 0 & 0 & \cdots & f(d_n) \end{pmatrix} V^{-1} \tag{A.20}$$

where d_i are the eigenvalues of A.

By diagonalising $\hat{\gamma}^{(0)T}$, we will have ${\gamma_D}^{(0)} \equiv V^{-1}\hat{\gamma}^{(0)T}V$, and we take the diagonal elements of ${\gamma_D}^{(0)}$ to form the vector $\vec{\gamma}^{(0)}$. We refer to the components of this vector as ${\gamma_i}^{(0)}$ which are the eigenvalues of $\hat{\gamma}^{(0)T}$, or in other words the diagonal elements of ${\gamma_D}^{(0)}$, so that

$$\hat{U}^{(0)}(\mu_b, \mu_0) = \eta^{\left(\frac{\hat{\gamma}^{(0)T}}{2\beta_0}\right)} = V \begin{pmatrix} \eta^{a_1} & 0 & \cdots & 0 \\ 0 & \eta^{a_2} & \cdots & 0 \\ \vdots & \vdots & \ddots & \vdots \\ 0 & 0 & \cdots & \eta^{a_n} \end{pmatrix} V^{-1} \equiv VDV^{-1}, \tag{A.21}$$

with

$$a_i \equiv \frac{{\gamma_i}^{(0)}}{2\beta_0}. \tag{A.22}$$

Hence $\hat{U}^{(0)}_{kl}$ can be written as

$$U^{(0)}_{kl} = \sum_{i,j} V_{ki} D_{ij} V^{-1}_{jl} = \sum_{i,j} V_{ki}\eta^{a_i}\delta_{ij}V^{-1}_{jl} = \sum_{i} V_{ki}V^{-1}_{il}\eta^{a_i} = \sum_{i} m^{(00)}_{kli}\eta^{a_i}, \tag{A.23}$$

with

$$m^{(00)}_{kli} \equiv V_{ki}V^{-1}_{il} \text{ (no summation over i).} \tag{A.24}$$

In order to obtain $\hat{U}^{(1)}$, we should add $\hat{\gamma}^{(1)}$ and β_1 as perturbations to the procedure and to obtain $\hat{U}^{(2)}$, we need to consider $\hat{\gamma}^{(2)}$ and β_2 as well. Eventually taking these into

consideration for $\hat{U}(\mu_b, \mu_0)$ based on Eq. (2.28) in [161], we obtain:

$$\hat{U}(\mu_b, \mu_0) = \left[\hat{1} + \frac{\alpha_s(\mu_b)}{4\pi}\hat{J}_1 + \left(\frac{\alpha_s(\mu_b)}{4\pi}\right)^2 \hat{J}_2\right] \hat{U}^{(0)}(\mu_b, \mu_0) \tag{A.25}$$
$$\times \left[\hat{1} - \frac{\alpha_s(\mu_0)}{4\pi}\hat{J}_1 - \left(\frac{\alpha_s(\mu_0)}{4\pi}\right)^2 \left(\hat{J}_2 - \hat{J}_1^2\right)\right].$$

Using $\hat{J}_1$ and $\hat{J}_2$ from Eqs. (71–72) in [162] we can write:

$$\hat{J}_1 = V S_1 V^{-1}, \qquad G_1 = V \hat{\gamma}^{(1)T} V^{-1}, \tag{A.26}$$
$$\hat{J}_2 = V S_2 V^{-1}, \qquad G_2 = V \hat{\gamma}^{(2)T} V^{-1}, \tag{A.27}$$
$$(S_1)_{ij} = \frac{\beta_1}{2\beta_0}\gamma_i^{(0)}\delta_{ij} - \frac{(G_1)_{ij}}{2\beta_0 + \gamma_i^{(0)} - \gamma_j^{(0)}}, \tag{A.28}$$
$$(S_2)_{ij} = \frac{\beta_2}{4\beta_0^2}\gamma_i^{(0)}\delta_{ij} - \frac{(G_2)_{ij}}{4\beta_0 + \gamma_i^{(0)} - \gamma_j^{(0)}} \tag{A.29}$$
$$+ \sum_k \frac{2\beta_0 + \gamma_i^{(0)} - \gamma_k^{(0)}}{4\beta_0 + \gamma_i^{(0)} - \gamma_j^{(0)}} \left[(S_1)_{ik}(S_1)_{kj} - \frac{\beta_1}{\beta_0}(S_1)_{ij}\delta_{jk}\right].$$

If we expand the above relation, for $\hat{U}^{(0)}$ we have

$$\hat{U}(\mu_b, \mu_0) = \hat{U}^{(0)}(\mu_b, \mu_0) + \frac{\alpha_s(\mu_0)}{4\pi}\left(\eta^{-1}\hat{J}_1\hat{U}^{(0)} - \hat{U}^{(0)}\hat{J}_1\right) \tag{A.30}$$
$$+ \left(\frac{\alpha_s(\mu_0)}{4\pi}\right) 2\left[\hat{U}^{(0)}\left(\hat{J}_1 2 - \hat{J}_2\right) - \eta^{-1}\hat{J}_1\hat{U}^{(0)}\hat{J}_1 + \eta^{-2}\hat{J}_2\hat{U}^{(0)}\right] + \cdots.$$

For $U^{(1)}$ we can write

$$U^{(1)} = \left(\eta^{-1}\hat{J}_1\hat{U}^{(0)} - \hat{U}^{(0)}\hat{J}_1\right). \tag{A.31}$$

Therefore

$$
\begin{aligned}
U^{(1)}_{kl} &= \sum_p \left[\eta^{-1}(\hat{J}_1)_{kp}(\hat{U}^{(0)})_{pl} - (\hat{U}^{(0)})_{kp}(\hat{J}_1)_{pl}\right] \\
&= \sum_{i,j,p} \left[\eta^{-1}(\hat{J}_1)_{kp}V_{pi}D_{ij}V^{-1}_{jl} - V_{ki}D_{ij}V^{-1}_{jp}(\hat{J}_1)_{pl}\right] \\
&= \sum_{i,j,p} \left[\eta^{-1}(\hat{J}_1)_{kp}V_{pi}\eta^{a_i}\delta_{ij}V^{-1}_{jl} - V_{ki}\eta^{a_i}\delta_{ij}V^{-1}_{jp}(\hat{J}_1)_{pl}\right] \\
&= \sum_i \sum_p \left[(\hat{J}_1)_{kp}V_{pi}V^{-1}_{il}\eta^{a_i-1} - V_{ki}V^{-1}_{ip}(\hat{J}_1)_{pl}\eta^{a_i}\right] \\
&= \sum_p \left[m^{(11)}_{kli}\eta^{a_i-1} + m^{(10)}_{kli}\eta^{a_i}\right],
\end{aligned}
\tag{A.32}
$$

with

$$
m^{(10)}_{kli} = \sum_p -V_{ki}V^{-1}_{ip}(\hat{J}_1)_{pl} \tag{A.33}
$$

$$
m^{(11)}_{kli} = \sum_p (\hat{J}_1)_{kp}V_{pi}V^{-1}_{il}. \tag{A.34}
$$

For $U^{(2)}$ we have

$$
\hat{U}^{(2)} = \left[U^{(0)}\left(\hat{J}_1^2 - \hat{J}_2\right) - \eta^{-1}\hat{J}_1\hat{U}^{(0)}\hat{J}_1 + \eta^{-2}\hat{J}_2\hat{U}^{(0)}\right]. \tag{A.35}
$$

Following the same procedure for $U^{(2)}$, we obtain:

$$
\hat{U}^{(2)} = \sum_i \left[m^{(22)}_{kli}\eta^{a_i-2} + m^{(21)}_{kli}\eta^{a_i-1} + m^{(20)}_{kli}\eta^{a_i}\right], \tag{A.36}
$$

where $m^{(nj)}_{kli}$ are:

$$
\begin{aligned}
m^{(20)}_{kli} &= \sum_p V_{ki}V^{-1}_{ip}(\hat{J}_1^2 - \hat{J}_2)_{pl}, \\
m^{(21)}_{kli} &= \sum_{p,m}\left(-(\hat{J}_1)_{kp}V_{pi}V^{-1}_{im}(\hat{J}_1)_{ml}\right), \\
m^{(22)}_{kli} &= \sum_p (\hat{J}_2)_{kp}V_{pi}V^{-1}_{il}.
\end{aligned}
\tag{A.37}
$$

As mentioned earlier $\hat{\gamma}^{(0)}$, $\hat{\gamma}^{(1)}$ and $\hat{\gamma}^{(2)}$ can be found in [90] and [160]. For β_0, β_1 and β_2 we have used [161]

$$
\beta_0 = \frac{33 - 2N_f}{3}, \qquad \beta_1 = \frac{306 - 38N_f}{3}, \qquad \beta_2 = \frac{2857}{2} - \frac{5033N_f}{18} + \frac{325f2}{54}, \tag{A.38}
$$

i	1	2	3	4	5	6	7	8	9
a_i	$\frac{14}{23}$	$\frac{16}{23}$	$\frac{6}{23}$	$-\frac{12}{23}$	0.4086	-0.4230	-0.8994	0.1456	-1

Table A.1.: The numbers a_i.

where N_f is the number of active flavours, which for B-decays is five. The magic numbers have been summarised in Tables A.2-A.20

i	1	2	3	4	5	6	7	8	9
$m_{11i}^{(00)}$	0	0	0.3333	0.6667	0	0	0	0	0
$m_{11i}^{(10)}$	0	0	-1.9869	0.7301	0	0	0	0	0
$m_{11i}^{(11)}$	0	0	1.9869	-0.7301	0	0	0	0	0
$m_{11i}^{(20)}$	0	0	-6.98112	15.6429	0	0	0	0	0
$m_{11i}^{(21)}$	0	0	-11.843	-0.7996	0	0	0	0	0
$m_{11i}^{(22)}$	0	0	18.8241	-14.8433	0	0	0	0	0
$m_{12i}^{(00)}$	0	0	1	-1	0	0	0	0	0
$m_{12i}^{(11)}$	0	0	5.9606	1.0951	0	0	0	0	0
$m_{12i}^{(20)}$	0	0	-13.4086	-52.1664	0	0	0	0	0
$m_{12i}^{(10)}$	0	0	-2.9606	-4.0951	0	0	0	0	0
$m_{12i}^{(22)}$	0	0	56.4723	22.265	0	0	0	0	0
$m_{12i}^{(21)}$	0	0	-17.6471	4.4848	0	0	0	0	0
$m_{21i}^{(00)}$	0	0	0.2222	-0.2222	0	0	0	0	0
$m_{21i}^{(10)}$	0	0	-1.3246	-0.2434	0	0	0	0	0
$m_{21i}^{(11)}$	0	0	0.6579	0.9100	0	0	0	0	0
$m_{21i}^{(20)}$	0	0	-4.65408	-5.2143	0	0	0	0	0
$m_{21i}^{(21)}$	0	0	-3.9216	0.9966	0	0	0	0	0
$m_{21i}^{(22)}$	0	0	4.9275	7.8658	0	0	0	0	0
$m_{22i}^{(00)}$	0	0	0.6667	0.3333	0	0	0	0	0
$m_{22i}^{(10)}$	0	0	-1.9737	1.3650	0	0	0	0	0
$m_{22i}^{(11)}$	0	0	1.9737	-1.3650	0	0	0	0	0
$m_{22i}^{(20)}$	0	0	-8.93903	17.3888	0	0	0	0	0
$m_{22i}^{(21)}$	0	0	-5.8435	-5.5901	0	0	0	0	0
$m_{22i}^{(22)}$	0	0	14.7825	-11.7987	0	0	0	0	0

Table A.2.: "Magic numbers" m_{1li} and m_{2li}.

i	1	2	3	4	5	6	7	8	9
$m_{31i}^{(00)}$	0	0	0.0106	0.0247	-0.0129	-0.0497	0.0092	0.0182	0
$m_{32i}^{(00)}$	0	0	0.0317	-0.0370	-0.0659	0.0595	-0.0218	0.0335	0
$m_{33i}^{(00)}$	0	0	0	0	-0.2897	-0.2006	0.1756	1.3146	0
$m_{34i}^{(00)}$	0	0	0	0	-0.1933	0.1579	0.1428	-0.1074	0
$m_{35i}^{(00)}$	0	0	0	0	-5.6115	-4.1477	0.8448	8.9144	0
$m_{36i}^{(00)}$	0	0	0	0	-2.5827	2.0187	0.0268	0.5372	0
$m_{41i}^{(00)}$	0	0	0.0159	-0.0741	0.0046	0.0144	0.0562	-0.0171	0
$m_{42i}^{(00)}$	0	0	0.0476	0.1111	0.0237	-0.0173	-0.1336	-0.0316	0
$m_{43i}^{(00)}$	0	0	0	0	0.1041	0.0583	1.0762	-1.2386	0
$m_{44i}^{(00)}$	0	0	0	0	0.0695	-0.0459	0.8752	0.1012	0
$m_{45i}^{(00)}$	0	0	0	0	2.0167	1.2047	5.1773	-8.3987	0
$m_{46i}^{(00)}$	0	0	0	0	0.9282	-0.5863	0.1643	-0.5061	0
$m_{51i}^{(00)}$	0	0	-0.0026	-0.0062	0.0018	0.0083	-0.0004	-0.0009	0
$m_{52i}^{(00)}$	0	0	-0.0079	0.0093	0.0094	-0.0010	0.0010	-0.0017	0
$m_{53i}^{(00)}$	0	0	0	0	0.0411	0.0336	-0.0079	-0.0668	0
$m_{54i}^{(00)}$	0	0	0	0	0.0274	-0.0264	-0.0064	0.0055	0
$m_{55i}^{(00)}$	0	0	0	0	0.7963	0.6945	-0.0382	-0.4527	0
$m_{56i}^{(00)}$	0	0	0	0	0.3666	-0.3380	-0.0012	-0.0273	0
$m_{61i}^{(00)}$	0	0	-0.0040	0.0185	0.0021	-0.0136	-0.0043	0.0012	0
$m_{62i}^{(00)}$	0	0	-0.0119	-0.0278	0.0108	0.0163	0.0103	0.0023	0
$m_{63i}^{(00)}$	0	0	0	0	0.0475	-0.0548	-0.0830	0.0903	0
$m_{64i}^{(00)}$	0	0	0	0	0.0317	0.0432	-0.0675	-0.0074	0
$m_{65i}^{(00)}$	0	0	0	0	0.9209	-1.1340	-0.3993	0.6124	0
$m_{66i}^{(00)}$	0	0	0	0	0.4239	0.5519	-0.0127	0.0369	0

Table A.3.: "Magic numbers" $m_{3li}^{(00)}, m_{4li}^{(00)}, m_{5li}^{(00)}$ and $m_{6li}^{(00)}$.

i	1	2	3	4	5	6	7	8	9
$m_{31i}^{(10)}$	0	0	-0.0631	0.0270	0.0681	-0.1910	-0.06786	-0.2080	0
$m_{32i}^{(10)}$	0	0	-0.0940	-0.1517	-0.2327	0.2288	0.1455	-0.4760	0
$m_{33i}^{(10)}$	0	0	0	0	0.6332	-0.9793	-5.0251	-0.7248	0
$m_{34i}^{(10)}$	0	0	0	0	0.0769	-0.6961	0.3634	-2.5304	0
$m_{35i}^{(10)}$	0	0	0	0	-28.9856	-60.1823	-16.284	-100.862	0
$m_{36i}^{(10)}$	0	0	0	0	11.5767	-3.2303	23.2477	-35.8962	0
$m_{41i}^{(10)}$	0	0	-0.0946	-0.0811	-0.0245	0.0555	-0.4158	0.1960	0
$m_{42i}^{(10)}$	0	0	-0.1410	0.4550	0.0836	-0.0664	0.8919	0.4485	0
$m_{43i}^{(10)}$	0	0	0	0	-0.2276	0.2844	-30.7946	0.6828	0
$m_{44i}^{(10)}$	0	0	0	0	-0.0276	0.2022	2.2268	2.384	0
$m_{45i}^{(10)}$	0	0	0	0	10.4169	17.4805	-99.7905	95.0275	0
$m_{46i}^{(10)}$	0	0	0	0	-4.1604	0.9383	142.465	33.8196	0
$m_{51i}^{(10)}$	0	0	0.0158	-0.0068	-0.0097	0.0320	0.0031	0.0106	0
$m_{52i}^{(10)}$	0	0	0.0235	0.0379	0.0330	-0.0383	-0.0066	0.0242	0
$m_{53i}^{(10)}$	0	0	0	0	-0.0899	0.1640	0.2269	0.0368	0
$m_{54i}^{(10)}$	0	0	0	0	-0.0109	0.1166	-0.0164	0.1285	0
$m_{55i}^{(10)}$	0	0	0	0	4.1134	10.0773	0.7354	5.1221	0
$m_{56i}^{(10)}$	0	0	0	0	-1.6429	0.5409	-1.0498	1.8229	0
$m_{61i}^{(10)}$	0	0	0.0237	0.0203	-0.0112	-0.0522	0.0321	-0.0143	0
$m_{62i}^{(10)}$	0	0	0.0352	-0.1138	0.0382	0.0625	-0.0688	-0.0327	0
$m_{63i}^{(10)}$	0	0	0	0	-0.1039	-0.2677	2.3753	-0.0498	0
$m_{64i}^{(10)}$	0	0	0	0	-0.0126	-0.1903	-0.1718	-0.1738	0
$m_{65i}^{(10)}$	0	0	0	0	4.7571	-16.4539	7.6973	-6.9290	0
$m_{66i}^{(10)}$	0	0	0	0	-1.8910	-0.8832	-10.9889	-2.4660	0

Table A.4.: "Magic numbers" $m_{3li}^{(10)}, m_{4li}^{(10)}, m_{5li}^{(10)}$ and $m_{6li}^{(10)}$.

i	1	2	3	4	5	6	7	8	9
$m_{31i}^{(11)}$	0	0	-0.1803	-1.0888	0.3220	1.3953	0.1085	-0.1219	0
$m_{32i}^{(11)}$	0	0	-0.5409	1.6331	1.6406	-1.6702	-0.2576	-0.2250	0
$m_{33i}^{(11)}$	0	0	0	0	7.2095	5.6327	2.0757	-8.8220	0
$m_{34i}^{(11)}$	0	0	0	0	4.8111	-4.4336	1.6880	0.7207	0
$m_{35i}^{(11)}$	0	0	0	0	139.668	116.483	9.9855	-59.8218	0
$m_{36i}^{(11)}$	0	0	0	0	64.2815	-56.6914	0.3169	-3.6050	0
$m_{41i}^{(11)}$	0	0	0.7401	-1.3510	-0.8211	0.5961	0.7670	0.4334	0
$m_{42i}^{(11)}$	0	0	2.2203	2.0265	-4.1830	-0.7135	-1.8215	0.7996	0
$m_{43i}^{(11)}$	0	0	0	0	-18.3819	2.4062	14.678	31.3526	0
$m_{44i}^{(11)}$	0	0	0	0	-12.2667	-1.8940	11.9366	-2.5613	0
$m_{45i}^{(11)}$	0	0	0	0	-356.107	49.7599	70.6109	212.602	0
$m_{46i}^{(11)}$	0	0	0	0	-163.897	-24.2177	2.2408	12.8119	0
$m_{51i}^{(11)}$	0	0	0.0133	0.1240	-0.0328	-0.1576	-0.0085	0.0165	0
$m_{52i}^{(11)}$	0	0	0.0310	-0.1861	-0.1669	0.1887	0.0201	0.0304	0
$m_{53i}^{(11)}$	0	0	0	0	-0.7333	-0.6363	-0.1620	1.1936	0
$m_{54i}^{(11)}$	0	0	0	0	-0.4893	0.5008	-0.1317	-0.0975	0
$m_{55i}^{(11)}$	0	0	0	0	-14.2052	-13.1577	-0.7791	8.0940	0
$m_{56i}^{(11)}$	0	0	0	0	-6.5379	6.4038	-0.0247	0.4878	0
$m_{61i}^{(11)}$	0	0	-0.0871	0.1279	0.0824	-0.0247	-0.0621	-0.0347	0
$m_{62i}^{(11)}$	0	0	-0.2614	-0.1918	0.4197	0.0295	0.1474	-0.0640	0
$m_{63i}^{(11)}$	0	0	0	0	1.84422	-0.0995522	-1.1874	-2.5111	0
$m_{64i}^{(11)}$	0	0	0	0	1.2307	0.0784	-0.9657	0.2051	0
$m_{65i}^{(11)}$	0	0	0	0	35.7275	-2.0587	-5.7124	-17.0279	0
$m_{66i}^{(11)}$	0	0	0	0	16.4435	1.0020	-0.1813	-1.0261	0

Table A.5.: "Magic numbers" $m_{3li}^{(11)}, m_{4li}^{(11)}, m_{5li}^{(11)}$ and $m_{6li}^{(11)}$.

i	1	2	3	4	5	6	7	8	9
$m_{31i}^{(20)}$	0	0	-0.221623	0.579366	1.17316	-1.38853	0.135066	-1.02839	0
$m_{32i}^{(20)}$	0	0	-0.425668	-1.93209	2.92926	3.32871	2.69087	-0.856585	0
$m_{33i}^{(20)}$	0	0	0	0	15.6719	-10.1006	-0.0487765	-11.775	0
$m_{34i}^{(20)}$	0	0	0	0	15.9377	1.94304	14.6555	15.6499	0
$m_{35i}^{(20)}$	0	0	0	0	39.256	-955.766	-18.5938	-1469.65	0
$m_{36i}^{(20)}$	0	0	0	0	324.798	59.1356	65.9104	599.472	0
$m_{41i}^{(20)}$	0	0	-0.332434	-1.7381	-0.421611	0.40331	0.827699	0.968895	0
$m_{42i}^{(20)}$	0	0	-0.638502	5.79627	-1.05272	-0.966852	16.49	0.807031	0
$m_{43i}^{(20)}$	0	0	0	0	-5.63218	2.93381	-0.298908	11.0938	0
$m_{44i}^{(20)}$	0	0	0	0	-5.72772	-0.564372	89.8106	-14.7446	0
$m_{45i}^{(20)}$	0	0	0	0	-14.1079	277.61	-113.945	1384.63	0
$m_{46i}^{(20)}$	0	0	0	0	-116.727	-17.1764	403.907	-564.792	0
$m_{51i}^{(20)}$	0	0	0.0554057	-0.144842	-0.166483	0.232504	-0.00609938	0.0522244	0
$m_{52i}^{(20)}$	0	0	0.106417	0.483023	-0.415692	-0.557379	-0.121516	0.0434998	0
$m_{53i}^{(20)}$	0	0	0	0	-2.224	1.69131	0.00220268	0.59797	0
$m_{54i}^{(20)}$	0	0	0	0	-2.26172	-0.325354	-0.661821	-0.794747	0
$m_{55i}^{(20)}$	0	0	0	0	-5.57083	160.039	0.839672	74.6328	0
$m_{56i}^{(20)}$	0	0	0	0	-46.0922	-9.90202	-2.97642	-30.4429	0
$m_{61i}^{(20)}$	0	0	0.0831086	0.434525	-0.192536	-0.379626	-0.0638441	-0.0706474	0
$m_{62i}^{(20)}$	0	0	0.159626	-1.44907	-0.480743	0.910075	-1.27195	-0.058845	0
$m_{63i}^{(20)}$	0	0	0	0	-2.57203	-2.76153	0.0230561	-0.808912	0
$m_{64i}^{(20)}$	0	0	0	0	-2.61566	0.531229	-6.92748	1.07511	0
$m_{65i}^{(20)}$	0	0	0	0	-6.4426	-261.308	8.7891	-100.961	0
$m_{66i}^{(20)}$	0	0	0	0	-53.3051	16.1678	-31.1551	41.182	0

Table A.6.: "Magic numbers" $m_{3li}^{(20)}, m_{4li}^{(20)}, m_{5li}^{(20)}$ and $m_{6li}^{(20)}$.

i	1	2	3	4	5	6	7	8	9
$m_{31i}^{(21)}$	0	0	1.0748	-1.1924	-1.6945	5.3637	-0.8020	1.3959	0
$m_{32i}^{(21)}$	0	0	1.6015	6.6880	5.7915	-6.4248	1.7201	3.1943	0
$m_{33i}^{(21)}$	0	0	0	0	-15.7599	27.5011	-59.394	4.8637	0
$m_{34i}^{(21)}$	0	0	0	0	-1.9149	19.5482	4.2949	16.9807	0
$m_{35i}^{(21)}$	0	0	0	0	721.438	1690.14	-192.468	676.858	0
$m_{36i}^{(21)}$	0	0	0	0	-288.139	90.7174	274.774	240.889	0
$m_{41i}^{(21)}$	0	0	-4.4115	-1.4795	4.3205	2.2913	-5.6714	-4.9608	0
$m_{42i}^{(21)}$	0	0	-6.5736	8.2987	-14.7664	-2.7446	12.1637	-11.3524	0
$m_{43i}^{(21)}$	0	0	0	0	40.1826	11.7481	-419.995	-17.2853	0
$m_{44i}^{(21)}$	0	0	0	0	4.8823	8.3507	30.3704	-60.3479	0
$m_{45i}^{(21)}$	0	0	0	0	-1839.43	722.001	-1361.	-2405.5	0
$m_{46i}^{(21)}$	0	0	0	0	734.661	38.7531	1943.02	-856.099	0
$m_{51i}^{(21)}$	0	0	-0.07947	0.1358	0.1723	-0.6059	0.0626	-0.1889	0
$m_{52i}^{(21)}$	0	0	-0.1184	-0.7620	-0.5890	0.7257	-0.13422	-0.4322	0
$m_{53i}^{(21)}$	0	0	0	0	1.6029	-3.1065	4.6343	-0.6581	0
$m_{54i}^{(21)}$	0	0	0	0	0.1948	-2.2081	-0.3351	-2.2975	0
$m_{55i}^{(21)}$	0	0	0	0	-73.3757	-190.915	15.0175	-91.5805	0
$m_{56i}^{(21)}$	0	0	0	0	29.3059	-10.2473	-21.4396	-32.5928	0
$m_{61i}^{(21)}$	0	0	0.5194	0.1400	-0.4335	-0.0948	0.4588	0.3973	0
$m_{62i}^{(21)}$	0	0	0.7740	-0.7855	1.4815	0.1136	-0.9840	0.9092	0
$m_{63i}^{(21)}$	0	0	0	0	-4.0314	-0.4861	33.9773	1.3844	0
$m_{64i}^{(21)}$	0	0	0	0	-0.4898	-0.34549	-2.4569	4.8334	0
$m_{65i}^{(21)}$	0	0	0	0	184.547	-29.8713	110.104	192.663	0
$m_{66i}^{(21)}$	0	0	0	0	-73.7071	-1.6033	-157.189	68.5673	0

Table A.7.: "Magic numbers" $m_{3li}^{(21)}, m_{4li}^{(21)}, m_{5li}^{(21)}$ and $m_{6li}^{(21)}$.

i	1	2	3	4	5	6	7	8	9
$m_{31i}^{(22)}$	0	0	0.6635	-12.8257	-4.8453	10.7966	1.6880	1.1284	0
$m_{32i}^{(22)}$	0	0	1.9905	19.2386	-24.6846	-12.9233	-4.0084	2.0820	0
$m_{33i}^{(22)}$	0	0	0	0	-108.475	43.5841	32.3005	81.6323	0
$m_{34i}^{(22)}$	0	0	0	0	-72.3881	-34.3059	26.2678	-6.6687	0
$m_{35i}^{(22)}$	0	0	0	0	-2101.46	901.305	155.387	553.549	0
$m_{36i}^{(22)}$	0	0	0	0	-967.189	-438.657	4.9311	33.3582	0
$m_{41i}^{(22)}$	0	0	2.7047	-28.4843	-2.2968	29.6401	5.9393	2.7007	0
$m_{42i}^{(22)}$	0	0	8.11407	42.7264	-11.7014	-35.4784	-14.1041	4.9828	0
$m_{43i}^{(22)}$	0	0	0	0	-51.4211	119.652	113.652	195.37	0
$m_{44i}^{(22)}$	0	0	0	0	-34.3145	-94.1806	92.4259	-15.9602	0
$m_{45i}^{(22)}$	0	0	0	0	-996.165	2474.37	546.745	1324.8	0
$m_{46i}^{(22)}$	0	0	0	0	-458.482	-1204.25	17.3504	79.8358	0
$m_{51i}^{(22)}$	0	0	-0.1220	0.8392	0.5410	-0.5153	-0.1202	-0.1420	0
$m_{52i}^{(22)}$	0	0	-0.3660	-1.2588	2.7564	0.6168	0.2854	-0.2620	0
$m_{53i}^{(22)}$	0	0	0	0	12.1127	-2.0802	-2.2995	-10.273	0
$m_{54i}^{(22)}$	0	0	0	0	8.0831	1.6374	-1.8701	0.8392	0
$m_{55i}^{(22)}$	0	0	0	0	234.656	-43.0187	-11.0624	-69.6614	0
$m_{56i}^{(22)}$	0	0	0	0	107.999	20.9368	-0.3511	-4.1980	0
$m_{61i}^{(22)}$	0	0	-0.7748	2.3718	0.5762	-2.0857	-0.6556	-0.2303	0
$m_{62i}^{(22)}$	0	0	-2.3243	-3.5577	2.9357	2.4965	1.5568	-0.4249	0
$m_{63i}^{(22)}$	0	0	0	0	12.9008	-8.4196	-12.5446	-16.6615	0
$m_{64i}^{(22)}$	0	0	0	0	8.6090	6.6272	-10.2017	1.3611	0
$m_{65i}^{(22)}$	0	0	0	0	249.923	-174.115	-60.3481	-112.981	0
$m_{66i}^{(22)}$	0	0	0	0	115.026	84.74	-1.9151	-6.8085	0

Table A.8.: "Magic numbers" $m_{3li}^{(22)}, m_{4li}^{(22)}, m_{5li}^{(22)}$ and $m_{6li}^{(22)}$.

i	1	2	3	4	5	6	7	8	9
$m_{71i}^{(00)}$	0.5784	-0.3921	-0.1429	0.0476	-0.1275	0.0317	0.0078	-0.0031	0
$m_{72i}^{(00)}$	2.2996	-1.0880	-0.4286	-0.0714	-0.6494	-0.0380	-0.0185	-0.0057	0
$m_{73i}^{(00)}$	8.0780	-5.2777	0	0	-2.8536	0.1281	0.1495	-0.2244	0
$m_{74i}^{(00)}$	5.7064	-3.8412	0	0	-1.9042	-0.1008	0.1216	0.0183	0
$m_{75i}^{(00)}$	202.901	-149.467	0	0	-55.2813	2.6494	0.7191	-1.5213	0
$m_{76i}^{(00)}$	86.4618	-59.6604	0	0	-25.443	-1.2894	0.0228	-0.0917	0
$m_{77i}^{(00)}$	0	1	0	0	0	0	0	0	0
$m_{78i}^{(00)}$	2.6667	-2.6667	0	0	0	0	0	0	0
$m_{81i}^{(00)}$	0.2169	0	0	0	-0.1793	-0.0730	0.0240	0.0113	0
$m_{82i}^{(00)}$	0.8623	0	0	0	-0.9135	0.0873	-0.0571	0.0209	0
$m_{83i}^{(00)}$	3.0292	0	0	0	-4.0143	-0.2945	0.4510	0.8196	0
$m_{84i}^{(00)}$	2.1399	0	0	0	-2.6788	0.2318	0.3741	-0.0670	0
$m_{85i}^{(00)}$	76.0879	0	0	0	-77.7679	-6.0904	2.2128	5.5576	0
$m_{86i}^{(00)}$	32.4232	0	0	0	-35.7924	2.9641	0.0702	0.3349	0
$m_{87i}^{(00)}$	0	0	0	0	0	0	0	0	0
$m_{88i}^{(00)}$	1	0	0	0	0	0	0	0	0

Table A.9.: "Magic numbers" $m_{7li}^{(00)}$ and $m_{8li}^{(00)}$.

i	1	2	3	4	5	6	7	8	9
$m^{(10)}_{71i}$	0.0021	-1.4498	0.8515	0.0521	0.6707	0.1220	-0.0578	0.0355	0
$m^{(10)}_{72i}$	9.9372	-7.4878	1.2688	-0.2925	-2.2923	-0.1461	0.1239	0.0812	0
$m^{(10)}_{73i}$	-5.0737	7.6871	0	0	6.2379	0.6255	-4.2771	0.1237	0
$m^{(10)}_{74i}$	-8.6840	8.5586	0	0	0.7579	0.4446	0.3093	0.4318	0
$m^{(10)}_{75i}$	2421.27	-1982.64	0	0	-285.55	38.4415	-13.86	17.2132	0
$m^{(10)}_{76i}$	-639.781	576.021	0	0	114.047	2.0633	19.7871	6.1260	0
$m^{(10)}_{77i}$	0	7.8152	0	0	0	0	0	0	0
$m^{(10)}_{78i}$	17.9842	-18.7604	0	0	0	0	0	0	0
$m^{(10)}_{81i}$	0.0008	0	0	0	0.9435	-0.2804	-0.1777	-0.1297	0
$m^{(10)}_{82i}$	3.7264	0	0	0	-3.2247	0.3359	0.3812	-0.2968	0
$m^{(10)}_{83i}$	-1.9026	0	0	0	8.7752	-1.4379	-13.1618	-0.4519	0
$m^{(10)}_{84i}$	-3.2565	0	0	0	1.0662	-1.0221	0.9517	-1.5776	0
$m^{(10)}_{85i}$	907.978	0	0	0	-401.702	-88.3699	-42.651	-62.8823	0
$m^{(10)}_{86i}$	-239.918	0	0	0	160.438	-4.7432	60.8902	-22.3794	0
$m^{(10)}_{87i}$	0	0	0	0	0	0	0	0	0
$m^{(10)}_{88i}$	6.7441	0	0	0	0	0	0	0	0

Table A.10.: "Magic numbers" $m^{(10)}_{7li}$ and $m^{(10)}_{8li}$.

i	1	2	3	4	5	6	7	8	9
$m_{71i}^{(11)}$	-4.3519	3.0646	1.5169	-0.5013	0.3934	-0.6245	0.2268	0.04956	0
$m_{72i}^{(11)}$	-17.3023	8.5027	4.5508	0.7519	2.0040	0.7476	-0.5385	0.0914	0
$m_{73i}^{(11)}$	-60.7794	41.2459	0	0	8.8066	-2.5212	4.3396	3.5852	0
$m_{74i}^{(11)}$	-42.9356	30.0198	0	0	5.8769	1.9845	3.5291	-0.2929	0
$m_{75i}^{(11)}$	-1526.64	1168.11	0	0	170.607	-52.1373	20.8762	24.3112	0
$m_{76i}^{(11)}$	-650.544	466.256	0	0	78.5215	25.3748	0.6625	1.4650	0
$m_{77i}^{(11)}$	0	-7.8152	0	0	0	0	0	0	0
$m_{78i}^{(11)}$	-20.0642	20.8404	0	0	0	0	0	0	0
$m_{81i}^{(11)}$	-1.4628	0	0.4687	2.6596	0.6448	-3.0787	0.0510	0.3518	0
$m_{82i}^{(11)}$	-5.8157	0	1.4062	-3.9894	3.2850	3.6851	-0.1424	0.6492	0
$m_{83i}^{(11)}$	-20.4295	0	0	0	14.436	-12.4282	1.1476	25.4531	0
$m_{84i}^{(11)}$	-14.4317	0	0	0	9.6335	9.7825	0.9332	-2.07932	0
$m_{85i}^{(11)}$	-513.142	0	0	0	279.663	-257.012	5.5205	172.598	0
$m_{86i}^{(11)}$	-218.664	0	0	0	128.714	125.086	0.1752	10.4012	0
$m_{87i}^{(11)}$	0	0	0	0	0	0	0	0	0
$m_{88i}^{(11)}$	-6.7441	0	0	0	0	0	0	0	0

Table A.11.: "Magic numbers" $m_{7li}^{(11)}$ and $m_{8li}^{(11)}$.

i	1	2	3	4	5	6	7	8	9
$m^{(20)}_{71i}$	-91.2189	81.3165	2.99191	1.11735	11.5573	0.886925	0.11496	0.175504	0
$m^{(20)}_{72i}$	-212.414	167.658	5.74652	-3.72617	28.8574	-2.12622	2.29032	0.146185	0
$m^{(20)}_{73i}$	-527.503	450.594	0	0	154.39	6.45179	-0.0415157	2.00952	0
$m^{(20)}_{74i}$	-749.114	579.46	0	0	157.009	-1.24112	12.4739	-2.67081	0
$m^{(20)}_{75i}$	7764.36	-5063.44	0	0	386.727	610.496	-15.826	250.809	0
$m^{(20)}_{76i}$	-22612.5	19501.2	0	0	3199.72	-37.7729	56.0992	-102.306	0
$m^{(20)}_{77i}$	0	44.4252	0	0	0	0	0	0	0
$m^{(20)}_{78i}$	15.4051	-18.7662	0	0	0	0	0	0	0
$m^{(20)}_{81i}$	-34.2071	0	0	0	16.2584	-2.03888	0.353763	-0.641144	0
$m^{(20)}_{82i}$	-79.6551	0	0	0	40.5956	4.88778	7.04792	-0.534035	0
$m^{(20)}_{83i}$	-197.814	0	0	0	217.191	-14.8315	-0.127755	-7.3411	0
$m^{(20)}_{84i}$	-280.918	0	0	0	220.875	2.8531	38.3855	9.75688	0
$m^{(20)}_{85i}$	2911.64	0	0	0	544.035	-1403.42	-48.7008	-916.245	0
$m^{(20)}_{86i}$	-8479.69	0	0	0	4501.27	86.833	172.632	373.738	0
$m^{(20)}_{87i}$	0	0	0	0	0	0	0	0	0
$m^{(20)}_{88i}$	5.77691	0	0	0	0	0	0	0	0

Table A.12.: "Magic numbers" $m^{(20)}_{7li}$ and $m^{(20)}_{8li}$.

i	1	2	3	4	5	6	7	8	9
$m_{71i}^{(21)}$	-0.0161	11.3308	-9.0418	-0.5490	-2.0699	-2.4008	-1.6767	-0.5673	0
$m_{72i}^{(21)}$	-74.7681	58.5182	-13.4731	3.0791	7.0744	2.8757	3.5962	-1.2981	0
$m_{73i}^{(21)}$	38.1746	-60.0759	0	0	-19.2511	-12.3094	-124.172	-1.9766	0
$m_{74i}^{(21)}$	65.3389	-66.8869	0	0	-2.3391	-8.7497	8.9790	-6.9008	0
$m_{75i}^{(21)}$	-18217.8	15494.7	0	0	881.254	-756.496	-402.382	-275.071	0
$m_{76i}^{(21)}$	4813.75	-4501.7	0	0	-351.969	-40.6047	574.456	-97.8957	0
$m_{77i}^{(21)}$	0	-61.0768	0	0	0	0	0	0	0
$m_{78i}^{(21)}$	-135.314	146.616	0	0	0	0	0	0	0
$m_{81i}^{(21)}$	-0.0054	0	-2.7939	2.9127	-3.3930	-11.8347	-0.4434	-4.0274	0
$m_{82i}^{(21)}$	-25.1314	0	-4.1632	-16.3374	11.5966	14.1759	0.9510	-9.2163	0
$m_{83i}^{(21)}$	12.8314	0	0	0	-31.5568	-60.6794	-32.8362	-14.0329	0
$m_{84i}^{(21)}$	21.962	0	0	0	-3.8342	-43.1317	2.3744	-48.9926	0
$m_{85i}^{(21)}$	-6123.46	0	0	0	1444.57	-3729.17	-106.406	-1952.87	0
$m_{86i}^{(21)}$	1618.02	0	0	0	-576.955	-200.162	151.91	-695.012	0
$m_{87i}^{(21)}$	0	0	0	0	0	0	0	0	0
$m_{88i}^{(21)}$	-45.4824	0	0	0	0	0	0	0	0

Table A.13.: "Magic numbers" $m_{7li}^{(21)}$ and $m_{8li}^{(21)}$.

i	1	2	3	4	5	6	7	8	9
$m_{71i}^{(22)}$	7.9088	-6.5297	7.7372	-8.8514	-3.9002	-3.3651	3.6324	1.4173	0
$m_{72i}^{(22)}$	31.4443	-18.1165	23.2117	13.2771	-19.8699	4.0279	-8.6259	2.6149	0
$m_{73i}^{(22)}$	110.458	-87.8817	0	0	-87.3171	-13.5844	69.5086	102.527	0
$m_{74i}^{(22)}$	78.0291	-63.9626	0	0	-58.2688	10.6925	56.5267	-8.3756	0
$m_{75i}^{(22)}$	2774.44	-2488.86	0	0	-1691.57	-280.921	334.383	695.234	0
$m_{76i}^{(22)}$	1182.27	-993.442	0	0	-778.539	136.722	10.6114	41.8965	0
$m_{77i}^{(22)}$	0	16.6516	0	0	0	0	0	0	0
$m_{78i}^{(22)}$	36.4636	-44.4043	0	0	0	0	0	0	0
$m_{81i}^{(22)}$	8.612	0	-8.5773	9.9240	15.2774	28.49	-10.4305	-3.4354	0
$m_{82i}^{(22)}$	34.2399	0	-25.732	-14.8861	77.8316	-34.1018	24.7694	-6.3384	0
$m_{83i}^{(22)}$	120.278	0	0	0	342.027	115.009	-199.594	-248.523	0
$m_{84i}^{(22)}$	84.9664	0	0	0	228.243	-90.5262	-162.317	20.3024	0
$m_{85i}^{(22)}$	3021.11	0	0	0	6625.99	2378.36	-960.183	-1685.24	0
$m_{86i}^{(22)}$	1287.38	0	0	0	3049.59	-1157.53	-30.4705	-101.556	0
$m_{87i}^{(22)}$	0	0	0	0	0	0	0	0	0
$m_{88i}^{(22)}$	39.7055	0	0	0	0	0	0	0	0

Table A.14.: "Magic numbers" $m_{7li}^{(22)}$ and $m_{8li}^{(22)}$.

i	1	2	3	4	5	6	7	8	9
$m_{91i}^{(00)}$	0	0	-0.0328	-0.0404	0.0021	-0.0289	-0.0174	-0.0010	0.1184
$m_{92i}^{(00)}$	0	0	-0.0985	0.0606	0.0108	0.0346	0.0412	-0.0018	-0.0469
$m_{93i}^{(00)}$	0	0	0	0	0.0476	-0.1167	-0.3320	-0.0718	0.4729
$m_{94i}^{(00)}$	0	0	0	0	0.0318	0.0918	-0.2700	0.0059	0.1405
$m_{95i}^{(00)}$	0	0	0	0	0.9223	-2.4126	-1.5972	-0.4870	3.5745
$m_{96i}^{(00)}$	0	0	0	0	0.4245	1.1742	-0.0507	-0.0293	-1.5186
$m_{99i}^{(00)}$	0	0	0	0	0	0	0	0	1

Table A.15.: "Magic numbers" $m_{9li}^{(00)}$.

i	1	2	3	4	5	6	7	8	9
$m_{91i}^{(10)}$	0	0	0.1958	-0.0442	-0.0112	-0.1111	0.1283	0.0114	-0.3596
$m_{92i}^{(10)}$	0	0	0.2917	0.2482	0.0382	0.1331	-0.2751	0.0260	-0.8794
$m_{93i}^{(10)}$	0	0	0	0	-0.1041	-0.5696	9.5004	0.0396	-0.4856
$m_{94i}^{(10)}$	0	0	0	0	-0.0126	-0.4049	-0.6870	0.1382	0.4172
$m_{95i}^{(10)}$	0	0	0	0	4.7639	-35.0057	30.7862	5.5105	62.3651
$m_{96i}^{(10)}$	0	0	0	0	-1.9027	-1.8789	-43.9516	1.9611	54.4557
$m_{99i}^{(10)}$	0	0	0	0	0	0	0	0	0

Table A.16.: "Magic numbers" $m_{9li}^{(10)}$.

i	1	2	3	4	5	6	7	8	9
$m_{91i}^{(11)}$	0	0	0.2918	0.04836	-0.0331	-0.0269	0.0200	-0.1094	0
$m_{92i}^{(11)}$	0	0	0.8754	-0.0725	-0.1685	0.0323	-0.0475	-0.2018	0
$m_{93i}^{(11)}$	0	0	0	0	-0.7405	-0.1088	0.3825	-7.9139	0
$m_{94i}^{(11)}$	0	0	0	0	-0.4942	0.0856	0.3111	0.6465	0
$m_{95i}^{(11)}$	0	0	0	0	-14.3464	-2.2495	1.8402	-53.6643	0
$m_{961i}^{(11)}$	0	0	0	0	-6.6029	1.0948	0.0584	-3.2339	0
$m_{99i}^{(11)}$	0	0	0	0	0	0	0	0	0

Table A.17.: "Magic numbers" $m_{9li}^{(11)}$.

i	1	2	3	4	5	6	7	8	9
$m_{91i}^{(20)}$	0	0	0.687795	-0.948054	-0.192814	-0.807654	-0.255352	0.0561848	-0.64363
$m_{92i}^{(20)}$	0	0	1.32104	3.1616	-0.481439	1.93618	-5.08731	0.0467986	-13.5825
$m_{93i}^{(20)}$	0	0	0	0	-2.57575	-5.87514	0.0922157	0.643316	7.77564
$m_{94i}^{(20)}$	0	0	0	0	-2.61944	1.13019	-27.7073	-0.855015	16.0333
$m_{95i}^{(20)}$	0	0	0	0	-6.45192	-555.931	35.1531	80.2925	102.043
$m_{96i}^{(20)}$	0	0	0	0	-53.3822	34.3969	-124.609	-32.7515	-98.8845
$m_{99i}^{(20)}$	0	0	0	0	0	0	0	0	0

Table A.18.: "Magic numbers" $m_{9li}^{(20)}$.

i	1	2	3	4	5	6	7	8	9
$m_{91i}^{(21)}$	0	0	-1.7394	0.0530	0.1741	-0.1036	-0.1478	1.2522	0
$m_{92i}^{(21)}$	0	0	-2.5918	-0.2971	-0.5949	0.1241	0.3170	2.8655	0
$m_{93i}^{(21)}$	0	0	0	0	1.6188	-0.5311	-10.9454	4.3631	0
$m_{94i}^{(21)}$	0	0	0	0	0.1967	-0.3775	0.7915	15.2328	0
$m_{95i}^{(21)}$	0	0	0	0	-74.1049	-32.6399	-35.4688	607.188	0
$m_{96i}^{(21)}$	0	0	0	0	29.5971	-1.7519	50.6366	216.094	0
$m_{99i}^{(21)}$	0	0	0	0	0	0	0	0	0

Table A.19.: "Magic numbers" $m_{9li}^{(21)}$.

i	1	2	3	4	5	6	7	8	9
$m_{91i}^{(22)}$	0	0	4.1531	-0.4627	-0.3404	-1.0326	0.0809	0.2167	0
$m_{92i}^{(22)}$	0	0	12.4592	0.6940	-1.7339	1.2359	-0.1921	0.3998	0
$m_{93i}^{(22)}$	0	0	0	0	-7.6197	-4.1683	1.5483	15.674	0
$m_{94i}^{(22)}$	0	0	0	0	-5.0848	3.2809	1.2592	-1.2804	0
$m_{95i}^{(22)}$	0	0	0	0	-147.615	-86.199	7.4486	106.285	0
$m_{96i}^{(22)}$	0	0	0	0	-67.9394	41.9523	0.2364	6.405	0
$m_{99i}^{(22)}$	0	0	0	0	0	0	0	0	0

Table A.20.: "Magic numbers" $m_{9li}^{(22)}$.

APPENDIX B

Calculation of $\mathcal{T}^{\pm}_{\perp,\parallel}$

In the heavy quark limit the matrix elements of $B \to K^*$ depend only on four independent funtions $\mathcal{T}^{\pm}_a$ corresponding to a transversly ($a = \perp$) and longitudinally ($a = \parallel$) polarised K^*. At next-to-leading order we have [91]:

$$\mathcal{T}_a = \xi_a C_a + \frac{\pi^2}{N_c}\frac{f_B f_{K^*,a}}{M_B}\Xi_a \sum_{\pm}\int \frac{d\omega}{\omega}\,\Phi_{B,\pm}(\omega)\int_0^1 du \Phi_{K^*,a}(u) T_{a,\pm}(u,\omega)\;, \tag{B.1}$$

where $N_c = 3$, $\Xi_\perp \equiv 1$, $\Xi_\parallel \equiv m_{K^*}/E_{K^*}$ and μ_f is the scale at which the typical virtualities of the hard scattering terms appear ($\mu_f = (\mu \times 0.5\,\mathrm{GeV})^{1/2} \simeq (m_b \Lambda_{\mathrm{QCD}})^{1/2}$) [91, 103].

In practice, we need $\mathcal{T}^{\pm}_{\perp,\parallel}$ which can be obtained by:

$$\begin{aligned} \mathcal{T}^+_a &= (\mathcal{T}_a,\ \text{in which } C_7^{eff} \to C_7^{eff} + C_7^{eff\prime})\;, \\ \mathcal{T}^-_a &= (\mathcal{T}_a,\ \text{in which } C_7^{eff} \to C_7^{eff} - C_7^{eff\prime})\;. \end{aligned} \tag{B.2}$$

These replacements lead to:

$$\mathcal{T}^+_\perp = \xi_\perp C^+_\perp + \frac{\pi^2}{N_c}\frac{f_B f_{K^*,\perp}}{M_B}\sum_{\pm}\int \frac{d\omega}{\omega}\,\Phi_{B,\pm}(\omega)\int_0^1 du \Phi_{K^*,\perp}(u) T^+_{\perp,\pm}(u,\omega)\;, \tag{B.3}$$

$$\mathcal{T}^-_\perp = \xi_\perp C^-_\perp + \frac{\pi^2}{N_c}\frac{f_B f_{K^*,\perp}}{M_B}\sum_{\pm}\int \frac{d\omega}{\omega}\,\Phi_{B,\pm}(\omega)\int_0^1 du \Phi_{K^*,\perp}(u) T^-_{\perp,\pm}(u,\omega)\;, \tag{B.4}$$

$$\mathcal{T}^+_\parallel = \xi_\parallel C^+_\parallel + \frac{\pi^2}{N_c}\frac{f_B f_{K^*,\parallel}}{M_B}\frac{m_{K^*}}{E_{K^*}}\sum_{\pm}\int \frac{d\omega}{\omega}\,\Phi_{B,\pm}(\omega)\int_0^1 du \Phi_{K^*,\parallel}(u) T^+_{\parallel,\pm}(u,\omega)\;, \tag{B.5}$$

$$\mathcal{T}^-_\parallel = \xi_\parallel C^-_\parallel + \frac{\pi^2}{N_c}\frac{f_B f_{K^*,\parallel}}{M_B}\frac{m_{K^*}}{E_{K^*}}\sum_{\pm}\int \frac{d\omega}{\omega}\,\Phi_{B,\pm}(\omega)\int_0^1 du \Phi_{K^*,\parallel}(u) T^-_{\parallel,\pm}(u,\omega)\;. \tag{B.6}$$

$f_{K^*,\perp}$, $f_{K^*,\parallel}$ and f_B can all be found in Table 5.1. $f_{K^*,\parallel}$ is scale dependent, but as its variation has a negligible effect, its scale dependency is usually ignored. However, $f_\perp$ is evolved using $f_\perp(\mu) = f_\perp(\mu_0)\,(\alpha_s(\mu)/\alpha_s(\mu_0))^{4/23}$, μ_0 the initial scale (usually 1 GeV) and $\mu \simeq m_b$.

B.1 Light-cone-distribution amplitudes Φ

To compute the integrals, it is necessary to know the light-cone-distribution amplitudes Φ. The K^* light-cone distribution amplitude can be expanded in terms of the Gegenbauer coefficients [91, 165]:

$$\Phi_{\bar{K}^*,a}(u) = 6u(1-u)\left\{1 + a_1(\bar{K}^*)_a\, C_1^{(3/2)}(2u-1) + a_2(\bar{K}^*)_a\, C_2^{(3/2)}(2u-1)\right\} . \quad \text{(B.7)}$$

The Gegenbauer polynomials are

$$C_1^{(3/2)}(x) = 3x \qquad C_2^{(3/2)}(x) = -\frac{3}{2} + \frac{15}{2}x^2 , \quad \text{(B.8)}$$

and the Gegenbauer coefficients $(a_1(\bar{K}^*)_a, a_2(\bar{K}^*)_a)$ are given in Table 5.1. They are scale dependent [165]:

$$a_n(\mu) = a_n(\mu_0)\left(\frac{\alpha_s(\mu)}{\alpha_s(\mu_0)}\right)^{(\gamma_{(n)}-\gamma_{(0)})/\beta_0} \quad \text{(B.9)}$$

with $\beta_0 = 11 - (2/3)n_f$. The one-loop anomalous dimensions are

$$\begin{aligned} \gamma_{(n)} = \gamma_{(n)}^{\parallel} &= C_F\left(1 - \frac{2}{(n+1)(n+2)} + 4\sum_{j=2}^{n+1} 1/j\right), \\ \gamma_{(n)}^{\perp} &= C_F\left(1 + 4\sum_{j=2}^{n+1} 1/j\right), \end{aligned} \quad \text{(B.10)}$$

where $C_F = 4/3$ and $\gamma_{(0)}$ is the anomalous dimension of the local current and vanishes for vector and axial-vector currents.

The two B light-cone distribution amplitudes $(\Phi_{B,+}, \Phi_{B,-})$ are not used directly as they appear as moments [91]. When calculating $\mathcal{T}_a$ where we have $T_{\perp,+}^{(1)}$ we will need the moment

$$\lambda_{B,+}^{-1} = \int_0^\infty d\omega \frac{\Phi_{B,+}(\omega)}{\omega} . \quad \text{(B.11)}$$

$\lambda_{B,+}^{-1}$ is given in Table 5.1 and evolves according to the following evolution relation [117]:

$$\lambda_B^{-1}(\mu) = \lambda_B^{-1}(\mu_0)\left\{1 + \frac{\alpha_s}{3\pi}\,\ln\frac{\mu^2}{\mu_0^2}\,(1 - 2\sigma_B(\mu_0))\right\}, \quad \text{(B.12)}$$

where $\sigma_B(1\,\text{GeV}) = 1.4 \pm 0.4$.
When computing $\mathcal{T}_a$ where we have $T_{\parallel,-}^{(1)}$, we will also need the moment

$$\lambda_{B,-}^{-1}(q^2) = \int_0^\infty d\omega \frac{\Phi_{B,-}(\omega)}{\omega - q^2/M_B - i\epsilon} \,, \tag{B.13}$$

which can be expressed as:

$$\lambda_{B,-}^{-1}(q^2) = \frac{e^{-q^2/(M_B\omega_0)}}{\omega_0} \left[-\text{Ei}(q^2/M_B\omega_0) + i\pi\right] \tag{B.14}$$

where $\text{Ei}(z)$ is the exponential integral function, and $\omega_0 = 2\bar{\Lambda}_{\text{HQET}}/3$; $\bar{\Lambda}_{\text{HQET}} = M_B - m_b$.

B.2 Form factor correction $C_a^{\pm}$

The following formulas are taken from [91], in which we applied (B.2).

$$C_a^{\pm} = C_a^{\pm(0)} + \frac{\alpha_s(\mu_b) C_F}{4\pi} C_a^{\pm(1)} \,. \tag{B.15}$$

At leading-order for $C_a^{\pm(0)}$ we have:

$$C_\perp^{\pm(0)} = (C_7^{eff} \pm C_7^{eff'}) + \frac{q^2}{2m_b M_B} Y(q^2) \,, \tag{B.16}$$

$$C_\parallel^{\pm(0)} = -(C_7^{eff} \pm C_7^{eff'}) - \frac{M_B}{2m_b} Y(q^2) \,, \tag{B.17}$$

with $Y(q^2)$ given in (5.11).
The next-to-leading order coefficients $C_a^{\pm(1)}$ contain a factorisable and a non-factorisable part:

$$C_a^{\pm(1)} = C_a^{\pm(\text{f})} + C_a^{\pm(\text{nf})} \,, \tag{B.18}$$

Term "non-factorisable" term contains all corrections that are not included in the definition of the QCD form factors for heavy-to-light transitions.
The factorisable corrections are [91, 103]

$$C_\perp^{\pm(\text{f})} = (C_7^{eff} \pm C_7^{eff'}) \left(\ln \frac{m_b^2}{\mu^2} - L + \Delta M \right) \,, \tag{B.19}$$

$$C_\parallel^{\pm(\text{f})} = -(C_7^{eff} \pm C_7^{eff'}) \left(\ln \frac{m_b^2}{\mu^2} + 2L + \Delta M \right) \,, \tag{B.20}$$

where L is defined in

$$L \equiv -\frac{m_b^2 - q^2}{q^2} \ln \left(1 - \frac{q^2}{m_b^2} \right) \,, \tag{B.21}$$

and ΔM depends on the mass renormalisation convention for m_b:

$$\begin{cases} \Delta M = 0 \,, & \overline{MS} \text{ scheme} \\ \Delta M = 3\ln(m_b^2/\mu^2) - 4(1-\mu_f/m_b) \,, & \text{Potential Substracted scheme} \\ \Delta M = 3\ln(m_b^2/\mu^2) - 4 \,, & \text{Pole Mass scheme} \end{cases} \tag{B.22}$$

The non-factorisable correction is obtained by computing matrix elements of four-quark operators and the chromomagnetic dipole operator [91].

$$\begin{aligned} C_F\, C_\perp^{\pm(\mathrm{nf})} &= -\bar{C}_2 F_2^{(7)} - C_8^{eff} F_8^{(7)} \\ &\quad - \frac{q^2}{2m_b M_B}\left[\bar{C}_2 F_2^{(9)} + 2\bar{C}_1\left(F_1^{(9)} + \frac{1}{6}F_2^{(9)}\right) + C_8^{eff} F_8^{(9)}\right] \,, \end{aligned} \tag{B.23}$$

$$\begin{aligned} C_F\, C_\parallel^{\pm(\mathrm{nf})} &= \bar{C}_2 F_2^{(7)} + C_8^{eff} F_8^{(7)} \\ &\quad + \frac{M_B}{2m_b}\left[\bar{C}_2 F_2^{(9)} + 2\bar{C}_1\left(F_1^{(9)} + \frac{1}{6}\,F_2^{(9)}\right) + C_8^{eff} F_8^{(9)}\right] \,. \end{aligned} \tag{B.24}$$

The quantities $F_{1,2}^{(7,9)}$ and $F_8^{(7,9)}$ are given in [166] and [167].

The barred Wilson coefficient $\bar{C}_2$ can be written in our convention (5.2)–(5.6) as [91]:

$$\begin{aligned} \bar{C}_1 &= \frac{1}{2}\,C_1 \,, \\ \bar{C}_2 &= C_2 - \frac{1}{6}\,C_1 \,, \\ \bar{C}_3 &= C_3 - \frac{1}{6}\,C_4 + 16\,C_5 - \frac{8}{3}\,C_6 \,, \\ \bar{C}_4 &= \frac{1}{2}\,C_4 + 8\,C_6 \,, \\ \bar{C}_5 &= C_3 - \frac{1}{6}\,C_4 + 4\,C_5 - \frac{2}{3}\,C_6 \,, \\ \bar{C}_6 &= \frac{1}{2}\,C_4 + 2\,C_6 \,. \end{aligned} \tag{B.25}$$

The effective Wilson coefficients $C_{7,9}^{eff}$ are given in (5.9) and (5.10). For C_8^{eff} we use

$$C_8^{eff} = C_8 + C_3 - \frac{1}{6}\,C_4 + 20C_5 - \frac{10}{3}C_6 \,. \tag{B.26}$$

B.3 Spectator scattering

For the hard scattering kernel we have

$$T_{a,\pm}(u,\omega) = T_{a,\pm}^{(0)}(u,\omega) + \frac{\alpha_s(\mu_f)C_F}{4\pi} T_{a,\pm}^{(1)}(u,\omega). \tag{B.27}$$

At leading-order we have the weak annihilation amplitude which has no analogue in the inclusive decay and generates the hard-(spectator)scattering term $T^{(0)}_{a,\pm}(u,\omega)$ [91]:

$$T^{(0)\pm}_{\perp,+}(u,\omega) = T^{(0)\pm}_{\perp,-}(u,\omega) = T^{(0)\pm}_{\parallel,+}(u,\omega) = 0, \tag{B.28}$$

$$T^{(0)\pm}_{\parallel,-}(u,\omega) = -e_q \frac{M_B\omega}{M_B\omega - q^2 - i\epsilon} \cdot \frac{4M_B}{m_b}(\bar{C}_3 + 3\bar{C}_4) \tag{B.29}$$

The next-to-leading order coefficients $T^{(1)}_a$ contain a factorisable as well as a non-factorisable part:

$$T^{(1)}_a = T^{(\mathrm{f})}_a + T^{(\mathrm{nf})}_a. \tag{B.30}$$

The hard scattering functions $T^{(1)}_{a,\pm}$ contain a factorisable term from expressing the full QCD form factors in terms of ξ_a, related to the α_s-correction [91, 103]:

$$T^{(\mathrm{f})\pm}_{\perp,+}(u,\omega) = (C_7^{eff} \pm C_7^{eff'})\frac{2M_B}{\bar{u}E_{K^*}}, \tag{B.31}$$

$$T^{(\mathrm{f})\pm}_{\perp,-}(u,\omega) = T^{(\mathrm{f})\pm}_{\parallel,-}(u,\omega) = 0 \tag{B.32}$$

$$T^{(\mathrm{f})\pm}_{\parallel,+}(u,\omega) = (C_7^{eff} \pm C_7^{eff'})\frac{4M_B}{\bar{u}E_{K^*}}, \tag{B.33}$$

where $\bar{u} = 1 - u$. The non-factorisable correction is obtained by computing matrix elements of four-quark operators and the chromomagnetic dipole operator [91].

$$\begin{aligned} T^{(\mathrm{nf})\pm}_{\perp,+}(u,\omega) = &-\frac{4e_d C_8^{eff}}{u + \bar{u}q^2/M_B^2} + \frac{M_B}{2m_b}\Big[e_u t_\perp(u,m_c)(\bar{C}_2 + \bar{C}_4 - \bar{C}_6) \\ &+ e_d t_\perp(u,m_b)(\bar{C}_3 + \bar{C}_4 - \bar{C}_6 - 4m_b/M_B\bar{C}_5) + e_d t_\perp(u,0)\bar{C}_3\Big], \end{aligned} \tag{B.34}$$

$$T^{(\mathrm{nf})\pm}_{\perp,-}(u,\omega) = 0, \tag{B.35}$$

$$\begin{aligned} T^{(\mathrm{nf})\pm}_{\parallel,+}(u,\omega) = &\frac{M_B}{m_b}\Big[e_u t_\parallel(u,m_c)(\bar{C}_2 + \bar{C}_4 - \bar{C}_6) \\ &+ e_d t_\parallel(u,m_b)(\bar{C}_3 + \bar{C}_4 - \bar{C}_6) + e_d t_\parallel(u,0)\bar{C}_3\Big], \end{aligned} \tag{B.36}$$

$$\begin{aligned} T^{(\mathrm{nf})\pm}_{\parallel,-}(u,\omega) = e_q \frac{M_B\omega}{M_B\omega - q^2 - i\epsilon}\Bigg[&\frac{8C_8^{eff}}{\bar{u} + uq^2/M_B^2} \\ &+ \frac{6M_B}{m_b}\Big(h(\bar{u}M_B^2 + uq^2, m_c)(\bar{C}_2 + \bar{C}_4 + \bar{C}_6) \\ &+ h(\bar{u}M_B^2 + uq^2, m_b^{\mathrm{pole}})(\bar{C}_3 + \bar{C}_4 + \bar{C}_6) \\ &+ h(\bar{u}M_B^2 + uq^2, 0)(\bar{C}_3 + 3\bar{C}_4 + 3\bar{C}_6) - \frac{8}{27}(\bar{C}_3 - \bar{C}_5 - 15\bar{C}_6)\Big)\Bigg]. \end{aligned} \tag{B.37}$$

Here $e_u = 2/3$, $e_d = -1/3$ and e_q is the electric charge of the spectator quark in the B meson. The functions $t_a(u, m_q)$ are given below

$$t_\perp(u, m_q) = \frac{2M_B}{\bar{u}E_{K^*}} I_1(m_q) + \frac{q^2}{\bar{u}^2 E_{K^*}^2} \left(B_0(\bar{u}M_B^2 + uq^2, m_q) - B_0(q^2, m_q)\right), \tag{B.38}$$

$$t_\parallel(u, m_q) = \frac{2M_B}{\bar{u}E_{K^*}} I_1(m_q) + \frac{\bar{u}M_B^2 + uq^2}{\bar{u}^2 E_{K^*}^2} (B_0(\bar{u}M_B^2 + uq^2, m_q) - B_0(q^2, m_q)), \tag{B.39}$$

where B_0 and I_1 are defined as

$$B_0(s, m_q) = -2\sqrt{4m_q^2/s - 1} \arctan \frac{1}{\sqrt{4m_q^2/s - 1}}, \tag{B.40}$$

$$I_1(m_q) = 1 + \frac{2m_q^2}{\bar{u}(M_B^2 - q^2)} \Big[L_1(x_+) + L_1(x_-) - L_1(y_+) - L_1(y_-)\Big], \tag{B.41}$$

and

$$x_\pm = \frac{1}{2} \pm \left(\frac{1}{4} - \frac{m_q^2}{\bar{u}M_B^2 + uq^2}\right)^{1/2}, \; y_\pm = \frac{1}{2} \pm \left(\frac{1}{4} - \frac{m_q^2}{q^2}\right)^{1/2}, \tag{B.42}$$

$$L_1(x) = \ln \frac{x-1}{x} \ln(1-x) - \frac{\pi^2}{6} + \mathrm{Li}_2\left(\frac{x}{x-1}\right). \tag{B.43}$$

It should be noted that m_q^2 must be replaced by $m_q^2 - i\epsilon$ when imaginary parts are involved. The barred coefficients are given in (B.25).

APPENDIX C

Form factors

To obtain the soft form factors we have used the factorisation scheme used in [103]:

$$\xi_\perp(q^2) = \frac{M_B}{M_B + m_{K^*}} V(q^2) \,, \tag{C.1}$$

$$\xi_\parallel(q^2) = \frac{M_B + m_{K^*}}{2E_{K^*}} A_1(q^2) - \frac{M_B - m_{K^*}}{M_B} A_2(q^2) \,. \tag{C.2}$$

The full form factors V and $A_{1,2}$ have been taken from light-cone sum rule (LCSR) calculations [114]:

$$V(q^2) = \frac{r_1}{1 - q^2/m_R^2} + \frac{r_2}{1 - q^2/m_{fit}^2} \,, \tag{C.3}$$

$$A_1(q^2) = \frac{r_2}{1 - q^2/m_{fit}^2} \,, \tag{C.4}$$

$$A_2(q^2) = \frac{r_1}{1 - q^2/m_{fit}^2} + \frac{r_2}{(1 - q^2/m_{fit}^2)^2} \,, \tag{C.5}$$

where the fit parameters $r_{1,2}, m_R^2$ and m_{fit}^2 are given in Table C.1.

	r_1	r_2	$m_R^2\,[\mathrm{GeV}^2]$	$m_{fit}^2\,[\mathrm{GeV}^2]$
V	0.923	-0.511	5.32^2	49.40
A_1		0.290		40.38
A_2	-0.084	0.342		52.00

Table C.1.: Fit parameters describing the q^2 dependence of the form factors V and $A_{1,2}$ in the LCSR approach [114].

Bibliography

[1] S. L. Glashow, Nucl. Phys. **22** (1961) 579;
S. Weinberg, Phys. Rev. Lett. **19** (1967) 1264;
A. Salam, Proc. 8th Nobel Symposium, Stockholm 1968, ed. N. Svartholm (Almqvist and Wiksells, Stockholm, 1968), p. 367.

[2] F. Englert and R. Brout, Phys. Rev. Lett. **13** (1964) 321;
P. W. Higgs, Phys. Rev. Lett. **13** (1964) 508;

[3] N. Cabibbo, Phys. Rev. Lett. **10** (1963) 531.

[4] M. Kobayashi and T. Maskawa, Prog. Theor. Phys. **49** (1973) 652.

[5] L. Wolfenstein, Phys. Rev. Lett. **51** (1983) 1945.

[6] M. A. Shifman, hep-ph/9510397.

[7] T. Inami and C. S. Lim, Prog. Theor. Phys. **65** (1981) 297 [Erratum-ibid. **65** (1981) 1772].

[8] S. L. Glashow, J. Iliopoulos and L. Maiani, Phys. Rev. D **2** (1970) 1285.

[9] J. Wess and B. Zumino, Phys. Lett. B **49** (1974) 52.

[10] S. R. Coleman and J. Mandula, Phys. Rev. **159** (1967) 1251.

[11] R. Haag, J. T. Lopuszanski and M. Sohnius, Nucl. Phys. B **88** (1975) 257.

[12] D. Bailin and A. Love, Bristol, UK: IOP (1994) 322 p. (Graduate student series in physics)

[13] S. Dimopoulos and H. Georgi, Nucl. Phys. B **193** (1981) 150.

[14] E. Gildener and S. Weinberg, Phys. Rev. D **13** (1976) 3333;
E. Gildener, Phys. Rev. D **14** (1976) 1667;
L. Susskind, Phys. Rev. D **20** (1979) 2619;
M. J. G. Veltman, Acta Phys. Polon. B **12** (1981) 437;
S. Dimopoulos and S. Raby, Nucl. Phys. B **192** (1981) 353;

E. Witten, Nucl. Phys. B **188** (1981) 513;
M. Dine, W. Fischler and M. Srednicki, Nucl. Phys. B **189** (1981) 575;
N. Sakai, Z. Phys. C **11** (1981) 153;
R. K. Kaul, Phys. Lett. B **109** (1982) 19;
R. K. Kaul and P. Majumdar, Nucl. Phys. B **199** (1982) 36.

[15] J. Beringer *et al.* [Particle Data Group Collaboration], Phys. Rev. D **86** (2012) 010001.

[16] J. R. Ellis, S. Kelley and D. V. Nanopoulos, Phys. Lett. B **260** (1991) 131;
U. Amaldi, W. de Boer and H. Furstenau, Phys. Lett. B **260** (1991) 447.

[17] S. P. Martin, In *Kane, G.L. (ed.): Perspectives on supersymmetry II* 1-153 [hep-ph/9709356].

[18] I. J. R. Aitchison, Cambridge, UK: Univ. Pr. (2007) 222 p

[19] H. E. Haber, In *Boulder 1992, Proceedings, Recent directions in particle theory* 589-686, and Calif. Univ. Santa Cruz - SCIPP 92-033 (93/04,rec.Jun.) 98 p [hep-ph/9306207].

[20] P. Fayet, Phys. Lett. B **64** (1976) 159.

[21] G. Jungman, M. Kamionkowski, K. Griest and , Phys. Rept. **267** (1996) 195 [hep-ph/9506380].

[22] I. Simonsen, hep-ph/9506369.

[23] H. P. Nilles, Phys. Rept. **110** (1984) 1.

[24] J. A. Bagger, In *Boulder 1995, QCD and beyond* 109-159 [hep-ph/9604232];
M. Drees, hep-ph/9611409;
S. Dawson, NATO Adv. Study Inst. Ser. B Phys. **365** (1997) 33 [hep-ph/9612229];
J. F. Gunion, In *Santa Barbara 1996, Future high energy colliders* 41-64 [hep-ph/9704349];
X. Tata, In *Campos do Jordao 1997, Particles and fields* 404-492 [hep-ph/9706307];
N. Polonsky, Lect. Notes Phys. M **68** (2001) 1 [hep-ph/0108236];
H. E. Haber, Nucl. Phys. Proc. Suppl. **101** (2001) 217 [hep-ph/0103095];
J. D. Lykken, hep-th/9612114;
P. Ramond,Bobeth:2002ch hep-th/9412234.

[25] E. Witten, Nucl. Phys. B **202** (1982) 253.

[26] S. Deser and B. Zumino, Phys. Lett. B **62** (1976) 335.

[27] A. H. Chamseddine, R. L. Arnowitt and P. Nath, Phys. Rev. Lett. **49** (1982) 970;
R. Barbieri, S. Ferrara and C. A. Savoy, Phys. Lett. B **119** (1982) 343;
L. J. Hall, J. D. Lykken and S. Weinberg, Phys. Rev. D **27** (1983) 2359.

[28] M. Dine, W. Fischler and M. Srednicki, Nucl. Phys. B **189** (1981) 575;
S. Dimopoulos and S. Raby, Nucl. Phys. B **192** (1981) 353;
M. Dine, A. E. Nelson, Y. Nir and Y. Shirman, Phys. Rev. D **53** (1996) 2658 [hep-ph/9507378];
G. F. Giudice and R. Rattazzi, Phys. Rept. **322** (1999) 419 [hep-ph/9801271].

[29] L. Randall and R. Sundrum, Nucl. Phys. B **557** (1999) 79 [hep-th/9810155];
G. F. Giudice, M. A. Luty, H. Murayama and R. Rattazzi, JHEP **9812** (1998) 027 [hep-ph/9810442];
D. K. Ghosh, A. Kundu, P. Roy and S. Roy, Phys. Rev. D **64** (2001) 115001 [hep-ph/0104217].

[30] V. D. Barger, M. S. Berger and P. Ohmann, Phys. Rev. D **47** (1993) 1093 [hep-ph/9209232];
V. D. Barger, M. S. Berger and P. Ohmann, Phys. Rev. D **49** (1994) 4908 [hep-ph/9311269].

[31] H. E. Haber and G. L. Kane, Phys. Rept. **117** (1985) 75.

[32] C. Csaki, Mod. Phys. Lett. A **11** (1996) 599 [hep-ph/9606414].

[33] J. Rosiek, hep-ph/9511250.

[34] G. F. Giudice and A. Masiero, Phys. Lett. B **206** (1988) 480;
J. E. Kim and H. P. Nilles, Phys. Lett. B **138** (1984) 150.

[35] J. F. Gunion and H. E. Haber, Nucl. Phys. B **272** (1986) 1 [Erratum-ibid. B **402** (1993) 567].

[36] J. F. Gunion and H. E. Haber, Nucl. Phys. B **278** (1986) 449.

[37] G. Degrassi, S. Di Vita, J. Elias-Miro, J. R. Espinosa, G. F. Giudice, G. Isidori and A. Strumia, JHEP **1208** (2012) 098 [arXiv:1205.6497 [hep-ph]].

[38] G. Degrassi, S. Heinemeyer, W. Hollik, P. Slavich and G. Weiglein, Eur. Phys. J. C **28** (2003) 133 [hep-ph/0212020].

[39] M. Misiak, S. Pokorski and J. Rosiek, Adv. Ser. Direct. High Energy Phys. **15** (1998) 795 [hep-ph/9703442].

[40] P. L. Cho, M. Misiak and D. Wyler, Phys. Rev. D **54** (1996) 3329 [hep-ph/9601360].

[41] C. Bobeth, A. J. Buras, F. Kruger and J. Urban, Nucl. Phys. B **630** (2002) 87 [hep-ph/0112305].

[42] L. J. Hall, V. A. Kostelecky and S. Raby, Nucl. Phys. B **267** (1986) 415.

[43] G. 't Hooft, C. Itzykson, (ed.), A. Jaffe, (ed.), H. Lehmann, (ed.), P. K. Mitter, (ed.), I. M. Singer, (ed.) and R. Stora, (ed.), NATO Adv. Study Inst. Ser. B Phys. **59** (1980) pp.1.

[44] A. J. Buras, P. Gambino, M. Gorbahn, S. Jager and L. Silvestrini, Nucl. Phys. B **592** (2001) 55 [hep-ph/0007313].

[45] J. R. Ellis and D. V. Nanopoulos, Phys. Lett. B **110** (1982) 44;
R. Barbieri and R. Gatto, Phys. Lett. B **110** (1982) 211.

[46] F. Gabbiani and A. Masiero, Nucl. Phys. B **322** (1989) 235.

[47] A. J. Buras, P. H. Chankowski, J. Rosiek and L. Slawianowska, Nucl. Phys. B **619** (2001) 434 [hep-ph/0107048];
S. Bergmann and G. Perez, Phys. Rev. D **64** (2001) 115009 [hep-ph/0103299];
S. Laplace, Z. Ligeti, Y. Nir and G. Perez, Phys. Rev. D **65** (2002) 094040 [hep-ph/0202010];
A. Ali and D. London, Eur. Phys. J. C **9** (1999) 687 [hep-ph/9903535];
L. J. Hall and L. Randall, Phys. Rev. Lett. **65** (1990) 2939;
G. D'Ambrosio, G. F. Giudice, G. Isidori and A. Strumia, Nucl. Phys. B **645** (2002) 155 [hep-ph/0207036];
A. J. Buras, P. Gambino, M. Gorbahn, S. Jager and L. Silvestrini, Phys. Lett. B **500** (2001) 161 [hep-ph/0007085].

[48] M. Ciuchini, G. Degrassi, P. Gambino and G. F. Giudice, Nucl. Phys. B **534** (1998) 3 [hep-ph/9806308].

[49] T. Appelquist and J. Carazzone, Phys. Rev. D **11** (1975) 2856.

[50] H. Georgi, Ann. Rev. Nucl. Part. Sci. **43** (1993) 209.

[51] A. Jaffe and E. Witten, Quantum Yang-Mills Theory,

[52] E. Fermi, Z. Phys. **88** (1934) 161.
La Ricerca Scientifica 2, Issue 12, 1933.

[53] T. D. Lee and C. -N. Yang, Phys. Rev. **104** (1956) 254.

[54] E. C. G. Sudarshan and R. e. Marshak, Phys. Rev. **109** (1958) 1860.
E. C. G. Sudarshan and R. E. Marshak, Proceedings of Padua- Venice Conference on Mesons and Newly Discovered Particles, September, 1957.

[55] R. P. Feynman and M. Gell-Mann, Phys. Rev. **109** (1958) 193.

[56] J. H. Christenson, J. W. Cronin, V. L. Fitch and R. Turlay, Phys. Rev. Lett. **13** (1964) 138.

[57] K. G. Wilson, Phys. Rev. **179** (1969) 1499.

[58] K. G. Wilson and W. Zimmermann, Commun. Math. Phys. **24** (1972) 87.

[59] G. Buchalla, A. J. Buras and M. E. Lautenbacher, Rev. Mod. Phys. **68** (1996) 1125 [hep-ph/9512380].

[60] G. 't Hooft and M. J. G. Veltman, Nucl. Phys. B **153** (1979) 365.

[61] J. M. Jauch and F. Rohrlich, Berlin, Germany: Springer-Verlag, 2 Revised edition (1980) 553 p.

[62] W. Pauli and F. Villars, Rev. Mod. Phys. **21** (1949) 434.

[63] W. A. Bardeen, R. Gastmans and B. E. Lautrup, Nucl. Phys. B **46** (1972) 319.

[64] M. S. Chanowitz, M. Furman and I. Hinchliffe, Nucl. Phys. B **159** (1979) 225.

[65] S. A. Gottlieb and J. T. Donohue, Phys. Rev. D **20** (1979) 3378.

[66] G. 't Hooft and M. J. G. Veltman, Nucl. Phys. B **44** (1972) 189.

[67] D. A. Akyeampong and R. Delbourgo, Nuovo Cim. A **17** (1973) 578.

[68] P. Breitenlohner and D. Maison, Commun. Math. Phys. **52** (1977) 11.

[69] W. A. Bardeen and A. J. Buras, Phys. Rev. D **20** (1979) 166 [Erratum-ibid. D **21** (1980) 2041].

[70] T. P. Cheng and L. F. Li, Oxford, Uk: Clarendon (1984) 536 P. (Oxford Science Publications)

[71] T. Muta, World Sci. Lect. Notes Phys. **78** (2010) 1.

[72] D. J. Gross and F. Wilczek, Phys. Rev. Lett. **30** (1973) 1343.

[73] H. D. Politzer, Phys. Rev. Lett. **30** (1973) 1346.

[74] F. J. Yndurain, Berlin, Germany: Springer (2006) 474 p

[75] M. E. Peskin and D. V. Schroeder, Reading, USA: Addison-Wesley (1995) 842 p

[76] H. Georgi, Menlo Park, Usa: Benjamin/cummings (1984) 165p

[77] Y. Grossman, "Just a Taste: Lectures on Flavor Physics"

[78] E. C. Poggio, H. R. Quinn and S. Weinberg, Phys. Rev. D **13** (1976) 1958.

[79] A. J. Buras and M. Munz, Phys. Rev. D **52** (1995) 186 [hep-ph/9501281].

[80] B. Grinstein, M. J. Savage and M. B. Wise, Nucl. Phys. B **319** (1989) 271.

[81] C. Bobeth, G. Hiller and G. Piranishvili, JHEP **0712** (2007) 040 [arXiv:0709.4174 [hep-ph]].

[82] A. K. Alok, A. Dighe and S. U. Sankar, Phys. Rev. D **78** (2008) 114025 [arXiv:0810.3779 [hep-ph]].

[83] S. Fukae, C. S. Kim, T. Morozumi and T. Yoshikawa, Phys. Rev. D **59** (1999) 074013 [hep-ph/9807254].

[84] D. Becirevic, N. Kosnik, F. Mescia and E. Schneider, Phys. Rev. D **86** (2012) 034034 [arXiv:1205.5811 [hep-ph]].

[85] K. G. Chetyrkin, M. Misiak and M. Munz, Nucl. Phys. B **520** (1998) 279 [hep-ph/9711280].

[86] T. Goto, Y. Okada, Y. Shimizu and M. Tanaka, Phys. Rev. D **55** (1997) 4273 [Erratum-ibid. D **66** (2002) 019901] [hep-ph/9609512].

[87] Y. -B. Dai, C. -S. Huang and H. -W. Huang, Phys. Lett. B **390** (1997) 257 [Erratum-ibid. B **513** (2001) 429] [hep-ph/9607389].

[88] W. Jaus and D. Wyler, Phys. Rev. D **41** (1990) 3405.

[89] A. J. Buras, M. Misiak, M. Munz and S. Pokorski, Nucl. Phys. B **424** (1994) 374 [hep-ph/9311345].

[90] C. Bobeth, M. Misiak and J. Urban, Nucl. Phys. B **574** (2000) 291 [hep-ph/9910220].

[91] M. Beneke, T. Feldmann and D. Seidel, Nucl. Phys. B **612** (2001) 25 [hep-ph/0106067].

[92] C. Greub, A. Ioannisian and D. Wyler, Phys. Lett. B **346** (1995) 149 [hep-ph/9408382].

[93] F. Kruger and L. M. Sehgal, Phys. Lett. B **380** (1996) 199 [hep-ph/9603237].

[94] W. Altmannshofer, P. Ball, A. Bharucha, A. J. Buras, D. M. Straub and M. Wick, JHEP **0901** (2009) 019 [arXiv:0811.1214 [hep-ph]].

[95] J. Charles, A. Le Yaouanc, L. Oliver, O. Pene and J. C. Raynal, Phys. Rev. D **60** (1999) 014001 [hep-ph/9812358].

[96] A. Khodjamirian, T. .Mannel, A. A. Pivovarov and Y. -M. Wang, JHEP **1009** (2010) 089 [arXiv:1006.4945 [hep-ph]].

[97] C. Bobeth, G. Hiller and D. van Dyk, JHEP **1107** (2011) 067 [arXiv:1105.0376 [hep-ph]].

[98] F. Kruger and J. Matias, Phys. Rev. D **71** (2005) 094009 [hep-ph/0502060].

[99] F. Kruger, L. M. Sehgal, N. Sinha and R. Sinha, Phys. Rev. D **61** (2000) 114028 [Erratum-ibid. D **63** (2001) 019901] [hep-ph/9907386].

[100] A. Faessler, T. Gutsche, M. A. Ivanov, J. G. Korner and V. E. Lyubovitskij, Eur. Phys. J. direct C **4** (2002) 18 [hep-ph/0205287].

[101] C. Bobeth, G. Hiller and G. Piranishvili, JHEP **0807** (2008) 106 [arXiv:0805.2525 [hep-ph]].

[102] T. Feldmann and J. Matias, JHEP **0301** (2003) 074 [hep-ph/0212158].

[103] M. Beneke, T. .Feldmann and D. Seidel, Eur. Phys. J. C **41** (2005) 173 [hep-ph/0412400].

[104] J. Matias, F. Mescia, M. Ramon and J. Virto, JHEP **1204** (2012) 104 [arXiv:1202.4266 [hep-ph]].

[105] U. Egede, T. Hurth, J. Matias, M. Ramon and W. Reece, JHEP **0811** (2008) 032 [arXiv:0807.2589].

[106] D. Becirevic and E. Schneider, Nucl. Phys. B **854** (2012) 321 [arXiv:1106.3283 [hep-ph]].

[107] C. Bobeth, G. Hiller and D. van Dyk, JHEP **1007** (2010) 098 [arXiv:1006.5013 [hep-ph]].

[108] A. V. Manohar and M. B. Wise, Camb. Monogr. Part. Phys. Nucl. Phys. Cosmol. **10** (2000) 1.

[109] B. Grinstein, SSCL-PREPRINT-017.

[110] C. S. Lim, T. Morozumi and A. I. Sanda, Phys. Lett. B **218** (1989) 343.

[111] M. Beneke, A. P. Chapovsky, M. Diehl and T. Feldmann, Nucl. Phys. B **643** (2002) 431 [hep-ph/0206152].

[112] M. J. Dugan and B. Grinstein, Phys. Lett. B **255** (1991) 583.

[113] M. Beneke and T. Feldmann, Nucl. Phys. B **592** (2001) 3 [hep-ph/0008255].

[114] P. Ball and R. Zwicky, Phys. Rev. D **71** (2005) 014029 [hep-ph/0412079].

[115] K. Nakamura *et al.* [Particle Data Group], J. Phys. G **37** (2010) 075021 and 2011 partial update for the 2012 edition.

[116] P. Ball, V. M. Braun and A. Lenz, JHEP **0708** (2007) 090 [arXiv:0707.1201].

[117] P. Ball and R. Zwicky, JHEP **0604** (2006) 046 [hep-ph/0603232].

[118] F. Mahmoudi, S. Neshatpour and J. Orloff, JHEP **1208** (2012) 092 [arXiv:1205.1845 [hep-ph]].

[119] N. Isgur and M. B. Wise, Phys. Rev. D **42** (1990) 2388.

[120] B. Grinstein and D. Pirjol, Phys. Lett. B **533** (2002) 8 [hep-ph/0201298].

[121] B. Grinstein and D. Pirjol, Phys. Lett. B **549** (2002) 314 [hep-ph/0209211].

[122] B. Grinstein and D. Pirjol, Phys. Rev. D **70** (2004) 114005 [hep-ph/0404250].

[123] M. Beylich, G. Buchalla and T. Feldmann, Eur. Phys. J. C **71** (2011) 1635 [arXiv:1101.5118 [hep-ph]].

[124] C. Bobeth, T. Ewerth, F. Kruger and J. Urban, Phys. Rev. D **64** (2001) 074014 [hep-ph/0104284].

[125] Y. Grossman, Z. Ligeti and E. Nardi, Phys. Rev. D **55** (1997) 2768 [hep-ph/9607473].

[126] F. Mahmoudi, Comput. Phys. Commun. **180** (2009) 1579 [arXiv:0808.3144].

[127] [LHCb Collaboration], LHCb-CONF-2012-002, presented at the 47th Rencontres de Moriond on Electroweak Interactions and Unified Theories.

[128] K. De Bruyn, R. Fleischer, R. Knegjens, P. Koppenburg, M. Merk, A. Pellegrino and N. Tuning, Phys. Rev. Lett. **109** (2012) 041801 [arXiv:1204.1737 [hep-ph]].

[129] P. Dimopoulos *et al.* [ETM Collaboration], JHEP **1201** (2012) 046 [arXiv:1107.1441].

[130] A. Bazavov *et al.* [Fermilab Lattice and MILC Collaboration], arXiv:1112.3051 [hep-lat].

[131] E. T. Neil *et al.* [for the Fermilab Lattice and for the MILC Collaborations], arXiv:1112.3978 [hep-lat].

[132] H. Na, C. J. Monahan, C. T. H. Davies, R. Horgan, G. P. Lepage and J. Shigemitsu, arXiv:1202.4914 [hep-lat].

[133] C. McNeile, C. T. H. Davies, E. Follana, K. Hornbostel and G. P. Lepage, Phys. Rev. D **85** (2012) 031503 [arXiv:1110.4510].

[134] C. Davies, arXiv:1203.3862 [hep-lat].

[135] J. Laiho *et al.*, http://www.latticeaverages.org/

[136] C. Bobeth, P. Gambino, M. Gorbahn and U. Haisch, JHEP **0404** (2004) 071 [hep-ph/0312090].

[137] J. Charles, O. Deschamps, S. Descotes-Genon, R. Itoh, H. Lacker, A. Menzel, S. Monteil and V. Niess *et al.*, Phys. Rev. D **84** (2011) 033005 [arXiv:1106.4041 [hep-ph]].

[138] A. J. Buras, J. Girrbach, D. Guadagnoli and G. Isidori, Eur. Phys. J. C **72** (2012) 2172 [arXiv:1208.0934 [hep-ph]].

[139] H. Albrecht *et al.* [ARGUS Collaboration], Phys. Lett. B **199** (1987) 451.

[140] RAaij *et al.* [LHCb Collaboration], Phys. Rev. Lett. **110** (2013) 021801 [arXiv:1211.2674 [Unknown]].

[141] R. Aaij *et al.* [LHCb Collaboration], arXiv:1203.4493 [hep-ex].

[142] S. Chatrchyan *et al.* [CMS Collaboration], arXiv:1203.3976 [hep-ex].

[143] T. Aaltonen *et al.* [CDF Collaboration], Phys. Rev. Lett. **107** (2011) 239903 [Phys. Rev. Lett. **107** (2011) 191801] [arXiv:1107.2304].

[144] [LHCb Collaboration], LHCb-CONF-2012-008, presented at the 47th Rencontres de Moriond on QCD and High Energy Interactions.

[145] [LHCb Collaboration], LHCb-PAPER-2012-011, in preparation.

[146] S. Bertolini, F. Borzumati, A. Masiero, G. Ridolfi, Nucl. Phys. B **353** (1991) 591.

[147] N. Oshimo, Nucl. Phys. B **404** (1993) 20.

[148] F. Borzumati, Z. Phys. C **63** (1994) 291 [hep-ph/9310212].

[149] F. Kruger and J. C. Romao, Phys. Rev. D **62** (2000) 034020 [hep-ph/0002089];
C. Bobeth, A. J. Buras and T. Ewerth, Nucl. Phys. B **713** (2005) 522 [hep-ph/0409293];
C. -S. Huang and Q. -S. Yan, Phys. Lett. B **442** (1998) 209 [hep-ph/9803366];
C. -S. Huang, W. Liao and Q. -S. Yan, Phys. Rev. D **59** (1999) 011701 [hep-ph/9803460];
C. Bobeth, M. Misiak and J. Urban, Nucl. Phys. B **567** (2000) 153 [hep-ph/9904413];
L. Hofer, U. Nierste and D. Scherer, JHEP **0910** (2009) 081 [arXiv:0907.5408 [hep-ph]];
H. E. Logan and U. Nierste, Nucl. Phys. B **586** (2000) 39 [hep-ph/0004139];
D'Ambrosio *et al.* in [47].

[150] http://superiso.in2p3.fr/

[151] S. Chatrchyan *et al.* [CMS Collaboration], Phys. Lett. B **716** (2012) 30 [arXiv:1207.7235 [hep-ex]].

[152] G. Aad *et al.* [ATLAS Collaboration], Phys. Lett. B **716** (2012) 1 [arXiv:1207.7214 [hep-ex]].

[153] B. C. Allanach, Comput. Phys. Commun. **143** (2002) 305 [hep-ph/0104145].

[154] F. Mahmoudi, Comput. Phys. Commun. **178** (2008) 745 [arXiv:0710.2067].

[155] S. Descotes-Genon, D. Ghosh, J. Matias, M. Ramon and , JHEP **1106** (2011) 099 [arXiv:1104.3342 [hep-ph]].

[156] T. Hurth, F. Mahmoudi, Nucl. Phys. B **865** (2012) 461 [arXiv:1207.0688 [hep-ph]].

[157] M. Misiak, H. M. Asatrian, K. Bieri, M. Czakon, A. Czarnecki, T. Ewerth, A. Ferroglia and P. Gambino *et al.*, Phys. Rev. Lett. **98** (2007) 022002 [hep-ph/0609232].

[158] M. Misiak and M. Steinhauser, Nucl. Phys. B **764** (2007) 62 [hep-ph/0609241].

[159] D. Asner *et al.* [Heavy Flavor Averaging Group Collaboration], arXiv:1010.1589 [hep-ex]. and online update at http://www.slac.stanford.edu/xorg/hfag

[160] M. Czakon, U. Haisch and M. Misiak, JHEP **0703** (2007) 008 [hep-ph/0612329].

[161] A. J. Buras, arXiv:1102.5650 [hep-ph].

[162] A. J. Buras, M. Gorbahn, U. Haisch and U. Nierste, JHEP **0611** (2006) 002 [hep-ph/0603079].

[163] P. Gambino, M. Gorbahn and U. Haisch, Nucl. Phys. B **673** (2003) 238 [hep-ph/0306079].

[164] C. -s. Huang, Commun. Theor. Phys. **2** (1983) 1265.

[165] P. Ball, M. Boglione, Phys. Rev. **D68** (2003) 094006 [hep-ph/0307337].

[166] H. H. Asatrian, H. M. Asatrian, C. Greub and M. Walker, Phys. Lett. B **507** (2001) 162 [hep-ph/0103087].

[167] H. H. Asatryan, H. M. Asatrian, C. Greub and M. Walker, Phys. Rev. D **65** (2002) 074004 [hep-ph/0109140].

[168] C. Bobeth, G. Hiller, D. van Dyk and C. Wacker, JHEP **1201** (2012) 107 [arXiv:1111.2558].